2020 10 12 10 74

Volume 12 Number 10 October 2020

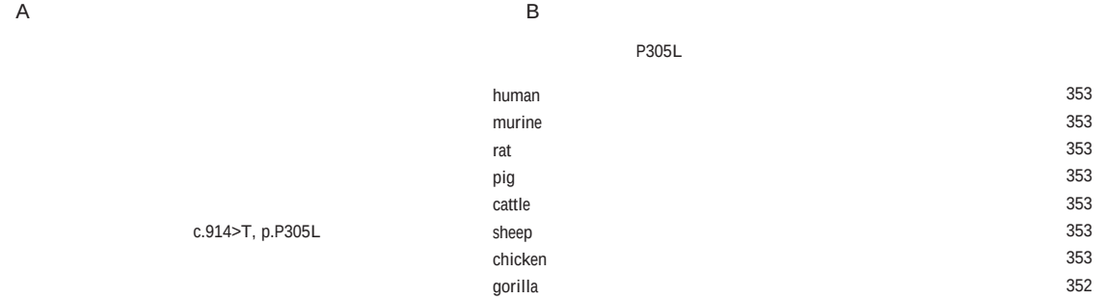

A. Sanger KIF1A c.914C>T p.P305L
B. KIF1A p.P305L KIF1A 294 353

P1297 Sanger KIF1A p.P305L

Figure P1297 Sanger sequencing results of proband family and KIF1A gene p.P305L amino acid sequence of different species

ISSN 1674-6929

. .

/

1998

2003

2003 2008 2011

2013 2008 2011

2017 2018 2018

SARS

2020 1

80

SCI 40 176.017 36.13

“ Characteristics of pediatric SARS CoV 2 infection and potential evidence for persistent fecal viral shedding ”

Nature Medicine 2020 6 16

32 1%

分子诊断与治疗杂志

HMSPL?J MD KMJCASJ?P BG?ELMQRGAQ ?LB RFCP?NW

0.0. /. /0 /. 52 @gkmlrfjw Tmjskc/0 Lsk`cp/. Marm`cp 0.0.

179 11 510620
020 32290789-206 32290789-201
jmdt vip.163.com
ISSN 1674-6929
CN 44-1656/R
46-283

440100190057

2020 10 18
RMB 15.00

Pcqnmlqg`jc Glqrgrsrgml	Sun Yat sen University
Qnmlqmp	China Family Doctors Magazine Publisher Co. Ltd.
Mpe_lgxcp	Da An Gene Co., Ltd. of SunYat sen University
Cbgrmpgl Afgcd	ZHANG Yipeng
Amlqsjr_lr	SHEN Ziyu
Cbgrmpgl Afgcd	LI Ming
K_l_egle Bgpcarmp	JIANG Xiwen
?qqmag_rc Cbgrmp	*LIU Yue*
Cbgrmpg_j Mddgac	<JOURNAL OF MOLECULAR DIAGNOSTICS AND THERAPY> Editorial Office
Cbgrmpq	LI Xiaolan LI Caizhen MO Yuanhao
Cbgrgle	China Family Doctors Magazine Publisher Co. Ltd.
?bb	11 Fl., Xianglong Building, 179# Tian he bei Lu, Guangzhou, China 510620
Rcj	020 32290789-206 32290789-201
CÎk_gj	jmdt@vip.163.com
AQQL	ISSN 1674-6929 CN 44-1656/R
Npglrgle	*TianYi Yofus Technology Co., Ltd.*
Ns`jgqf B_rc	2020.10.18
Npgac	RMB 15.00

分子诊断与治疗杂志

2020 10 12 10

HMSPL?J MD
KMJCASJ?P BG?ELMQRGAQ ?LB RFCP?NW

Monthly Volume 12 Number 10 October 2020

AMLRCLRQ

COMMENTS

ORIGINAL ARTICLES

REVIEWS

DNA RNA

Progress of research on gene editing toward therapeutic applications

HUA Liang ZHU Bing
Central Laboratory of Guangzhou Women and Children s Medical Center Guangzhou Guangdong China 510120

ABSTRACT Gene editing refers to a new technology for site specific modification of the genome. Using this technology you can accurately locate a certain site in the genome cut the target DNA or RNA fragment at this site and insert a new gene fragment. This process simulates the natural mutation of genes by artificial means and then achieves the purpose of modifying and editing the original genome of the organism. Since its birth gene editing technology has experienced five generations of development the technology has become more and more mature and the editing accuracy has also been improved. It has been more and more widely used in various biological fields including disease treatment and has become a research hotspot in recent years. This article briefly reviews the progress of researches on gene editing technology and the therapeutic applications.

KEY WORDS Gene editing Therapeutic application

DNA DNA double strand break DSB DSB DNA NHEJ HRR 2015 NHEJ NHEJ DNA DSB indel

1

NHEJ DSB DNA HDR

510120
E mail zhubing0327@163.com

DSB ıı w I Ψ ﻨﻌ Ж

´ ᾅ Ḩ ъ

Ḩ Ẩ в ﻨ ˝ ЖỎ

ﻨ Ẩ M ɟ

2

1986 Smithies [1] Ỏ

Ньж ﻨﻌ ɥ

ᅥ ɟ Kirk R [2] Ỉ †

Ỉ I ɔ ﻨﻌ

ıı Ỏﻨﻌ ɟ

ᴬ Ỉ 'Y ж ᅥ ٷ

ﻨﻌ ΨἏ Ḩ DNA ɟ ¥

Ньﻨﻌ ж Ỉ 'Y ה ẹ

ч ﻨﻌ ς Ђ Y ɟ

2.1 م

م ᵐ Ẻ 'Y΄H Ḩ 12~45 bp ῎Ω Ỉ 'Y ɟ ẹ Нь

῎Ω У DSB w ᾅ ٷﻨﻌ

Ψ Ỉ ﻨﻌ Ẩ ﻨﻌ Ά

╥ﻨﻌ Ặ ɟ

ﻨﻌ ฿ Ẩ AAV I Ψ ɟ ӂ Нь ẹ

Ἇ wש ǖ م ٷжﻨﻌ

ɔ ᾅ´ Ḩ ʄ ẹ ɔ ᾅ Ἇ ɟ

2.2 Zinc finger protein ZFP

ZFP ᵐ Cys2 His2 ﻄ ´

DNA ﻋ ɟ ZFN ζ ฿ Нь ᾄ ᅥ ´

DNA ῎Ω ZFP ᅥ ' w J I ɔ

ﺉ'Y΄H DNA Ỉ 'Y Fok I ɟ ᾀ ᵐ έ

´ DNA Fok I Ξ Y Жﻨ ᾅ

ﻨﻌ Ḩ DNA 'Y΄H У DSB ɟ

˜ ´ ӂ ẹ ᾄ DNA

῎Ω ٷ

ɔ ; DNA ῎Ω ᵐ Ђ

ὓ ﻨﻌ ´ T

ﻨﻌ ɟ 'Y ' У ה

ẹ Ђᵐ ȉ ɟ

2.3 ﻋ Transcription activator like effector nucleases TALEN

Ά ZFN ч TALEN ς Ξ ǖ ᵐ

ǖ 33 35 Y ﻨ ╥ẃ ḨНь

12 Ḩ ᅥ 13 Ḩ Ξ Y ' ﻨ ﻨ ᾄ ´

DNA ῎Ω ẹ ∩ᵐ ˜ Ἇ N 5′T

w ɔ ' w ḨНь 12

Ḩ ᅥ 13 Ḩ Ξ Y ' ﻨ ﻨ ᾅ ˜ ῎Hωὓ

ă DNA ῎Ω ɟ ᵐ ǖ Ά ZFN

Ἇ Ỉ 'Y Fok I ɟ TALEN ٷᵐ ɔ

ẋ Ђ ZFN ٷ ╥

ᅥ ɟ ὢ ٷж ᅥ I

Ψ NHEJ ᅥ HDR ɟ ӂ TALEN

I ZFN ʄ З Ҝ ฿ J

ъ ἏЂẹ Нь ﻨﻌ ɟ

2.4 ﻉ ῎Ω/

ﻉ ῎Ω Ặ clustered regularly interspaced short palindromic repeats/CRISPR associated proteins CRISPR/Cas

CRISPR/Cas9 sgRNA Ά DNA Ψ ٦ PAM ῎Ω ɔ ﻨﻌ Ў Ő

Cas9 r‡A "‡@‡b‡@TǤAH

ﻏﻰžﺤﻟT G ῏ђ ⓢ ŐŐ ѯ з ӂX

2.6 غ نحر ٨
Ꝁ ॥ ٨ ˘
ژ ´ ᾷ ɔ ى dCas9 ɘ ᾳ
dCas9 ˜ ᾳ ´ DNA ئۆ
Ḩ ɘ غ نحر ɟ З ژ
dCas9 ´ Ђ CRISPR ئۆ ٨
غ نحر م ΄Y dCas9 غ نحر
Ẻ ẫ ٨
ε I Ỉ غ نحر ॥ ٨ Ђ نحر ɟ

З

غ نحر ж ئۆ I Ỉ ٨ I ˥
Ђ ' ɟ I Ỉ غ نحر ฿ ˜
غ نحر I
˜ I З ॥ ' Њ
Ə Ḣ ɟ

3.1 I غ نحر
I غ نحر ъ ж ɔ ˥
ئۆ غ نحر ˜ ع Ḩ ɯ
ᾷ ɟ
Ҕ ئۆ Њ Ђ Ά φ ẍ
ɟ غ نحر ᾷ ˜
ɔ Ђ ٨ ẍ
╥ غ نحر ɟ Χ Ο ´ ẍ ɞ
ɞΟ ´ ẍ ɞ ɘ
Ế ̏ ɞ Ế ̏ ɞWiskott Aldrich
´ ٨ β ئىΨ [4,5] ɟ
غ نحر ٨ NHEJ غ نحر Ẩ
Ə Њ ฿ ٨ ئى
Ψ ئۆ Ỉ [6] ɟ ʄ HRR نحر
غ ς Ὸ Ὼ ɟ ئۆ ῗ
Ꝁ Ψ ה Ђ ฿ I
ї [7] ئىΨ [8] [9] ٨ Χ
IgM ´ [10] ɟ

3.2 I Ỉ غ نحر
ɔ ῗ ъ ɘ
I Ə˜ ئى ع I Ỉ
Ὼ I Ỉ غ نحر ɟ
Ế ̏ Duchenne muscular dystrophy DMD غ نحر ϶ ٨
϶ ɟ ᾳ AAV I Cas9 ٨ sgRNAs
ᾷ DMD I Ỉ ʄ DMD غ نحر
Ő NHEJ غ نحر ॥
ъ ΰ ʄ ٨ ɔ ٨
' ɔ [11,12] ɟ
ᾳ AAV I ´ NHEJ غ نحر
ЊΨ Ꝁ ɟ Ꙩ
ΰ ᾷ Ψ З
ɟ Φ [13] I Ꝁ
϶ [14] ɯ ש ç Ẉ 10 [15] ɟ
Њ غ نحر غ نحر ų
ẹ ʄ I Ỉ I Ỉ HRR ɟ
Њ ᵐ З ų
ї [16] ɞφ ى אָ [17] ɞ ɞ
ɞ ٨ [18,19] ɟ Ꙩ
̓ ᵐ ų Ψ غ نحر ى
϶ ε ى [20] ɟ

3.3 غ نحر
غ نحر ̓ Њ ɟ ж ٢
gRNA ٨ AAVs Cas9 ' ˘ Ђ
HIV غ نحر Ψ LTR ٨ gag ┘ DNA نحر
غ [21] ɟᵐ ٨ ϶ ╥
˜ HIV غ نحر Ξ Y ̏ ̓ ┘ طر Ξ Y gRNA
' ɯ ẫ Ặ [22] ɟ
ɸ ى Ẻ Ẫ ɵ ´ DNA cccDNA
ẹ ئۆ Ψ Њ Ѣ ΄Y cccDNA ẅ
٨ Ő غ
' ɟ ж ٢ HBV ˜
gRNA ᾳ Cas9 ΄Y ΄H cccDNA Y
٨ ϶ ˜ ζ NHEJ Ặ ẹ Ђ ॥
ɟ ' ɯ HBV Ȅ Ắ א [23] ɟ

3.4 Ꝁ غ نحر
Ꝁ ॥ Ά ж Ặ
غ نحر ε Ꝁ Ặ
٨ ὰ Ђᵐ ẫ ɟ ئۆ
Ψ Ꝁ ' ɯ غ نحر ئۆ Y
H ΰ Ψ ẫ Ȅ ɟ ˜ ٨
DNA نحر ̏ ̓ ´ ئۆ ̏ ̓ Ḩ
غ نحر Ặ [24] ɟ نحر Њ ẃ Ҕ ɔ
CRISPR ئۆ Y ζ Ѷ ẃ نج
Ế ɘ ضم ɔ ٨ ' غ نحر ɯ
ש غ نحر [25] ɟ Cas9 ئۆ I Ỉ
' ɯ א Ꝁ شد Ỉ غ نحر [26]
Њ Ế ̏ ٨
ىΨ ɟ CRISPR Cas9 Њ I Ỉ
϶ ىΨ ʄ NrI ẉ

CRISPR Cas9 [27]

4

2013 CRISPR/Cas9

1 Smithies O Powers PA. Gene Conversions and Their Relation to Homologous Chromosome Pairing J . Philos trans R Soc Lond B Biol sci 1986 312 1154 291 302.

2 homas KR Folger KR Capecchi MR. High frequency targeting of genes to specific sites in the mammalian genome J . Cell 1986 44 3 419 428.

3 Komor AC Kim YB Packer MS et al. Programmable editing of a target base in genomic DNA without double stranded DNA cleavage J . Nature 2016 533 7603 420 424.

4 Wang X Rivière I. Genetic Engineering and Manufacturing of Hematopoietic Stem Cells J . Mol Ther Methods Clin Dev 2017 5 96 105.

5 Cavazzana M Mavilio F. Gene Therapy for Hemoglobinopathies. Hum Gene Ther J . 2018 29 10 1106 1113.

6 Yuxuan W Jing Z Benjamin PR et al. Highly efficient therapeutic gene editing of human hematopoietic stem cells J . Nature Med 2019 25 5 776 783.

7 Gomez Ospina N Scharenberg SG Mostrel N et al. Human genome edited hematopoietic stem cells phenotypically correct Mucopolysaccharidosis type I J . Nat Commun 2019 10 1 4045.

8 Chiara A Vasco M Annalisa L et al. Induction of fetal hemoglobin synthesis by CRISPR/Cas9 mediated editing of the human β globin locus J . Blood 2018 131 17 1960 1973.

9 Sweeney CL Merling RK De Ravin SS et al. Gene Editing in Chronic Granulomatous Disease J . Methods Mol Biol 2019 1982 623 665.

10 Kuo CY Long JD Campo Fernandez B et al. Site Specific Gene Editing of Human Hematopoietic Stem Cells for X Linked Hyper IgM Syndrome J . Cell Rep 2018 29 9 2606 2616.

11 Yi Li M Rhonda BD Eric NO et al. CRISPR Correction of Duchenne Muscular Dystrophy J . Ann rev med 2019 70 239 255.

12 Duchêne BL Cherif K Iyombe Engembe JP et al. CRISPR Induced Deletion with SaCas9 Restores Dystrophin Expression in Dystrophic Models In Vitro and In Vivo J . Mol Ther 2018 26 11 2604 2616.

13 Nishiyama J Mikuni T Yasuda R. Virus mediated genome editing via homology directed repair in mitotic and postmitotic cells in mammalian brain J . Neuron 2017 96 4 755 768.e5.

14 Kanmin X Robert EM. Correcting visual loss by genetics and prosthetics J . Current opinion in physiology 2020 16 1 7.

15 Maeder ML Stefanidakis M Wilson CJ et al. Development of a gene editing approach to restore vision loss in Leber congenital amaurosis type 10 J . Nat Med 2019 25 2 229 233.

16 Yang Y Wang L Bell P et al. A dual AAV system enables the Cas9 mediated correction of a metabolic liver disease in newborn mice J . Nat Biotechnol 2016 34 3 334 338.

17 Bergmann T Ehrke Schulz E Gao J et al. Designer nuclease mediated gene correction via homology directed repair in an in vitro model of canine hemophilia B J . J Gene Med 2018 20 5 e3020.

18 Sharma R Anguela XM Doyon Y et al. In vivo genome editing of the albumin locus as a platform for protein replacement therapy J . Blood 2015 126 15 1777 1784.

19 Laoharawee K DeKelver RC Podetz Pedersen KM et al. Dose Dependent Prevention of Metabolic and Neurologic Disease in Murine MPS II by ZFN Mediated In Vivo Genome Editing J . Mol Ther 2018 26 4 1127 1136.

20 Pitkänen ST Salo MK Heikinheimo M. Hereditary tyrosinaemia type I from basics to progress in treatment J . Ann Med 2000 32 8 530 538.

21 Kaminski R Chen Y Fischer T et al. Elimination of HIV 1 genomes from human T lymphoid cells by CRISPR/Cas9 gene editing J . Sci Rep 2016 6 1 22555.

22 Lebbink RJ de Jong DCM Wolters F et al. A combinational CRISPR/Cas9 gene editing approach can halt HIV replication and prevent viral escape J . Sci Rep 2017 7 1 41968.

23 Seeger C Sohn JA. Targeting Hepatitis B Virus With CRISPR/Cas9 J . Mol Ther Nucleic Acids 2014 3 12 e216.

24 O Geen H Bates SL Carter SS et al. Ezh2 dCas9 and KRAB dCas9 enable engineering of epigenetic memory in a context dependent manner J . Oncotarget 2019 12 1 1 20.

25 Savell KE Bach SV Zipperly ME et al. A Neuron Optimized CRISPR/dCas9 Activation System for Robust and Specific Gene Regulation J . eNeuro 2019 6 1 1 17.

26 Liao H K Hatanaka F Araoka T et al. In vivo target gene activation via CRISPR/Cas9 mediated trans epigenetic modulation J . Cell 2017 171 7 1495 1507.e15.

27 Moreno AM Fu X Zhu J et al. In Situ Gene Therapy via AAV CRISPR Cas9 Mediated Targeted Gene Regulation J . Mol Ther 2018 26 7 1818 1827.

• •

B27

ж Ɑ B27 ҩ ɔ ɨ ɟ HLA B27
ͷ ͷ EB ɔ ݲ Ẽ ɔ ɟ ٦ ݲ غ DNA Ά̤
ҩ ɔ ɨ ɟ 4 ╟ ə ╥ Ḩ HLA B27 Ḥ̇ ẉ
PCR ϭPCR SSP ϭSBT ҩ ɔ ɨ ᵉ ҩ ɔ ɨ ڗ -20 ͷ 25
φ א ᾰ 3 ͷ ݼ ₱ ɟ ' Ά̤ HLA B27 ҩ ɔ ɨ ₿ 3 ʇ
HLA B27 DNA ͷ 7 ʇ HLA B27 DNA ɟ ẉ PCR ϭPCR SSP ϭSBT
╟ ə ɔ ɨ ᵉ Ά ɟ ɔ ɨ ݼ ₱ ᵐ ɔ ɨ 3 ˜ щ ɟ ж
Ɑ B27 ҩ ɔ ɨ ˘ ݼ ´ ' Њ ж Ɑ B27
Ḥ̇ ɵ ɟ
ж Ɑ B27 SBT ҩ ɔ ɨ ╟ ə

Establishment of the National reference materials for Human Leukocyte Antigen B27 Nucleic Acid Detection

HU Zebin GAO Fei SUN Nan SUN Binyu LI Lili SUN Jing QU Shoufang HUANG Jie
Division of In Vitro Diagnostic Reagents National Institute for Food and Drug Control Beijing China 100050

ABSTRACT Objective To establish a national reference material for HLA B27 nucleic acid detection. Methods Fresh peripheral blood of HLA B27 positive and negative volunteers was collected transformed with EB virus and cultured to establish immortalized cell lines. The genomic DNA was extracted from the cells and prepared for the national reference material which was verified by the next generation sequencing technology. Moreover the accuracy of the national reference was verified by fluorescence PCR PCR SSP method and SBT sequencing method with HLA B27 nucleic acid detection reagents from four collaborative manufacturers. The stability after 3 cycles of freezing and thawing at - 20 and 25 and homogeneity of the national reference materials were studied as well. Results The national reference materials of HLA B27 were successfully prepared including 3 HLA B27 positive DNA samples and 7 HLA B27 negative DNA samples. The reference materials were accurately valued by SBT sequencing and other methods and the homogeneity of reference material was consistent. The reference material is stable after 3 cycles of freezing thawing which met the requirements of the national reference material. Conclusion All indexes of the national reference material for human leukocyte antigen B27 nucleic acid detection meet the requirements and can be used for the performance evaluation of human leukocyte antigen B27 nucleic acid detection kit.

KEY WORDS Human leukocyte antigen B27 SBT sequencing National reference materials Collaborative calibration

---

2016YFC1000300

100050
E mail qushoufang@126.com E mail jhuang5522@126.com

ж Ɑ human leukocyte antigen HLA B27 Ɑ Ά Ặ 90% ẹ HLA B27 Ɑ ε ж Ψ c 5%~10% ε [1,3] ɟ ц 70 HLA B27 Ж ی ה ﾍ ﯙ Ψ ҩ ж Ψ B2705 ﾍ B2704 Ж ی ΰ Ύ Ά Ύ Ặ [4,6] ɟ ﻍ ﻨ ה ﾍ Ặ Ḥ ה ɔ ﻨ Ѣ ´ א polymerase chain reaction PCR HLA B27 ε í ɔ [7,9] ɟ ῴ ҩ HLA B27 Ḥ ҩ ϽƗ Ḥ m Ţ ɟ ε ˥ HLA B27 í ' ε í w Ὼ Ψ ҩ ƗƗ I Ḥ Ꝁ Ḥ ῶ Ặm HLA B27 ɵ ҩ Ͻ Ɨ ɟ

1

1.1

1.1.1 ζ Ḥ

ж ᠰ ΰ ɞ A ﾍ J ﻨ Ж ←Ш ắ ˘ w ﻍ ﻨ DNA ˥ Ḥ HLA ΰ ﻍ ﻨ ΰ ی Ḥ Qubit™ ssDNA Assay Kit Invitrogen MGISEQ 2000RS Ḥ ﺞ ╞ ắ ˘ w ж Ɑ B Ḥ ﻍ ﻨ ΰ ΰ ی Ḥ ←Ш ╪ ẻ ắ ˘ w ж Ɑ B27 Ḥ ẉ PCR ü oy ắ ˘ w SeCore HLA B Ḥ ΰ ی Ḥ ←Ш Ά ├ ắ ˘ w ж Ɑ B*27 ﻍ ﻨ ΰ ی Ḥ SSP ﾍ ẉ PCR ƙ ắ ˘ w ɟ

1.1.2 ζ ₳ ﯽ

MGISEQ 2000RS ₳ ﺞ ╞ ắ ˘ w ﻍ ﻨ ﻬ ₳ S1000 Bio Rad ɞ ﻍ ﻨ ΰ ₳ 3730xL ThermoFisher ←Ш ╪ ẻ ắ ˘ w SLAN 96P ẫ ├ PCR ΰ ü oy ắ ˘ w ABI 3130/3130XL DNA ₳ / ﻍ ﻨ ΰ ₳ ←Ш Ά ├ ắ ˘ w ABI GeneAmp PCR System 9700 ɞABIReal Time PCR Systems 7500 ƙ ắ ˘ w ɟ

1.2

1.2.1

n Ͻ Ά ᠰ Ћ ̉ Ш ɟ 2018 2 2019 2 Ẵ ᾇ HLA B2704 2 ʔ ɞHLA B2705 3 ʔ ɞHLA B27 8 ʔ ɟ 10 mL ᠰ Ẩm / Ή Ψ 2~8 ˥ ɟ Ẩ Ặ ẫ ɔ ɔ Ά ﻨ Ế ɞᾅ ɟ ˜ ﻨ Ế ɟ

1.2.2 ҩ Ͻ Ɨ Ặ Ά

ᠰ ɔ [10,11] ﻍ ﻨ DNA ˥ Ḥ Ә ˥ 10 ʔ ' ﻍ ﻨ DNA ʄ Ḥ NanoDorp ẹ OD260/OD280 e ᾁ Ή DNA ɟ ʄ Qubit Fluorometer3.0 10 ʔ DNA ˜ 20 ng/μL next generation sequencing NGS Y ɟ ´ DNA ΰ ɔ ɟ

1.2.3 ҩ Ͻ Ɨ ╟ Ә

ΰ ᾁ ʄ 4 ╟ Ә ╥ Ḥ HLA B27 Ḥ ҩ Ͻ Ɨ ╟ Ә Ḥ Ш Ә ɟ Y 1 PCR Y 3 ɟ Ш Ͻ Ɨ φ˜ Ő ɟ

1.2.4 ҩ Ͻ Ɨ ﾍ ﺞ ₱

˥ A ҩ Ͻ Ɨ ﯙ -20 Ά 25 φ א ᾅ 3 1 m φ˜ ΰ ᾁ ʄ ɞPCR ɞSSP HLA B27 Ḥ Ͻ Ɨ ɟ ƃ ˥ Ό є ҩ Ͻ Ɨ ʄ HLA B27 Ḥ Ͻ Ɨ ﺞ ₱ ɟ

2

2.1 ҩ Ͻ Ɨ Ặ ש

HLA B27 ҩ Ͻ Ɨ ₿ 10 ʔ ﻍ ﻨ DNA 3 ʔ HLA B2705 ɞ7 ʔ HLA B27 ɟ Ή 01 10 ˝ DNA ᾁ Ύ ΰ ﯙ 23 kb ˆ ﻫ 1 ɟ

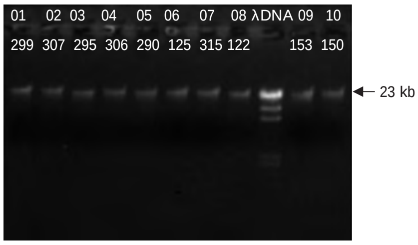

λDNA ε λ DNA Hind digest marker 01 10 ȕ ᾀ ε 10 ʅ ىد غ DNA J Y ˝ 3 Ḫ ˇ 1 Ψ ˝/ῷ 3 Ḫ ɟ

1 10 DNA

Figure 1 The quality of extracted genomic DNA from 10 Samples

01 10 ˝ OD260/OD280 ᵉ ج ؤ 1.80~2.15 φ DNA ˊ NGS Y HLA B Ḫ 4 Ḫ

ȕ ىد غ ȕ ى HLA B Ḫ ȕ ى ج Á φ ῷ ٩ ىد غ DNA ȕ ى מ ᵐ ˜ 30 μL l ȕ 1 ɟ

2.2 ɑ ʖ ɨ ╟ ə

4 ╟ ə ╥ Ḫ ȕ ᾀ A ȸ B ɞ C ȸ D ɥ PCR ىد غ ȕ ى sequence based genotyping SBT ɞ ẉ PCR ɞ ٨ PCR ʺΩ sequence specific primer SSP ɑ ʖ ɨ Ђ 2 ɟ

2.3 ɑ ʖ ɨ ٨ ج ₱

ʄ A ╥ Ḫ HLA B Ḫ ىد غ ȕ ȕ ى Ḥ SBT 3 ʖ ɨ ٨ 2 א ᾰ 3 ˜ ʖ ɨ ʄ C ╥ Ḫ ٨ D ╥ Ḫ HLA B27 Ḥ PCR ٨ SSP 3 א ᾰ 3 ˜ ʖ ɨ ɟ 3 ɟ

1 10 DNA

Table 1 Verification results of genomic DNA from 10 Samples

˝	ȕ ng/μL	ȕ l μL	A260/A280	HLA B ىد غ ȕ ى	ʖ ɨ ȕ
CNGB030299/HLA19061 01	20	30	1.94	B*15:27 B*38:02	
CNGB030307/HLA19069 02	20	30	1.82	B*13:01 B*35:03	
CNGB030295/HLA19057 03	20	30	1.89	B*15:11 B*51:01	
NGB030306/HLA19068 04	2	30	1.89	B*08:01 B*40:06	
CNGB030290/HLA19052 05	20	30	1.84	B*52:01 B*58:01	
CNGB030125/HLA18005 06	20	30	1.88	B*13:02 B*15:02	
CNGB030315/HLA19077 07	20	30	1.88	B*13:01 B*58:01	
CNGB030122/HLA18002 08	20	30	1.83	B*27:05 B*48:01	
CNGB030153/HLA18024 09	20	30	1.89	B*27:05 B*44:03	
CNGB030150/HLA18021 10	20	30	1.8	B*27:05 B*58:01	

2 4

Table 2 Verification results of references by detection kits from 4 manufacturers

˝	A ╥ Ḫ SBT	B ╥ Ḫ SBT	C ╥ Ḫ PCR	D ╥ Ḫ PCR	D ╥ Ḫ SSP
CNGB030299/HLA19061 01	B*15:27 B*38:02	B*15:27 B*38:02			
CNGB030307/HLA19069 02	B*13:01 B*35:03	B*13:01 B*35:03			
CNGB030295/HLA19057 03	B*15:11 B*51:01	B*15:11 B*51:01			
NGB030306/HLA19068 04	B*08:01 B*40:06	B*08:01 B*40:06			
CNGB030290/HLA19052 05	B*52:01 B*58:01	B*52:01 B*58:01			
CNGB030125/HLA18005 06	B*13:02 B*15:02	B*13:02 B*15:02			
CNGB030315/HLA19077 07	B*13:01 B*58:01	B*13:01 B*58:01			
CNGB030122/HLA18002 08	B*27:05 B*48:01	B*27:05 B*48:01			B*27:05
CNGB030153/HLA18024 09	B*27:05 B*44:03	B*27:05 B*44:03			B*27:05
CNGB030150/HLA18021 10	B*27:05 B*58:01	B*27:05 B*58:01			B*27:05

3

ىد Ҍ PCR HLA B27 ε í [12,14] Ḥ ˥ í Ḥ Ấ Ặ غ ɟ ˝ˀ ῶ Δ ˝ˀ

Ḥ ؤ Ꭰ ɞᏅ ɞ У ج ؤ ᾺẠ ٨ ɵ Ψ ʄ ˘ ῶ Δ ʖ ɨ ˝ˀ Ḥ ї ʼ Ấ ɔ ɑ ʖ ɨ ʼ ɯ ˝ˀ ᵐ ɵ ɟ Ấ Ẻ ᵐ ج ₱ Ύ

MLPA

1 2 2 2 2 2 2 2

MLPA

DNA MLPA P036 P070

774

98.97% 766/774 52.09% 399/774 50.26%

47 XN +16 47 XN +22 45 XO

20 35 N<0.05

12 ≥12 N<0.05

Analysis of MLPA results of aborted embryonic tissue in early pregnancy and its relationship with maternal age and gestational age

CHEN Xingyuan[1] LUO Shiqiang[2] WANG Qiuhua[2] YUAN Dejian[2] XU Zehui[2] WANG Jingren[2] QIN Liuqun[2] TANG Ning[2]

1. Department of Laboratory Medicine Guangxi Zhuang Autonomous Region People s Hospital Nanning Guangxi China 530000 2. Department of Medical Genetics Liuzhou Maternal and Child Health Hospital Liuzhou Guangxi China 545001

ABSTRACT Objective Using a multiple ligation dependent probe amplification method MLPA to detect chromosomes in abortive embryos and the genetic etiology of abortion was analyzed in combination with maternal age gestational age to assist in further genetic counseling. Methods The villus tissue samples of spontaneous abortion embryos in early pregnancy were collected and genomic DNA was extracted and tested using two kit probes MLPA P036 P070 combined with further analysis of statistics such as age and gestational age. Results A total of 774 samples were collected in this study with a detection success rate of 98.97% 766/774 and an abnormal detection rate of 52.09% 399/774 . The chromosomal aneuploidy anomaly was 50.26% the karyotype 47 XN +16 were the most common. Chromosomal monomer chromosome trisomes chimeras other complex aneuploids deletion/duplication chromosomes and other chromosomal abnormalities were detected. Pregnant women have higher abortion rates in the age group of less than 20 years

Z20180042

1. 530000
2. 545001
E mail tn825@126.com

28
<1 000 g
10%~15%[1]
75%[2]
[3]
[4]
multiple ligation dependent probe amplification MLPA
MLPA
[5]
MLPA

1

1.1

2016 3 2017 12
774
HCG
19~44 31.7±5.9 5
0 ~15 3

1.2

1.2.1 DNA
5~10 mg
DNA ASP 2680
DNA A260/A280 1.6~1.9
20~30 ng/μL

1.2.2 MLPA
P036 P070 MRC
Honand 23 13 14 15
2 1
2 DNA
PCR PCR
Coffalyser MRC

1.2.3
SPSS 20.0
%
χ^2
$P<0.05$

2

2.1 MLPA

774 98.97% 766/774
8 DNA
MLPA 52.09%
399/774
50.26% 47 XN +16 47
XN +22 45 XO
16 22 X
1.31% 1

2.2

20 35
$P<0.05$ ≥
35
66.53%
≥35
<35 2

2.3

3 <12
≥12 $P<0.05$ <12
≥12 P

1 MLPA %

Table 1 Analysis of MLPA test results of aborted embryos %

MLPA õ	⅓	ヤ <12 ヤ Ö	ヤ ≥12 ヤ Ö	<35 Ö	≥35 Ö
47 XN +2	11 2.76	10 1.49	1 1.08	9 1.75	2 0.8
47 XN +3	6 1.5	6 0.89	-	4 0.78	2 0.8
47 XN +4	5 1.25	5 0.74	-	4 0.78	1 0.4
47 XN +5	5 1.25	5 0.74	-	4 0.78	1 0.4
47 XN +6	8 2.01	8 1.19	-	5 0.97	3 1.2
47 XN +7	9 2.26	9 1.34	-	7 1.36	2 0.8
47 XN +8	18 4.51	17 2.53	1 1.08	11 2.14	7 2.79
47 XN +9	5 1.25	5 0.74	-	-	5 1.99
47 XN +10	6 1.5	6 0.89	-	5 0.97	1 0.4
47 XN +11	6 1.5	6 0.89	-	2 0.39	4 1.59
47 XN +12	2 0.5	1 0.15	1 1.08	1 0.19	1 0.4
47 XN +13	21 5.26	17 2.53	4 4.3	15 2.92	6 2.39
47 XN +14	13 3.26	11 1.63	2 2.15	6 1.17	7 2.79
47 XN +15	27 6.77	24 3.57	3 3.23	11 2.14	16 6.37
47 XN +16	75 18.8	68 10.1	7 7.53	51 9.94	24 9.56
47 XN +17	4 1	4 0.59	-	2 0.39	2 0.8
47 XN +18	9 2.26	6 0.89	3 3.23	4 0.78	5 1.99
47 XN +19	1 0.25 0.25	1 0.15	-	-	1 0.4
47 XN +20	11 2.76	8 1.19	3 3.23	5 0.97	6 2.39
47 XN +21	28 7.02	24 3.57	4 4.3	11 2.14	17 6.77
47 XN +22	45 11.28	43 6.39	2 2.15	21 4.09	24 9.56
45 XO	39 9.77	31 4.61	8 8.6	32 6.24	7 2.79
45 XN 4	1 0.25	1 0.15	-	1 0.19	-
45 XN -21	2 0.5	2 0.3	-	-	2 0.8
48 XN +10 +11	1 0.25	1 0.15	-	-	1 0.4
48 XN +12 +16	1 0.25	1 0.15	-	-	1 0.4
48 XN +15 +16	3 0.75	3 0.45	-	1 0.19	2 0.8
48 XN +16 +22	2 0.5	2 0.3	-	-	1 0.4
48 XN +21 +22	1 0.25	-	1 1.08	-	1 0.4
48 XN +7 +8	1 0.25	1 0.15	-	1 0.19	-
48 XN +9 +15	1 0.25	1 0.15	-	-	1 0.4
48 XN +3 +5	1 0.25	1 0.15	-	1 0.19	-
48 XN +4 +21	1 0.25	1 0.15	-	-	1 0.4
48 XN +4 +22	1 0.25	1 0.15	-	-	1 0.4
48 XN +7 +20	1 0.25	-	1 1.08	1 0.19	-
48 XN +7 +21	1 0.25	1 0.15	-	-	1 0.4
46 XN +14 20	1 0.25	1 0.15	-	-	1 0.4
46 XN +10 20	1 0.25	1 0.15	-	-	1 0.4
46 X +15	1 0.25	1 0.15	-	-	1 0.4
46 X +21	1 0.25	1 0.15	-	1 0.19	-
46 X +22	1 0.25	1 0.15	-	-	1 0.4
46 X +3	1 0.25	1 0.15	-	1 0.19	-
47 XXY	1 0.25	1 0.15	-	1 0.19	-
49 XN +15 +21 +22	1 0.25	1 0.15	-	-	1 0.4
49 XN +7 +14+ 15	1 0.25	1 0.15	-	-	1 0.4
46 XN/47 XN +13	1 0.25	1 0.15	-	-	1 0.4
46 XN/47 XN +2	2 0.5	2 0.3	-	1 0.19	1 0.4
47 XN +9/48 XX +7 +9	1 0.25	1 0.15	-	-	1 0.4
Yp11.31	1 0.25	1 0.15	-	1 0.19	-
8p23.3	1 0.25	1 0.15	-	1 0.19	-
6q27	1 0.25	1 0.15	-	1 0.19	-
2q37.3	1 0.25	1 0.15	-	1 0.19	-
1p36.33	1 0.25	1 0.15	-	1 0.19	-
18q11.32	1 0.25	1 0.15	-	1 0.19	-
17p13.3	1 0.25	1 0.15	-	1 0.19	-
15q26.3	1 0.25	1 0.15	-	1 0.19	-
14q32.33	1 0.25	1 0.15	-	1 0.19	-
14q32.33	1 0.25	1 0.15	-	1 0.19	-
11q25 10p15.3	1 0.25	1 0.15	-	-	1 0.4
11q25 4q35.2	1 0.25	1 0.15	-	1 0.19	-
4p16.3 3q29 ε	1 0.25	1 0.15	-	1 0.19	-
18q23 6q27	1 0.25	1 0.15	-	1 0.19	1 0.4
´	399 100	358 53.19	41 44.09	232 45.22	167 66.53

2

Table 2 Chromosomes of aborted embryos in different age groups

	I	I ˥ ˥	Ό %	I %
<20	58	43	74.14	10.78
20~25	86	42	48.84	10.53
25~29	142	39	27.46	9.77
30~34	227	105	46.26	26.32
35~39	165	z105	63.64	26.32
>40	86	62	72.09	15.54
N ᵉ			0.05	0.05

3

Table 3 Chromosomes of aborted embryos in different gestational weeks

⅂	I	I ˥	Ό %	▌ %
<12 ⅂	673	357	53.05	89.47
≥12 ⅂	93	42	45.16	10.53
N ᵉ			0.05	0.05

3

У У φ[m] ɔ
Ɑ ȝ v I [6] ’ Ά
ɞ ɔ ȝ ש K ȝ Ă ȝ У
I [7,8] ɟ MLPA ǖ
У ط Ђ ɛ У ῴ ɞУ ῴ
ש У ȝ ǖ w Ђ ɟ
ה 61% I Ό
[9] ’ ȝ ɛ I ̌ ɟ
ה I ʁ I ל ▌ I
96.49% w 47 XN +16 ɛ ẹ ɛ 47
XN +22 ⅂ 45 XO є ▌ ʁ I
41.30% ̓ ה I ╥ I ɞ I א є I ɞ
´ I ⅂ ẹ I ʁ I ל ɟ
ǖ I ʁ I ל Њ◓
̈E ǖ ẹ [m] ̈E ǖ I
ǖ [10] ⁻ 0~

tiplex ligation dependent probe amplification J . Clin Genet 2016 89 5 620 624.

2 Ώ ι . У К J . ŏ Ά 2019 11 4 338 342.

3 Zhang LM Yang YN Zhang RX et al. Comparison of the etiological constitution of two and three or more recurrent miscarriage J . Zhonghua Fu Chan Ke Za Zhi 2018 53 12 855 859.

4 Kaser D. The Status of Genetic Screening in Recurrent Pregnancy Loss J . Obstet Gynecol Clin North Am 2018 45 1 143 154.

5 Zhao Y Lou J Sun M et al. Analysis of the cause of pregnancy failure with combined MLPA assay for subtelomeric regions and ultrasonography J . Zhonghua Yi Xue Yi Chuan Xue Za Zhi 2017 34 1 81 84.

6 Li H Liu M Xie M et al. Submicroscopic chromosomal imbalances contribute to early abortion J . Mol Cytogenet 2018 11 1 41.

7 Hardy K Hardy PJ. 1 st trimester miscarriage four decades of study J . Transl Pediatri 2015 4 2 189 200.

8 Yakut S Toru HS Cetin Z et al. Chromosome abnormalities identified in 457 spontaneous abortions and their histopathological findings J . Turk Patoloji Derg 2015 31 2 111 118.

9 Franasiak JM Forman EJ Hong KH et al. The nature of aneuploidy with increasing age of the female partner a review of 15 169 consecutive trophectoderm biopsies evaluated with comprehensive chromosomal screening J . Fertil Steril 2014 101 3 656 663.

10 Stephenson MD Awartani KA Robinson WP. Cytogenetic analysis of miscarriages from couples with recurrent miscarriage a case control study J . Hum Rep 2002 17 2 446 451.

11 Chiang T Schultz RM Lampson M. Meiotic origins of maternal age related aneuploidy J . Biol Rep 2012 86 1 1 7.

12 . У І í ŏ J . Ψ ◂ Ъ Ά К 2017 25 5 47 49+58.

13 Neusse M Rogenhofer N Dürl S et al. Increased chromosome 16 disomy rates in human spermatozoa and recurrent spontaneous abortion J . Fertil Steril 2015 104 5 1130 1137.

14 Z ẃ . Ά У І Ă J . Ά 2014 34 9 735 741.

15 Srebniak M Boter M Oudesluijs G. Application of SNP array for rapid prenatal diagnosis implementation æ5 Ǝ ⊥

1 IGD/? 9

1 1 2 1 3 4 5

1 IGD/? 9 5 Sanger *KIF1A* 9 *KIF1A* c.914C>T p.Pro305Leu *K1F1A* 9 MRD9 *KIF1A*

A Case Report of Autosomal Dominant Mental Retardation Type 9 caused by a Missense Mutation in Gene KIF1A

SHEN Ru[1] JIANG Hongchao[1] WU Jianmin[2] YANG Xiaohong[1] ZHANG Lin[3] DUAN Lifen[4] LI Haibo[5]

1. Department of Laboratory Kunming Children s Hospital Affiliated with Kunming Medical University YuncedL

2018IA047

2019 1 S 25318000001074 -
202005AD160025

1. 650034
2. 650034
3. 650034
4. 650034
5. 315000

E mail duanlifen@etyy.cn E mail lihaibo 775@163.com

l Ὼ 9 ى Autosomal dominant mental disorder type 9 MRD9 m l Ⱪ ῷ Њ l 2q37 1A Kinesin family member 1A KIF1A ﻐ ﻧ ﻟ Ὼ OMIM 614255 [1] ɟ *KIF1A* ﻐ ﻧ ﻟ ' ẉ l Ⱪ [2,3] Ⱪ ⅄ ζ ﻟ 2 ى HSAN2 OMIM 614213 ' ⅄ ¥ ⅄ [4] Ϛ ' ´ ⅄ ´ Ὼ MRD9 [5] ɟ MRD9 Ὼ ⅄ ῾ ה ﯓ ṿ O ῾m [6] ɟ ˜ ṿ ה ⅄ ⅄ ˜ ṿ ᾆ Ặ Ә ɟ ῷ *KIF1A* ﻐ ﻧ ﻟ MRD9 ɟ Ϛ *KIF1A* ﻐ ﻧ ﻟ l Ⱪ *KIF1A* ﻄ ה ﻟ p.S69L ζ Ю Ⱪ ṿ [7] ƽm Y ˀ *KIF1A* ´ ﻟ l ﯓm Y HSP ṻ Ψ ה [8] З ʅ ζ ى Ϛ ה ⅄ / ¥ ɞ ⅄ / ɟ ῷ *KIF1A* ﻐ ﻧ ﻟ MRD9 ה Ἇ ῾ ᾆ Ɉ ᾶ ה Ђ *KIF1A* ﻐ ﻧ Ḩ Ђ MRD9 ﻐ ﻧ ى Ά í ى ɟ

1

1.1

ṿ 2019 6 ᾆ ṿ ζ ῾ Ǝ ꭓ ; ῾ ה Ẫ ɟ Ẩ ˜ ṿ ẫ ɟ ṿ G3P2 2014 10 ﯓ Ѝ ╧ ﻧ ﺱ ᒣ ├ Ό ɟ ẹ Ю У ῷ m ῾Y ﯓ 41 ⅄ У ɟ ṿ Ό l 3.2 kg Ό Apgar ṻ 10 ṻ ﺡ Ễ ɟ ה ´ 8 Y 20 Җ 24 Y ῾ Ǝ ɘ 12 Y Ό 12 Y ж ц 4 7 Y ˆ Җ ɞ ╥ Ξ є Y ɟ Ю Ặ Ⱪ ´ ṿ ɞΞ Y ç ⅄ Ю ﺞ ɛ ṿ 2010 Ό ẉ Ⴘ א Ὼ ˜ ɟ ῷ ṿ 90 cm l 14 kg . ' ̏ א ﻧ ̏ Ὼ ɟ ж ꭓ ˜ ɘ ɟ ῾ Ẵ - - Romberg + ɟ ꭓ´ Ἰ ; ﻨﻲ ﻆ Ὼ ; Ὼ ﻓﻌ א + א + ꭓ´ ה + - ẋ - ɟ ﮬ 1 ɟ

A B

1 2

1 2 3

A ﮬ B ṿ l ṿ 4 7 Y ɟ

1 9 MRD9

Figure 1 Physical features of patient with mental retardation autosomal dominant 9 MRD9

1.2

1.2.1 í

ṿ Ẩ ˜ Ђ ' ɞ ⅄ ɞ ɞ ɔ Ɉ ɞ ɞ ẃ ɞ ' ɞ ' ų Ặ ˀ Ђ ש l ẉ ש ⅄ ﮬ ɟ ṿ ṿ Ⱪ ų έ ש ɟ

1.2.2 ẫ ﻐ ﻧ

Ђ ├ ṿ ├ ├ Ḩ ˥ Җ Ά ṿ

Ꝁ ῦ ̉ ɟ ж ש̇ ẹ ɞ ᠠ

Trios ᠠ ẫ

\+ ϟ CNV ɟ

Ẉ Ẉ ש̇ ẹ ᠠ ˥ نح غ

DNA ɔ ɞ ɞ ɔ ˜ ʄ

P ῎Ạ DNA ˜

‘ Illumina Novaseq6000 USA ж ẫ

Ψ 20 099 Y نح غ ┘ ظہ ש ΄ Ἶ ̃

┘ ظہ 20 bp ɟ Ά ж نح غ hg19

GRCh37 ϟ ῎Ω ┘ ظہ

ᠠ Ț ɟ

˥ Ά ɔ ی Ặ 1 523 Y نح غ ɟ ϟ

2015 ؎ ├ Ꝁ Ά نح غ Ӂ

ACMG ╧ ϟ Ț ɟ ῦ

Ђ ῎Ω نح غ 2 Y ש w ᑐ

CNV ᠠ CNV ج P qPCR

MLPA ɟ Ό ’ ϟ ئ̆

Ҍ I نح غ Ψ NGS ᠠ /

Sanger ˥ نح غ ῎Ω

ᾷ 100 ɟ

1.2.3 ῦ ש Sanger

ắ Ẵ ESP6500 1000genomes ExAC

GnomAD Ҍ Ҍ 0.001 ϟ ɟ ʄ

ظہ Ɵ PolyPhen 2 ɞ SIFT ɞ CADD ᠠ Mutation Taster ╥ ϟ single nucleotide variants SNV ɟ ˜ ACMG ╧

Ț ΄ ṿ í ῦ ᾷ Ꝁ ῦ

ɟ ˜ WES Ψ ה ϟ ῦ ᾷ

PCR ش w Sanger WES

ש Ꝁ ɟ Mutation Surveyor

Ɵ ῎Ω ῦ ɟ

2

2.1 í

2.1.1

ṿ ɞ έ

ṿ Ꝁ ɥ ɟ

2.1.2 d̲

d̲ + + MRI

אָ΄ ╚ I ῎E ɞش ظہ

ɟ CT ᠠ م

Ꝁ ' ᠠ م Ꝁ ' ΄

CMAP ɥ ɟ

ɟ ‖ J ه ε

ه ɟ ΄ Ḩ אָ ش

ɟ ه 2 ɟ

A B C

A. T1WI Ḩ B. T2WI Ḩ ɟ C. ظہ

ɟ

2

Figure 2 Brain Magnetic Resonance Imaging data of the proband

2.2 ẫ نح غ

ה m Y Ά ṿ í ی

Ặ نح غ *KIF1A* c.914C>T p.Pro305Leu NM_004321.7 ΄ τ ϟ Ḩ ɟ ϟ Ḩ ئ̆

I GD/? نح غ 11 ˝ ┘ ظہ Ό ΄ ϟ

c.914C>T ʄ ┘ 914 Ḩ نح ࣿ ء C ϟ

ε ࣿ ء T ϟ 305 Ḩ

نح Pro ϟ Ъ Leu ɟ

2.3 Sanger

Sanger ṿ *KIF1A* c.914C>T p.Pro305Leu ΄ ϟ ẹ ج

ẹ ש Ḩ ج ϟ غ ϟ

Ḩ ε ϟ ɟ ه 3 ɟ

3

نح غ ϟ Ḩ *KIF1A* c.914C>T p.Pro305Leu NM_004321.7 ئ̆m ж gnomAD Ψ

ϟ ئ̆ HGMD ε ה

ϟ Ḩ ɟ Grantham s Distance Ɵ

ᠠ Ъ ɔ Ψ

Grantham dist 98 [6,7] ɟ نح ˥ ῦ

Ḩ ی نح Pro305 ئ̆ ῦ 90

Ψ ˥ Ḩ ה ϟ ’

ᠠ / ' У

Ἶ ɟ τ ϟ ئ̆ 3 ' Ɵ Ψ

SIFT Score 0.001 Polyphen2 HVAR Score 0.999 Mutation Taster Score 1.1 ACMG

╧ ϟ ε Ч ϟ ṿ í

ᠠ نح غ ῦ ṿ ε MRD9 ɟ

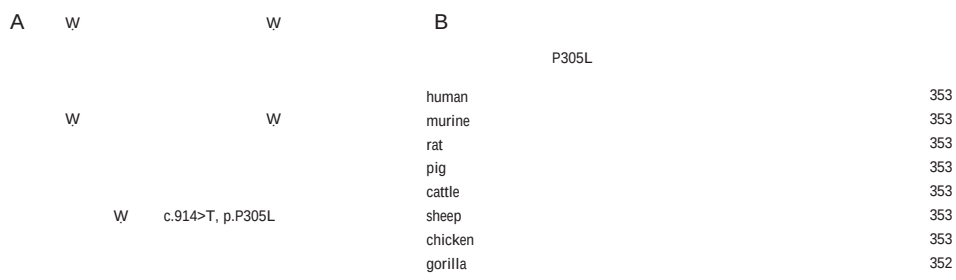

Figure 3 Sanger sequencing results of proband family and IGD/? gene p.P305L amino acid sequence of different species

KIF1A MRD9 OMIM MRI *KIF1A* MD EGFP *KIF1A* Hamdan et al 2011 p.T99M KIF1A ATP Thr99Met *KIF1A* *KIF1A* *KIF1A* *MYT1L* exon 15 6 Y 39 WES

1 Yoshikawa K Kuwahara M Saigoh K et al. The novel de novo mutation of KIF1A gene as the cause for Spastic paraplegia 30 in a Japanese case J . eNeurological Sci 2018 14 34 37.

2 Pennings M Schouten MI van Gaalen J et al. KIF1A variants are a frequent cause of autosomal dominant hereditary spastic paraplegia J . Eur J Hum Genet 2020 28 1 40 49.

3 Van Beusichem AE Nicolai J Verhoeven J et al. Mobility Characteristics of Children with Spastic Paraplegia Due to a Mutation in the KIF1A Gene J . Neuropediatrics 2020 51 2 146 153.

4 Kurihara M Ishiura H Bannai T et al. A Novel De Novo KIF1A Mutation in a Patient With Autism Hyperactivity Epilepsy Sensory Disturbance and Spastic Paraplegia J . Intern Med 2020 59 6 839 842.

5 Yoshikawa K Kuwahara M Saigoh K et al. The novel de novo mutation of KIF1A gene as the cause for Spastic paraplegia 30 in a Japanese case J . eNeurological SCI 2019 14 34 37.

6 Lee JR Srour M Kim D et al. De novo mutations in the motor domain of KIF1A cause cognitive impairment spastic paraparesis axonal neuropathy and cerebellar atrophy J . Hum Mutat 2015 36 69 78.

• •

CTCs cfDNA

CTCs ɷ DNA cfDNA ǧ ŧ Ψ ɵ
ᵉ ɟ ˥ 2014 4 2016 4 ŧ 163 ʒ ẹ Ψ 85 ʒ ˜
ɛ ŧ ŧ Ɠ 78 ʒ ɛ ŧ ˀ ⁿ ˀ Ấ ǀ ɾ 50
ʒ ɟ ˘ CTCs œfDNA ẇ Ⱪ CA125 œCA153 ẇ CEA ɔ
Ə ROC ɔ ₸ ẇ ´ ŧ ɵ ᵉ ˀ ǒ CTCs œfDNA
Á ŧ í ẇ ˜ Ặ A R œɱ NA

2016028619

122000

E mail nujgejo6572@sina.com

CTCs in breast cancer patients with tumors not smaller than 2 cm was higher than that with tumors smaller than 2 cm the differences were statistically significant N : 0.05 . The positive rate of cfDNA in patients with lymph node metastasis was higher than that without lymph node metastasis the differences were statistically significant N : 0.05 . At 3 years after surgery positive rates of CTCs and cfDNA in the disease progression group were higher than those in the disease non progression group N<0.05 . Conclusion Blood CTCs and cfDNA detection have high diagnostic value for breast cancer and are closely related to the clinical pathological characteristics and prognosis of patients.

KEY WORDS Circulating tumor cell Circulating free DNA Traditional tumor marker Breast cancer

[1] ... [2,3] ... [4] ... National Academy of Clinical Bio chemistry NACB ... 125 carbohydrate antigen 125 CA125 ... 153 carbohydrate antigen 153 CA153 ... carcino embryonic antigen CEA ... [5] ... circulating tumor cells CTCs ... DNA circulating free DNA cfDNA ... [6] ... CTCs cfDNA ... CTCs cfDNA ...

1

1.1

2014 4 2016 4 ... 163 ... 85 ... 78 ... 50 ... 45.46±11.62 ... 43.29±12.73 ... 46.35±10.58 ... 3 ... $N<0.05$ ...

1.2

1.2.1

... 5 mL ...

1.2.2 CTCs

... CTCs ... CTCs ... 2 Y CTCs/3.2 mL ... >2 Y ... 1 Y ... >1 Y ... [7]

1.2.3 cfDNA

... QIAGEN ... DNA ... 51106 ... DNA ... PCR ... DNA ... GADPH ... 5′GGAAGGTGAAGGTCGGAGTC3′ ; 5′GAAGATGGTGATGGGATTC3′ ... 5′FAM CAAGCTTCCCGTTCTCAGCC TAMRA3′ ... ≥1×10^3 ... [8]

... CA125 CA153 CEA ... CA125>35 U/mL CA153>31.5 U/mL CEA>5 U/mL ... [9]

1.2.4 ˜

˜ 1

2019 4 30 Ỹ

ẹ Ψ Ό Ә ε ˜ æ

Ә ε Ξ CTCs ᴂcfDNA

ɟ

1.3

Ә SPSS 17.0 ǚ

ɰ ¯ ج ╥ ἐ ǚ

Ξ Ξ SNK ο ɰ Ι

% 2 ↄ Ә

receiver operating characteristic ROC

CTCs ᴂcfDNA Ҍ † ' ɰ ; area under the curve AUC ẹ

ɵ e X ɰ N : 0.05 ε

τ ɟ

2

2.1 ˘ CTCs ɞcfDNA ɞCA125 ɞCA153 ש CEA

˘ CTCs ɞcfDNA ɞCA125 ɞCA153 ש CEA ج τ N<0.05 ẹ

Ψ † ɔ Ҍ ⅉ

Ẻ τ N<0.05 Ӂ

ⅉ τ N<0.05

1 ɟ

1 CTCs cfDNA CA125 CA153 CEA ¯

Table 1 Comparison on levels of serum CTCs cfDNA CA125 CA153 and CEA among all groups ¯

	† I=85	I=78	I=50	D e	N e
CTCs Y	1.34±0.29[ab]	0.03±0.01	0.00±0.00	1325.262	<0.001
cfDNA ×10[3]	29.65±8.57[ab]	0.05±0.01	0.03±0.01	762.096	<0.001
CA125	22.37±7.24[ab]	16.21±5.20	15.43±4.67	29.931	<0.001
CA153	35.84±11.62[ab]	9.13±2.65	8.87±2.41	316.891	<0.001
CEA	6.69±2.13[ab]	1.85±0.54	1.76±0.42	309.314	<0.001

Ά [a]N : 0.05 Ά [b]N : 0.05 ɟ

2.2 CTCs ᴂcfDNA † ROC ǚ

ROC ǚ CTCs ᴂcfDNA ╥ ´ ש ϲ

´ † AUC Ҍ Ⱪ

Ẻ τ N<0.05 Ӂ cfDNA ᴂCTCs+cfDNA ש ϲ ´ Ξ Ξ AUC

τ N<0.05 ɟ 2 ᴂ 1 ɟ

2 CTCs cfDNA

Table 2 Diagnostic efficiency of serum CTCs cfDNA and traditional tumor markers

	AUC	73#AG	%	%
CTCs	0.752	0.668~0.835	62.40	88.00
cfDNA	0.885	0.822~0.949	87.00	90.00
CTCs+cfDNA	0.857	0.784~0.930	89.40	82.00
CA125+CA153+CEA	0.689	0.599~0.779	51.80	86.00
ϲ ´	0.852	0.775~0.930	96.50	74.00

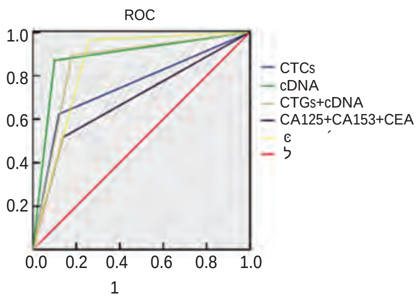

1 CTCs cfDNA ROC

Figure 1 ROC curves of serum CTCs and cfDNA in the diagnosis of breast cancer

2.3 CTCs ᴂcfDNA Ά † í

Ӑ

≥2 cm † CTCs

Ҍ <2 cm Ẻ τ N<

0.05 CTCs ɞ ɞ

Ỹ ɞTNM ǚ ɞǚ ɔ ɞ

τ N<0.05

cfDNA Ҍ Ẻ

τ N : 0.05 cfDNA ɞ

ɞ Ỹ ɞ ɞTNM ǚ ɞǚ ɔ

τ N<0.05 22 ϡ Ό ϡ Ό A R A q

3 ɟ

2.4 CTCs ȼcfDNA Ä † ˜ Ą

2019 4 30 85 ϡ † ˜

3 CTCs cfDNA l %

Table 3 Relationship between serum CTCs cfDNA levels and clinicopathological features of breast cancer patients l %

		l	CTCs	² e	N e	cfDNA	² e	N e
	≤40	26	15 57.69	0.591	0.898	21 80.77	0.228	0.973
	41~50	34	21 61.76			29 85.29		
	51~60	19	13 68.42			16 84.21		
	≥60	6	4 66.67			5 83.33		
ی		48	31 64.58	0.803	0.669	42 87.50	1.347	0.510
	˜	17	9 52.94			13 76.47		
		20	13 65.00			16 80.00		
Ỹ		22	14 63.64	0.021	0.885	19 86.36	0.173	0.677
		63	39 61.90			52 82.54		
cm	≥2	42	31 73.81	4.642	0.031	36 85.71	0.288	0.591
	<2	43	22 51.16			35 81.40		
TNM ŏ		19	9 47.37	2.932	0.402	15 78.95	0.552	0.907
		36	23 63.89			30 83.33		
		21	14 66.67			18 85.71		
		9	7 77.78			8 88.89		
ŏ ɔ	ɧ ŏ ɔ	18	14 77.78	3.702	0.157	17 94.44	2.769	0.250
	Ψ ŏ ɔ	22	15 68.18			19 86.36		
	ŏ ɔ	45	24 53.33			35 77.78		
		31	22 70.97	1.543	0.214	30 96.77	6.222	0.013
		54	31 57.41			41 75.92		

CTCs cfDNA

1 Salatino M Girotti MR Rabinovich GA. Glycans pave the way for immunotherapy in triple negative breast cancer J . Cancer Cell 2018 33 2 155 157.

2 Desantis C Ma J Bryan L et 2018 0 1 33 J Ca

• •

VEGF IL 18 MCP 1

1 2 3 4 1 1 1 5

ǚ ῴ PE VEGF ɗIL 18 ɗMCP 1 ש Ά ל Ặ
ɟ ǚ Њ 2017 2 2020 2 í 118 ʢ PE í ẹ ǚ ε
PE 63 ʢ ɗPE 55 ʢ ɟ ̓ ˥ 60 ʢ ̓ Ə ε
3 ж VEGF ɗIL 18 ɗMCP 1 ש ל ǚ ẹ Ặ ɟ PE
Ȉ ẛ VEGF ɞ ч 18 IL 18 ɞ╥ ɔ 1 MCP 1 Њ PE
ש Ể τ N<0.05 PE ظ
AA ɞ ♥ HCT ȸ J l D D Њ PE ש AA ɗHCT ȸ D

192102310368
1. 473000
2. 473000
3. 473000
4. 473000
5. 473000
E mail uvax19717@sina.cn

were observed in the three groups and their correlation was analyzed. Results Serum vascular endothelial growth factor VEGF interleukin 18 IL 18 monocyte chemoattractant protein 1 MCP 1 levels of patients in the severe PE group were significantly higher than those in the mild PE group and the control group N<0.05 . The levels of arachidonic acid induced maximum platelet aggregation rate AA hematocrit HCT and D dimer DD of patients in the severe PE group were significantly higher than those in the mild PE group and the control group. The levels of AA HCT and D D increased with the severity of the disease and the difference was statistically significant N<0.05 . Correlation analysis showed that AA HCT D D VECG IL 18 and MCP 1 were all positively correlated N<0.05 . Conclusion As the disease progresses in patients with preeclampsia serum VEGF IL 18 MCP 1 levels increase. VEGF IL 18 MCP 1 and hemorheological indicators are positively correlated which can be used to judge the condition of patients with preeclampsia Predictive indicators.

KEY WPRDS Pre eclampsia Hemorheology indicators Monocyte chemoattractant protein 1 Vascular endothelial growth factor Interleukin 18

♥ ǚ ɷ ה ε 8%~13% ǚ ɷ ה ε 9.5%~10.5%[1] ɟ O ї ɟ У ɻ ף ṿ ה ש H ζ Ɑ ǵ ɟ ῷ pre eclampsia PE У φ[m] ɯ Ό ♥ ɞ ε ζ ¥ ã Ώ ל ɔ ɟ PE ' ǚ ε PE ɻ PE PE ש ' ה ε PE ṿ ɔ ɞ ɞ ῌ ' ש ɔ ῺO ' ● ש ɞ ṿ ● [2] ɟ ῷ í Њ PE ה Ặ Ж Ə ε ṿ ● ל ɔ ᾶ í ɟ Ặ PE ה Ặ Ά ǚ ӿ ש ל ǚ[m] [3] ɟ PE ה Ψ ǚ א ч 18 interleukin 18 IL 18 Ə ε ǵ ' א ● [4] ɟ Ї ǵ vascular endothelial growth factor VEGF ῷ í ɔ ắ א Ҟ ẹ ל ɔ PE Ẻ τ ɟ ╥ ɔ 1 monocyte chemoattractant protein 1 MCP 1 í ה У ● ǵ ' Ẻ ɔ Ə [5] ɟ ǵ ǚ PE VEGF ɞIL 18 ɞMCP 1 ש Ά ל Ặ ɻ ; ɟ

1

1.1

ɿ 2017 2 2020 2 118 ʢ ῷ O ǚ ε PE I=63 ש PE I=55 ɟ ẹ Ψ PE Ά ε 20 ɻ Ό ♥ ≥140/90 mmHg ɞ ≥300 mg/24 h ¥ ɔ ɞ PE Ά ε PE 20 ɻ Ό ♥ ≥160/110 mmHg ɞ ≥2.0/24 h ɞ ╗ ɞ ῈE [6] ɟ ᵬ 60 ʢ Ə ε ɟ [m] τ N<0.05 Ẻ ' 1 ɟ

1 3

Table 1 Comparison of general information of 3 groups of patients

ᾶ	I		ɻ ɻ	BMI kg/m²
PE	63	27.19±5.32	34.15±3.79	24.22±3.17
PE	55	27.56±5.47	34.75±3.42	24.51±3.03
	60	27.89±5.75	34.52±3.73	24.14±3.19
D	-	0.25	0.41	0.22
N	-	0.780	0.666	0.803

Ẩ Ά ħ Ψ ɷ Ά У ђ[6] Ά ε PE ج ε ╥ ɞ ש ɟ ש ج Щ Ά ǚ O ɞ ɞ ã ẹ ђ ɞO ה ǚ ɥ ɞ ɞӿ ǚ í ɟ

1.2

1.2.1 VEGF ɞIL 18 ɞMCP 1

ǚ ج 5 mL Є ɯ 5 min 3 500 rpm/min ɿ

ɔ Ҍ ; 80 Ψ ἁ ɟ ƒ ẍ ٩ Ψ VEGF ɑIL 18 ɞ MCP 1 Ḥ ắ ˘ w Y O Ḥ Ш Ό Δ ж ٩ Ә ɟ

1.2.2 ל

₿ ⌊

arachidonic acid AA ɞ ♥ hematocrit HCT ɑD J l D Dimer D D ɟ ẹ Ψ AA Є w Ѧ ڙ ε ﻪ Sigma ắ ˘ SC 2000 ﻱ ˝ 4 Ѧ HCT ← Ш ה ắ ˘ w Vin trobe ♥ w 3 000 r/min 30 min ♥ e D D Є w ẍ Ѧ ڙ ε ﺋ ﻪ ắ ˘ Neth star ῦ Ѧ ɟ

1.3

˘ ɔ VEGF ɑIL 18 ɑMCP 1 Ỹ w ש ל ῦ VEGF ɞ IL 18 ɑMCP 1 Ά ל Ặ ɟ

1.4

SPSS 18.0 Ө ῦ ¯ D l % 2 Ặ ῦ Spearman Ặ ῦ ɟ w N<0.05 ε Ḗ τ ɟ

2

2.1 3 VEGF ɑIL 18 ɑMCP 1 Ỹ 3 VEGF ɑIL 18 ɑMCP 1 PE >PE > τ N<0.05 ɟ 2 ɟ

2.2 ˆ˟ ж ל 3 ж AA % ɑHCT % ɑD D μg/mL PE >PE > τ N<0.05 ɟ 3 ɟ

2 3 VEGF IL 18 MCP 1 ¯

Table 2 Expression of serum VEGF IL 18 and MCP 1 in the 3 groups ¯

ᾯ	l	VEGF ng/L	IL 18 pg/ml	MCP 1 pg/mL
PE	63	126.45±29.41	167.16±20.75	267.05±37.56
PE	55	162.05±50.24	194.05±17.42	422.04±53.01
	60	39.16±8.41	103.15±27.01	140.26±20.46
D e		210.28	258.33	756.28
N e		0.000	0.000	0.000

3 ¯

Table 3 Hemorheology indexes of different population ¯

ᾯ	l	AA %	HCT %	D D μg/mL
PE	63	57.06±7.05	0.35±0.03	1.21±0.26
PE	55	73.47±8.48	0.38±0.05	1.98±0.21
	60	30.81±6.01	0.30±0.01	0.53±0.11
D e		515.76	84.19	724.59
N e		0.000	0.000	0.000

2.3 ῦ PE VEGF ɑIL 18 ɑMCP 1 ש Ά ל Ặ Ặ ῦ AA ɞHCT ɞD D ɞVECG ɞ IL 18 ɑMCP 1 φ ﺞ ε Ặ N<0.05 4 ɟ

3

˟ ẫ ה ε 1/200 ﻪ ﻍ H ж 5 ˛ ж[7] ɟ PE Ә ε O ה φm ҁ У ש م У ṿ H ζ Ƈ ﻍ φm[8] ɟ PE ˊ ' ﺲש ל ה ﺆה ῴ ɞ ɞ Ὼ ɞ ῴ[9] ɟ m ה Ὼ ﺆ ' ˜ Ẩ Ό ﻼ ٩ ɞ ♥ ╗ ɞ ẉ א ש ﻳ ' ש א O ● ﻼ ●[10] ɟ

4 PE VEGF IL 18 MCP 1

Table 4 Levels of VEGF IL 18 and MCP 1 in PE patients and their correlation with hemorheology indexes

	AA %		HCT %		D D μg/mL		VEGF ng/L		IL 18 pg/mL		MCP 1 pg/mL	
	p e	N e	p e	N e	p e	N e	p e	N e	p e	N e	p e	N e
AA %	-	-	0.571	0.001	0.331	0.033	0.495	0.003	0.943	0.000	0.834	0.002
HCT %	0.571	0.001	-	-	0.915	<0.001	0.413	0.005	0.392	0.003	0.765	0.001
D D μg/mL	0.331	0.033	0.915	<0.001	-	-	0.516	0.002	0.467	0.005	0.912	0.000
VEGF ng/L	0.495	0.003	0.413	0.005	0.516	0.002	-	-	0.685	0.007	0.864	0.002
IL 18 pg/mL	0.645	0.012	0.513	0.002	0.439	0.003	0.510	0.002	-	-	0.739	0.001
MCP 1 pg/mL	0.761	0.001	0.812	0.000	0.561	0.001	0.903	0.000	0.812	0.002	-	-

Ặ ṿ Ά

ש̇ Ặ PE

Њ Ỉ

Ỉ כ Ỉ [11] ɟ VEGF

Ỉ Ỉ ῦ ئۆ ; \\ ӊ

ῷ í ɔ ắ א Ҡ

ɟ Ặ ש̇ †

Ψ VEGF ╗ [12] ɟ ה IL 18 ל

Ά ה ה ئۆ ' ΐ

ئۆ Ψ Ỹ ' ΐ

/ Ị УאʊỤ У ש̇ ɸ ђ У /΄ɷ ╕ ╕ · Ψ

Ş Ş

• •

sFGL2

1 2 1 1

θ ϕ ى CHB Ⳓ Ψ ' ч 2 sFGL2
ί τ ɟ ˥ ێ 140 ʢ CHB Ә ε ϕ ى CHB ẹ Ψ 25
ʢ CHB ˥̉ Γ ى 42 ʢ Ә ε Γ ى
CHC ˥̉ ꟾ ɟ ж 68 ʢ ɟ ӝ Ⳋ ˘ sFGL2
´ א ˘ Ⳓ Ψ qDEJ0 mRNA ꜩ ێ ˘ Spearman ǚ
ꜩ Ά CHB ˘ ί Ặ ɟ ێ 3 ˜ Ố sFGL2 Ⳑ Ⳓ
Ψ qDEJ0 mRNA ꜩ ῴ˜ ɟ CHB sFGL2 Ⳑ qDEJ0 mRNA
ج Ђ CHC Ⳑ Ẻ τ N<0.05 CHC Ⳑ sFGL2 Ⳑ qDEJ0
mRNA τ N>0.05 ɟ Spearman Ặ ǚ sFGL2 Ⳑ qDEJ0 mRNA
Ά HBV DNA ɵALT ɵAST Ⳳ Ặ N<0.05 Ά GGT ɵT Bil ɵAFP Ặ N>0.05 ɟ ˜
sFGL2 Ⳑ qDEJ0 mRNA ῴ ج ; Ẻ τ N<0.05 ɟ CHB
sFGL2 ╗ Ά HBV DNA ɵALT ɵAST ʹY Ặ ˜ sFGL2 ; ɟ
' ч 2 ϕ ى ӝ Ⳋ ´ א

The clinical significance of detection of sFGL2 in peripheral blood of patients with chronic hepatitis B

HONG Xiaolv[1] PAN Xiaoping[2] XU Peiyan[1] HUANG Xiaohua[1]
1. Department of Infection Diseases Huadu District People s Hospital Guangzhou Guangdong China 510800 2. Department of Clinical Laboratory Huadu District People s Hospital Guangzhou Guangdong China 510800

ABSTRACT Objective To evaluate the clinical value of soluble fibrinogen like protein 2 sFGL2 in peripheral blood of patients with chronic hepatitis B CHB . Methods Enzyme linked immunosorbent assay and real time fluorescent quantitative PCR were detected the levels of plasma sFGL2 and qDEJ0 mRNA in peripheral blood of 140 CHB patients CHB group in which 25 cases were treated with antiviral drugs antiviral group ɵ42 HCV patients CHC group and 48 healthy cases control group comparing the differences among those groups Spearman correlation was analyzed between sFGL2 level and clinical indexes in CHB patients estimating the differences in the levels of plasma sFGL2 and qDEJ0 mRNA before and after antiviral treatment in antiviral group of 25 cases. Results The levels of plasma sFGL2 and qDEJ0 mRNA in the CHB group were higher than those in the CHC group and the control group the difference were statistically significant N<0.05 no statistical difference between the CHC group and the control group in plasma sFGL2 and qDEJ0 mRNA N>0.05. Spearman correlation analysis showed that sFGL2 concentration and qDEJ0 mRNA expression were positively correlated with HBV DNA ALT and AST N<0.05 but not correlated with GGT T Bil and AFP N>0.05 . The concentration of sFGL2 and the expression of qDEJ0

1. 510800
2. 510800
E mail pxpwh@163.com

mRNA after antiviral treatment were significantly lower than before antiviral treatment and the difference was statistically significant N<0.05 . Conclusion SFGL2 is significantly increased in CHB patients which is closely related to the abnormalities of HBV DNA load ALT and AST and sFGL2 is significantly decreased after antiviral treatment.

KEY WORDS Soluble fibrinogen like protein 2 Chronic hepatitis B ELISA qRT PCR

2 soluble fibrinogen like protein 2 sFGL2

7q11.23 7 kb 2 1 [1] sFGL2

[2] sFGL2 [3] [4] [5] sFGL2 [6,7] sFGL2 CHB sFGL2 CHB CHB

1

1.1

2019 8 1 ~2020 1 22 CHB 140 CHB 86 54 38.96±12.07 25 CHB 16 9 40.65±13.41 42 CHC 35 7 40.95±6.24 68 26 42 36.71±12.85 D=2.492 N=0.116

2019 [8] 2019 [9]

1.2

1.2.1

5 mL 3 5 mL 30 min 1.5 mL -80 1 500 rpm 20 min -80

1.2.2 sFGL2

2 sFGL2 sFGL2 CHB HBV DNA alanine aminotransferase ALT aspartate aminotransferase AST γ glutamyl transferase GGT total bilirubin T Bil alpha fetoprotein AFP

1.2.3 qDEJ0 mRNA

Trizol Invitrogen RNA cDNA cDNA sFGL2 F AGGCAGAAACGGACTGTTGT sFGL2 R CCAGGCGACCATGAAGTACA GAPGH GAPGH F TGCACCACCAACTGCTTAGC GAPGH R GGCATGGACTGTGGTCATGAG SYBR™ Premix 10 μL Forward primer 10 pmol/μL 2 μL Reverse primer 10 pmol/μL 2 μL cDNA 3 μL H_2O 8 μL 95 2 min 40 95 10 s 60 45 s $2^{-\Delta\Delta Ct}$ ΔCT=CT CT ΔΔCT= ΔCT ΔCT 3 Ct

1.3

SPSS 13.0 Θ ῦ ‾ Ξ r D Ặ ῦ Pearson N<0.05 ε τ ɟ

2

2.1 3 sFGL2 ⁄ qDEJ0 mRNA

3 sFGL2 ⁄ qDEJ0 mRNA CHB >CHC > τ N<0.05 ɟ 1 ɟ

1 3 sFGL2 qDEJ0 mRNA ‾

Table 1 Coparing the levels of plasma sFGL2 and qDEJ0 mRNA in 3 groups ‾

ᾳ	sFGL2 ng/mL	sFGL2 mRNA
CHB	93.59±38.96	63.44±38.96
CHC	26.08±5.14	12.09±6.70
	16.68±3.39	8.24±5.94
D ᵉ	193.449	102.275
N ᵉ	<0.001	<0.001

2.2 sFGL2 ⁄ qDEJ0 mRNA Ά CHB ˘ ί Ặ ῦ

Spearman ῦ sFGL2 Ά HBV DNA ɞALT ɞAST \ Ặ N<0.05 Ά GGT ɞ T Bil ɞAFP Ặ N<0.05 2 ɟ

ί	sFGL2		qDEJ0
	p ᵉ	N ᵉ	0.982
HBV DNA LogF	0.982	<0.001	346
ALT	0.336	<0.001	0.954
AST	0.346	<0.001	.1490.3360.005
GGT	0.149	0.079	
T Bil	0.045	0.595	
AFP	0.005	0.954	

2.3 ῷ ˜ sFGL2 ⁄ qDEJ0 mRNA

3 Y ˜ sFGL2 ⁄ qDEJ0 mRNA ῷ ; ڿ τ N<0.05 3 ɟ

3

ῷ ɸ ى hepatitis B virus HBV ẍ Ҡ Ἂ щ ˝ T ẹ T regulatory T cell Treg ۆ ẹ ה ה Ψ Ặ Ә [10] ɟ sFGL2 ζ T ῦ Treg ˈ ˝ ˈ ۼ ẹ ˈ ε [11] Ά Ặ ҁ ۺ ẹ Ψ COLAK [12] sFGL2 ۆ Ψ AI [13] sFGL2 ۆ ẍ ╗ ẹ ╗ Ά AIH O YU [14] ۆ ה Ψ sFGL2 ʼ I ϽΆ ה ɟ

sFGL2 ۆ Ặ Ψ T Ẻ ‖ ῦ Ә ɟ I sFGL2 ʼ Ἂ Tregs ʄ Th1/Th2 [15] ɟ I Ἰ Ψ Foerster [16] ۆ Γ ى ⁴ Ψ sFGL2 Ά ῦ ⁄ ˜ Ὑ Ặ א ⁄ ɔ Ὸ ⁴ sFGL2 ɟ sFGL2 Ά Ὑ Ặ ɟ Ὸ sFGL2 ɔ ى ῦ ϽΆ HBV Ặ T ˈ T ۺ ẍ ɔ HBV ˜ ɔ ε CHB Ặ Ȯ ۼ ɸm [17] ɟ ɔ sFGL2 ʼ Ἂ Ђ I Њ HBV T I У ẍ ɔ ъ ˛ HBV Ἂ ⁄ m ה ɟ ۼ sFGL2 ۆ CHB Ψ ה ה ѡ ۺ ί ῦ Ψ Ә ᵉ Ẫ ɟ Ѝ [18] sFGL2 ۆ HBV DNA ˝ ˀ Ặ sFGL2 Ά CHB

3 sFGL2 qDEJ0 mRNA ‾

Table 3 Coparing the levels of plasma sFGL2 and qDEJ0 mRNA befor and after antiviral treatment in 25 CHB cases ‾

	I	ῷ	˜	r ᵉ	N ᵉ
sFGL2	25	127.41±24.07	74.40±22.97	48.463	<0.001
qDEJ0 mRNA	25	97.26±12.38	25.72±12.52	22.068	<0.001

ʹ ʹY Ặ ɟ З sFGL2 ϡ Ά Ђ سج ъ ĩ̈ ´ ʹ ɟ غ sFGL2 ʹ ɛ Ţ CHB O غ ʹ Ə ɛ CHB ɞ ϡ ɔ ɞ í ؤ̌ í Ə Ψ ɟ Ψ CHB 3 ˜ sFGL2 ς ; Ά Ꭹ [19] m sFGL2 Ά ʹY Ặ ɟ غ sFGL2 ʹ ɛ CHB ɟ c Ҥ sFGL2 ؤ̌ CHB ꟃ Ψ ա ẅ ȕ CHB ῷ ˜ ϡ ɔ ẅ ẹ ῎Ạ ; m HBV sFGL2 غ نح ʹ ա ẅ sFGL2 ῎Ạ Tregs Ặ ῎Ạ ɟ ɔ sFGL2 Ə ɛ m ẍ ȕ̃ ؤ̌ CHB Ψ Ẻ ẍ Ə ɟ ؤ̌ CHB ꟃ Ψ Ά í ʹY Ặ ʹ Ə ɛ CHB ɞ ϡ ɔ ɞ í ɟ̀ sFGL2 ؤ̌ CHB ˜ ; ς ʹ Ə ɛ CHB ؤ̌ í Ə Ψ ɟ

1 Liu M Leibowitz JL Clark da et a1. Gene transcription of fgl2 in endothelial cells is controlled by Ets 1 and Oet I and requires the presenee of both Sp1 and Sp3 J . Eur J Bio chem 2003 270 10 2274 2286.

2 Liu XG Liu Y Chen F. Soluble fibrinogen like protein 2 sFGL2 the novel effector molecule for immunoregulation J . Oncotarget 2017 8 2 3711 3723.

3 Ye X Ding J Chen Y et al. Adenovirus mediated artificial miRNA targetting fibrinogen like protein 2 attenuates the se verity of acute pancreatitis in mice J . Biosci Rep 2017 37 6 1 12.

4 Li WZ Yang Y Liu K et al. FGL2 prothrombinase contrib utes to the early stage of coronary microvascular obstruction through a fibrin dependent pathway J . Int J Cardiol 2019 274 1 27 34.

5 Tang M Cao X Li P et al. Increased expression of Fibrino gen Like Protein 2 is associated with poor prognosis in pa tients with clear cell renal cell carcinoma J . Sci Rep 2017 7 1 12676.

6 Ở ɛ̈ . ی fgl2 ̏H ᗡ غ نح J . ╞ Ψ ├ 2003 32 6 613 615.

7 . ی ɸ ی Ψ ж ч غ نح ẅ ẹ í Ặ J . Ψ ╞ 2004 12 7 385 388.

8 Ψ ╞ ├ Ж Ж ȕ Ж Ψ ╞ ├ Ж ȕ Ж . ɸ ی ╧ 2019 J . í 2019 35 12 2648 2669.

9 Ψ ╞ ├ Ж ȕ Ж Ψ ╞ ├ Ж Ж ȕ Ж . Г ی ╧ 2019 J . í 2019 35 12 2670 2686.

10 Gehring AJ Protzer U. Targeting Innate and Adaptive Im mune Responses to Cure Chronic HBV Infection J . Gastro enterology 2019 156 2 325 337.

11 Chan CW Kay LS Khadaroo RG et al. Soluble fibrinogen like protein 2/fibroleukin exhibits immunosuppressive proper ties Suppressing T cell proliferation and inhibiting maturation of bone marrow derived dendritic cells J . J Immunol 2003 170 8 4036 4044.

12 Colak Y Senates E Ozturk O et al. Plasma fibrinogen like protein 2 levels in patients with non alcoholic fatty liver dis ease J . Hepatogastroenterology 2011 58 112 2087 2090.

13 Ai G Yan W Yu H et al. Soluble Fgl2 restricts autoim mune hepatitis progression via suppressing Tc17 and conven tional CD8+ T cell function J . J Gene Med 2018 20 7 8 e3023.

14 Yu H Liu Y Wang H et al. Clara Cell 10 kDa Protein Alle viates Murine Hepatitis Virus Strain 3 Induced Fulminant Hepatitis by Inhibiting Fibrinogen Like Protein 2 Expression J . Front Immunol 2018 9 1 2935.

15 Luft O Khattar R Farrokhi K et al. Inhibition of the Fibrin ogen Like Protein 2 FcγRIIB/RIII immunosuppressive path way enhances antiviral T cell and B cell responses leading to clearance of lymphocytic choriomeningitis virus clone 13 J . Immunology 2018 154 3 476 489.

16 Foerster K Helmy A Zhu Y et a1. The novel immunoregu latory molecule FGL2 a potential biomarker for severity of chronic hepatitis C virus infection J . J Hepatol 2010 53 4 608 615.

17 Dembek C Protzer U Roggendorf M. Overcoming immune tolerance in chronic hepatitis B by therapeutic vaccination J . Curr Opin Virol 2018 30 1 58 67.

18 Й . ч 2 ؤ̌ Ψ ẅ í τ J . P ├ 2018 39 6 876 879.

19 Ꭹ . ẍ غ ȕ ی ч 2 ؤ̌ ɸ ی Ψ ϡ ɔ J . Ψ ╞ ɔ 2017 37 11 750 755.

The value of amniocentesis in the prenatal diagnosis of chromosomal abnormalities in non invasive high risk cases of prenatal screening

LIU Hui FANG Huiqin CHEN Wei YAN Yalan YUAN Jing

Prenatal Diagnosis Center of Obstetrics and Gynecology the First Affiliated Hospital of Anhui Medical University Hefei Anhui China 230022

ABSTRACT Objective To explore the value of amniocentesis in the prenatal diagnosis of chromosomal abnormalities in non invasive high risk cases of prenatal screening. Methods A total of 105 non invasive high risk cases of prenatal screening admitted to our hospital from January 2017 to December 2019 were selected as the research objects and genetic counseling was given. After the patient s informed consent amniocentesis karyotype analysis was performed. Based on the clinical follow up results statistical amniocentesis karyotype analysis was performed to detect various types of chromosomal abnormalities 13 trisomy syndrome 18 trisomy syndrome 21 trisomy syndrome sex chromosomes etc. and the sensitivity accuracy and specificity of diagnosing various types of chromosomal abnormalities. Receiver operating characteristic curve ROC and area under ROC AUC were used to analyze the efficacy of amniotic fluid puncture karyotype analysis for diagnosis of total chromosomal abnormalities. Results Among 105 non invasive high risk cases of prenatal screening there were 83 cases of chromosomal abnormalities in clinical

---

2017 1708085MH214

230022

E mail yuanjing_ahmu@163.com

follow up including 9 cases of 13 trisomy syndrome 13 cases of 18 trisomy syndrome 51 cases of 21 trisomy syndrome and 10 cases of sex chromosome abnormalities. Based on the clinical follow up results the sensitivity of amniocentesis karyotype analysis for 13 trisomy syndrome was 88.89% the accuracy was 96.19% and the specificity was 96.88%. Amniotic fluid puncture karyotype analysis for the diagnosis of 18 trisomy syndrome had a sensitivity of 92.31% accuracy of 99.05% and specificity of 100.00%. The sensitivity of amniocentesis karyotype analysis for diagnosis of 21 trisomy syndrome was 98.04% accuracy was 97.14% and specificity was 96.30%. Amniotic fluid puncture karyotyping analysis had a sensitivity of 90.00% an accuracy of 98.10% and a specificity of 98.95% the sensitivity of amniocentesis karyotype analysis for diagnosis of total chromosomal abnormalities was 95.18% specificity was 72.73% and accuracy was 90.48%. Conclusion Amniotic fluid puncture has a high prenatal diagnosis value for chromosomal abnormalities in NIPT high risk populations and can provide a reliable reference for eugenics and postnatal care genetic counseling.

KEY WORDS Amniotic fluid puncture Non invasive prenatal diagnosis High risk Chromosome abnormality Sensitivity Specificity Accuracy

ҩ Ό ' Ẉ ṿ 20 ˛
~30 ˛ Ẉ Ό ṿ 100 ˛ ˆ
Ό ה ҩ [1] ɟ l
ṿ Ό ζ Ɑ ġ φm ' Ὼ ӊ ; ɞ
ה ɞה ɞ Ύ ῴ
l ṿ Ό˜
ɞ Ӂ ɞ ġ У ῴ
Ά Ἇ Ό ж İ τ
[2] ɟ J ӎ ה
ὰ У ῴ Noninvasive prenatal test
NIPT ئۆ í ἇ Ẻ
l Ό ٩ ӊ ˆ ئۆ У ῴ
ṿ l Ψ ἇ Ə [3] ɟ ӂ Ђ
NIPT ϶ ἇ ɞ ṿ ɞ ġ
ἳ Ἇ ӊ í NIPT ж
щ ῃ γ m [4] ɟ ɯ
ɯ ῃ ɛ ƚ Ἇ Ń م NIPT ɞ
ῃ m ɯ í
ɛ ῃ [5] ɟ Ђ
ῃ ئۆ NIPT ж Ψ
ɵ e ٦ ; ɟ

1

1.1 m

٦ 2017 1 2019 12
105 ʢ У ῴ ὰ ʢ 20~45
ج 36.24±4.30 ٩ 13~20 ٩ ج
18.54±1.60 ٩ ὲ У 63 ʢ У 42 ʢ ɟ
Ӊ ۱ Ӝ Ἇ ج
ῃ ɞ' ئۆ ϶ ῃ
ˀ Ш ɟ
Ẩ Ἇ ϶ У ῴ У ῴ
ὰ ϶ ῃ
' ˊ ╥ ṿ
ɟ Ἇ У ῴ ὰ ӂ
ῃ í
ˊ '
Ρ ῞Η ' ẈẆ У
l >37.4 Ό
ε ˜ Ẩ ῴ 1 Ἲ ڗ ˊ
l ﬡ ɟ

1.2

1.2.1 NIPT

5 mL 10 000 rpm
10 min ٦ Ψ DNA ɞ
PCR ඣ J ӎ
מ ΰ ἇ˘ l Z e ɟ
ẹ Ψ 13 ɞ18 ɞ21 ˝ l Z e ئۆ -3.0~3.0 م Ἲ ε
ӊ Ό م ε ɟ ẹ ђ l
ש l ٜ Ẻ l Ỹ Ə ε ה ٦ ɟ

1.2.2 ῃ ي ΰ

NIPT Є Ʀ ⁄ ئۆ
ˀ ˜ Ђ 18~30 ٩ ῃ ɟ ٦
20 mL ΰ Ђ Ξ Y Ἲ ;
2 000 rpm 7 min ٦ 0.5~1 mL
Ђ 25 mL T ﺠ Ế Ψ ﺠ Ế ﺠ Ά
₱˜ ﺠ Ế Ψ ﺠ Ế 37 ɞ5% CO_2 9 10
d Ỹ ﺠ Ế ﺠ Ђ
϶ ɞӊ ɞ ز ҩ ٩ J
ز ˜ G ; 20 Y

ΰ Ψ ΰ ˥ 4 Y ΰ ל
ж Ꝁ ɷ ꟿ ˜ l Ȁ Ά IS
CN2013 ی ΰ ɟ Ȃ ή ώ ج
ی ε Rh ẹ g, ε Rh ч Ȃ
У ώ ή ˜ ◗ RhD ẍ ɟ

1.2.3 í

ε ‟E ˥ ש 2 Y ж ⅄
У ˜ ɞ У ʇ
מ ɟ

1.3

SPSS 22.0 ϴ
ա ¯ r l %
^{2} ɔ ə Receiver operating characteristic ROC ש ROC ; Area under the curve AUC ΰ ή ی ΰ
l ɟ N : 0.05 ε τ ɟ

2

2.1 í

105 ʇ У ώ ὰ ʇ í
l 83 ʇ 79.05% ẹ Ψ ₿ 13 є l ´
9 ʇ 10.84% 18 є l ´ 13 ʇ 15.66% 21
є l ´ 51 ʇ 61.45% l 10 ʇ
12.05% ɟ

2.2 ή ی ΰ Ό˘ ی l
Ỹ

í 105 ʇ ή ی ΰ Ό˘
ی l Ỹ ɟ 1 ɟ

1 13 l=105

Table 1 Amniotic fluid puncture karyotype analysis detected 13 trisomy syndrome l=105

í	13 є l ´			18 є l ´			21 є l ´			l		
	8	1	9	12	1	13	50	1	51	9	1	10
	3	93	96	0	92	92	2	52	54	1	94	95
	11	94	105	12	93	105	52	53	105	10	95	105

2.3 ΰ ή ی ΰ ˘ ی l ˘ l ɞΆ ɞ
τ N<0.05 2 ɟ

ա í ε Ά ή ی ΰ

2

Table 2 Amniotic fluid puncture karyotype analysis for diagnosis of various types of chromosomal abnormalities

l ΰ	%	Ά %	%
13 є l ´	88.89 8/9	96.19 101/105	96.88 93/96
18 є l ´	92.31 12/13	99.05 104/105	100.00 92/92
21 є l ´	98.04 50/51	97.14 102/105	96.30 52/54
l	90.00 9/10	98.10 103/105	98.95 94/95
^{2} e	2.504	52.049	4.090
N e	0.475	0.562	0.252

= ж / ж + ˆ ж ×100% Ά = + / ʇ ×100% = / ʇ + ˆ ʇ ×100% ɟ

2.4 ή ی ΰ Ό l Ỹ

í Ό l 83 ʇ l
22 ʇ ή ی ΰ Ό l
85 ʇ l 20 ʇ ɟ 3 ɟ

2.5 ΰ ή ی ΰ l

ա í ε Ά ή ی ΰ
l ε 95.18% ε
72.73% Ά ε 90.48%

3

NIPT DNA

NIPT

21 21

60%

• •

Th1/Th2

1 1 2

Th1/Th2 Ά O ɞ Ҡ Ặ ɉ
2017 10 2019 10 Њ ICU ͻ 62 ʇ 28 d ˜ ί
Ǖ ε H 20 ʇ ˧ 42 ʇ Ǖ ᾀ Њ Ẩ ICU ῴ 1 d Ẩ ICU ˜ 1 ɞ7 ɞ14 d
Ξ ˥ Ψ Th1 IFN γ⁺CD3⁺CD4⁺T ש Th2 IL 4⁺CD3⁺CD4⁺T
Th1/Th2 ᵉ Ǖ Ξ Th1 ɞTh2 ש Th1/Th2 ᵉ ɉ ı ´
Ҡ Ǖ ᾀ Ҡ 24 ʇ ˧ Ҡ 38 ʇ Ǖ Ξ Th1 ɞTh2 ש Th1/Th2
ᵉ ɉ ˜ 1 ɞ7 ɞ14 d Th1 ש Th1/Th2 ᵉ Њ H Ẻ
τ N : 0.05 Th2 Ά H τ N<0.05 ɉ Ҡ Th1 ש
Th1/Th2 ᵉ Њ Ҡ Ẻ τ N : 0.05 Th2 Ά Ҡ
τ N<0.05 ɉ Th1/Th2 ᵉ ӈ O
´ Ҡ Th1 Th1/Th2 ˜ Th1 ˜ ɉ
Th1/Th2 O Ҡ

Relationship between Th1/Th2 cell imbalance and disease severity lung injury in patients with sepsis

CHEN Lijun[1] WANG Jia[1] ZHANG Wenjing[2]

1. Emergency Department the First Affiliated Hospital of Hebei North University Zhangjiakou Hebei China 075000 2. Department of Thoracic Surgery the First Affiliated Hospital of Hebei North University Zhangjiakou Hebei China 075000

ABSTRACT Objective To explore the relationship between Th1/Th2 cell imbalance and disease severity lung injury in patients with sepsis. Methods Sixty two patients with sepsis who were treated in ICU of the hospital from October 2017 to October 2019 were divided into the death group 20 cases and the survival group 42 cases according to the clinical outcomes after 28 d of treatment. At 1 d before entering ICU and at 1 7 and 14 d after entering ICU contents of Th1 cells IFN γ⁺CD3⁺CD4⁺ T lymphocytes and Th2 cells IL 4⁺ CD3⁺CD4⁺T lymphocytes in peripheral venous blood in both groups were detected by flow cytometry. The ratio of Th1/Th2 was calculated. The contents of Th1 and Th2 cells and Th1/Th2 were analyzed and compared between the two groups. According to presence or absence of lung injury they were further divided into the lung injury group 24 cases and lung non injury group 38 cases . The contents of Th1 and Th2 cells and Th1/Th2 were analyzed and compared between the two groups. Results At 1 7 and 14 d after treatment contents of Th1 cells and Th1/Th2 in the survival group were significantly higher than those in the death group N< 0.05 while differences in contents of Th2 cells were not statistically significant between the two groups N>

20200521

1. 075000
2. 075000
E mail 704750797@qq.com

0.05 . The contents of Th1 cells and Th1/Th2 in the lung injury group were significantly higher than those in the lung non injury group N : 0.05 while the differences in contents of Th2 cells were not statistically significant between the two groups N<0.05 . Conclusion The decrease of Th1/Th2 ratio indicates the aggravation of disease severity and poor prognosis. The pro inflammatory Th1 cells are increased in patients with sepsis and lung injury and the Th1/Th2 balance drifts to Th1.

KEY WORDS Sepsis Th1/Th2 cell imbalance Disease severity Lung injury

ж I א ʾ ζ ε ɞ ɧ ɞ ɞ ɞ ɔ ε O ɬ ẋ ɞ ɞ ɞ ã ש [1] ɉ ῷ ã ж 1 900 600 H 1/4 ς 300 O ϊ [2] ɉ ẍ ẍ б Ψ Ậ Ə [3] ɉ T Th ж I ẍ Ψ ẅ ζ ǚ ε Th1 Th2 Th1/Th2 Ά I ẍ א Ύ Ậ [4] ɉ ɔ ; Th1/Th2 Ά O ɞ Ќ Ậ ; ɉ

1

1.1

2017 10 2019 10 Ѣ ICU ɔ 62 Ə ε Ẩ Ã Ậ Ã [5] ɉ Ã O ɥ ẍ ã ש Ќ ɉ 28 d ĩ ǚ ε H 20 42 ɉ H 12 8 60~78 68.40±2.73 Ẩ ICU ῷ 1 d Th1 % 15.35±8.78 Th2 % 1.63±0.85 Th1/Th2 11.92±9.01 ɉ 23 19 61~79 68.58±2.76 Ẩ ICU ῷ 1 d Th1 % 15.46±8.35 Th2 % 1.57±0.88 Th1/Th2 11.85±9.08 ɉ Ő ı Ќ ǚ ᾇ Ќ 24 Ќ 38 Ќ Ã Ậ [6] ɉ Ќ 10 14 59~76 67.38±2.63 Ќ 17 21 59~78 68.12±2.75 Ξ τ N<0.05 ɉ ├ Ң Ж Ã ש ẹ Щ ɉ

1.2 Ά

ǚ ᾇ Ѣ Ẩ ICU ῷ 1 d Ẩ ICU 1 ɞ 7 ɞ14 d Ѧ BD FACSCalibur Ψ Th1 IFN γ⁺CD3⁺CD4⁺T ש Th2 IL 4⁺CD3⁺CD4⁺T Th1/Th2 ɉ ǚ H Ά ɞ Ќ Ќ Th1 ɞTh2 ש Th1/Th2 ɉ

1.3

SPSS 18.0 Θ ǚ w r ɉ I % ² ɉ N<0.05 ε τ ɉ

2

2.1 2 1 ɞ7 ɞ14 d Th1 ɞTh2 1 ɞ7 ɞ14 d Th1 Ѣ H Ẻ τ N : 0.05 ɉ 1 d H Th2 Ѣ 7 ɞ14 d Th2 Ѣ H τ N<0.05 ɉ 1 ɉ

2.2 Ά H 1 ɞ7 ɞ14 d Th1/Th2 1 ɞ7 ɞ14 d Th1/Th2 Ѣ H Ẻ τ N<0.05 ɉ 2 ɉ

2.4 14 d Ĩ Ќ Ά Ќ Th1 ɞ Th2 ש Th1/Th2 Ќ Th1 ש Th1/Th2 Ѣ Ќ Ẻ τ N<0.05 Th2 Ά Ќ τ N<0.05 ɉ 3 ɉ

1 7 14 d Th1 Th2

Table 1 Comparison of Th1 Th2 cell content between survival group and death group at 1 7 and 14 d after treatment

		Th1 %			Th2 %		
		1 d	7 d	14 d	1 d	7 d	14 d
	42	17.18±5.72	20.23±6.61	22.89±8.72	1.72±0.83	2.12±0.76	2.08±0.81
H	20	12.86±5.21	13.54±6.12	15.48±5.26	1.95±0.86	2.05±0.66	1.98±0.69
r		2.858	3.813	4.917	1.008	0.353	0.476
N		0.006	0.000	0.000	0.317	0.725	0.636

2 1 7 14 d Th1/Th2

Table 2 Comparison of Th1/Th2 cell content between survival group and death group at 1 7 and 14 d after treatment

		Th1/Th2		
		1 d	7 d	14 d
	42	16.92±9.05	16.12±6.56	13.49±6.18
H	20	11.95±8.72	10.17±6.48	9.76±6.33
r		2.045	3.351	2.205
N		0.045	0.001	0.031

3 14 d Th1 Th2 Th1/Th2

Table 3 Comparison of Th1 and Th2 cell contents and Th1/Th2 values between lung injury group and non lung injury group

		Th1 %	Th2 %	Th1/Th2
Ҡ	24	18.79±9.26	2.05±0.34	11.27±7.39
Ҡ	38	12.45±8.63	1.98±0.46	6.85±5.21
r		2.739	0.642	2.762
N		0.008	0.523	0.007

3

[7] [8] Th1 Th2 Th1/Th2 [9] Th1/Th2

Th1/Th2 Th1 Th2 Th1/Th2 Th1/Th2 [10] [11] [12] Th1 Th2 Th1/Th2 Th1/Th2 Th1 6 interleukin 6 IL 6 8 interleukin 8 IL 8 10 interleukin 10 IL 10 IL 10 tumor necrosis factor α TNF α [13]

Th1 Th1/Th2 Th1 [14] Th1 γ interferon γ IFN γ IFN γ TNF α

ъ Ќ Th2 ˜Ω ζ ŭ ч 4
interleukin 4 IL 4 ė
Ќ ė ´ Ќ R f 0

miRNA 4534

miRNA 4534
2014 1 2016 6 64 30
30
qRT PCR miRNA 4534 ROC
miRNA 4534 miRNA 4534
miRNA 4534 miRNA 4534
N : 0.05 miRNA 4534
N<0.05 ROC miRNA 4534 AUC 0.839 0.777~
0.931 N : 0.05 2.52 76.56% 98.33%
miR 4534 N<0.05 TNM /
miR 4534 / N<0.05 miR 4534
N<0.05 3 62
40.32% 25/62 26.27±9.92 miR 4534 3
N<0.05 miRNA 4534 AUC 0.914 0.814~0.970
N<0.05 15.69 miRNA 4534 N<0.05
miRNA 4534
miRNA 4534

Relationship between serum miRNA 4534 level and pathological staging and prognosis of patients with lung cancer

YANG Shouyan[1] DENG Binbing[2] MENG Xiong[2] WANG Xi[2] MU Qiantu[2]
1. Department of Oncology PLA Army 958 Hospital Chongqing China 400020 2. Department of Respiratory and Critical Care Medicine PLA Army 958 Hospital Chongqing China 400020

ABSTRACT Objective To investigate the relationship between serum micro ribonucleotide miRNA 4534 level and pathological staging and prognosis of patients with lung cancer. Methods Sixty four patients with lung cancer lung cancer group who were treated between January 2014 and June 2016 were selected

cstc2015shmszx10129

1. 400020
2. 400020
E mail 345589984@qq.com

miRNA 4534 and pathological features in patients with lung cancer was analyzed. At 3 years of follow up the relationship between miRNA 4534 and prognosis of patients with lung cancer was evaluated. Results The relative expression level of miRNA 4534 in the lung cancer group was higher than that in the benign lung disease group and the control group the difference was statistically significant N<0.05 and there was no significant difference in the relative expression level of miRNA 4534 between the benign lung disease group and the control group the difference was not statistically significant N>0.05 . ROC curve showed that the area under the curve AUC optimal cut off value sen

TACRTACCACCATACCCAA 3′ ɟ Takara ắ ˘ ´ U6 Ϋ Ω ε ~ 5′ CTCGCTT CGGCAGCACA 3′ א ~ 5′ AACGCTTCAC GAATTTGCGT 3′ ɟ Θ ε Ỉ ל א l ɟ $2^{-\Delta\Delta Ct}$ miRNA ɟ

1.3

SPSS 19.0 Θ ŏ ⁎ ŏ w ¯ ⁎ ŏ w Ψ Ң ẖ ŏ Ң p25 p75 Ξ r Mann Whitney U Kruskal Walls H k w l % ² Ά ROC Ţ miRNA 4534 ה Ẇ ~ ⁎ pear son ŏ mirRNA 4534 Ά Ă N< 0.05 τ ɟ

2

2.1 3 miRNA 4534 miRNA 4534 Ң ∤ τ N<0.05 ∤ miRNA 4534 τ N<0.05 1 ɟ

1 3 miRNA 4534

Table 1 Comparison of relative expression level of miRNA 4534 among the 3 groups

ά	l	miRNA 4534
	64	17.82 2.74 27.44
	30	1.38±0.58[a]
	30	1.17±0.53[a]
X [e]		46.563
N [e]		0.000

2.2 miRNA 4534 ROC ROC miRNA 4534 ה ; AUC ε 0.839 95%AG 0.777~0.931 N<0.05 ȳ í [e] ε 2.52 76.56% 98.33% ₯ 1 ɟ

2.3 miRNA 4534 Ά í Ă ⁎ ά в вЧ ´ в в ى miR 4534 τ N< 0.05 TNM / miR 4534 Ң / τ N : 0.05 miR 4534 Ң τ N<0.05 2 ɟ

2.4 Ỹ 3 64 ҄ 62 ҄ 3.13% 2/64 ɟ 62 ҄ Ψ 3 25 ҄ в 40.32% 25/62 26.27± 9.92 Y ɟ

2.5 miRNA 4534 Ά ~ Ă 3 в ᴓ ң Ң ң τ N<0.05 3 ₯ 2 ɟ

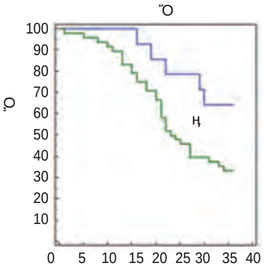

2 miRNA 4534

Figure 2 Survival curves of miRNA 4534 with high and low expression levels

2.6 miRNA 4534 ˜ ˜ ROC

ш 3 Ỉ H Ə ε ˜ ˜ Ą ROC miRNA 4534 ˜ ˜ AUC ε 0.914 95% CI 0.814~0.970 P<0.05 ӯ í e ε 15.69 ɟ ฿ 3 ɟ

2.7 miRNA 4534 Ά Ą ǖ

Pearson Ą ǖ miRNA 4534 Ά \ Ą Ą p ; -0.386 N=0.002 ɟ

2 3 2 ӱ ă Ə p υ Ȯ

3

ٷ

╥ Y miRNA ϧ ɔ Ά Ą miRNA ' ٷ Ψ Ό 2 3 2ῷ 4 Ų Ύ RNA ʄ miRNA ε ὰ [5] ɟ Ą miRNA 4534 Ḥ Ҍ I 22q13.1 miRNA Ά ῷ Ώ Ą Ą 1 VASH 1 ῷ Ώ ה s ῷ ٷ 2 / [6] ɟ miRNA 4534 ῷ ẹ ٷ Ψ ɟ VASH 1 ' ϧ Ά Ḥ Ώ

Q UŽ

2 3 2 ʄ Ą Ų

2 3 2 Ų

ALP CYFRA21 1

1 2 1 3

ALP 19 21 1 CYFRA21 1 2017 1 2019 7 ALP CYFRA21 1 ROC ALP CYFRA21 1 127 44.88% 57/127 N<0.05 N>0.05 ALP CYFRA21 1 N<0.05 ALP CYFRA21 1 N<0.05 ALP AUC >95.23 U/L 57.89% 70.00% AUC 0.765 ALP CYFRA21 1 >0.459 70.18% 70.00% ALP CYFRA21 1 19 21 1

Predictive value of serum calcium ions ALP and CYFRA21 1 for early bone metastases of lung cancer

ZHAO Chedong[1] XU Qian[2] MA Jing[1] ZHANG Jian[3]

1. Department of Clinical Laboratory the First Affiliated Hospital of Xi an Jiaotong University Xi an Shanxi China 710061 2. Department of Clinical Laboratory Xi an Fourth hospital Xi an Shanxi China 710004 3. Department of Dermatology the First Affiliated Hospital of Xi an Jiaotong University Xi an Shanxi China 710061

ABSTRACT Objective To analyze the predictive value of serum calcium ions alkaline phosphatase ALP and cytokeratin 19 fragment 21 1 CYFRA21 1 for bone metastases of lung cancer. Methods Between January 2017 and July 2019

YK201522

1. 710061
2. 710004
3. 710061
E mail yiiling10@163.com

types of lung cancer were compared. Serum levels of calcium ion ALP and CYFRA21 1 were compared between patients with and without bone metastasis and patients with different degrees of bone metastases. The receiver operating characteristic ROC curves were used to analyze the predictive value of serum calcium ion ALP and CYFRA21 1 in bone metastases from lung cancer. Results The incidence of bone metastases in this study was 44.88% 57/127 . The incidence of bone metastases from adenocarcinoma was significantly higher than those from squamous cell carcinoma small cell carcinoma and adenosquamous carcinoma. However there were no significant differences in the incidences of bone metastases from squamous cell carcinoma small cell carcinoma and adenosquamous carcinoma N<0.05 . Serum levels of calcium ion ALP and CYFRA21 1 were significantly higher in lung cancer patients with bone metastasis than in those without bone metastasis N : 0.05 and significantly higher in patients with multiple bone metastases than in those with single bone metastasis N<0.05 . In terms of single index diagnosis the area under the curve AUC of ALP was the largest with >95.23 U/L as the cut off value. And its sensitivity and specificity for predicting bone metastases from lung cancer were 57.89 % and 70.00%. The AUC of combined prediction was 0.765 significantly larger than that of each index single prediction N<0.05 . With >0.459 as the cut off value the sensitivity and specificity for predicting bone metastases from lung cancer were 70.18 % and 70.00%. Conclusion Combined prediction of serum calcium ion ALP and CYFRA21 1 can improve the prediction efficiency which is better for early warning of lung cancer bone metastases.

KEY WORDS Serum calcium ion Alkaline phosphatase Cytokeratin 19 fragment antigen 21 1 Lung cancer Bone metastasis

φm ẹ ה ש

H ج Ḩ [1] ɟ 57% ؤ ה ẹ Ψ . φm 30%~40% [2] ɟ ה c ɞ ɞ Ặ Ï Θ skeletal related events SREs O ĩ ς ε Ж├ H ع φ m Ặ ה Ψ Ḩ c 6~10 Y O ~ [3] ɟ Ω w ε ζ ж ữ ؤ ȳ [4] ẃ ɔ neuron specific enolase NSE ɞ ữ ặ c ε 46.15% ɞ 72.00% ɟ ɞ alkaline phosphatase ALP ש 19 ɑ 21 1 cytokeratin 19 fragment 21 1 CYFRA21 1 ς í ẹ ؤ Ψ í ж ɔ ɞ Y I ع ĩ ς [5,6] ɟ щ ï ắ ɞ' w í ữ ɞALP ש CYFRA21 1 ɵ w ε í w ל Ẻ I ; ɟ

1

1.1 m

ε Ỉ 2017 1 2019 7 ɟ Ẩ Ά ɞ ε CT d̠ Ч Ά [7] ɟ Ά ų Ặ ɑ ה ה ɟ Ẩ 127 ʢ ẹ Ψ 79 ʢ 48 ʢ 49~84 ج 61.22±12.45 44 ʢ ɞ 38 ʢ ɞ 27 ʢ ɞ 18 ʢ ɟ ├ Ḩ Ж Ά ש Ш ɟ

1.2

1.2.1 ɞALP ש CYFRA21 1

ῴ ɔ ש Ặ ẫ ɔ ữ Ѧ ל e م 2.11~2.52 mmol/L ɞ ALP 45~125 U/L cobas e602 ɔ ה ẉ ẫ ẍ ữ CYFRA21 1 ɟ

1.2.2

ج Є 3 Y / ɔ ש d̠

computedtomography CT ה positron emission tomography PET CT CT ɞ Ă ḏ magnetic resonance imaging MRI ش ی ◗ ' ε ɟ ẹ Ψ ŭ ε ╥ ה 4 ה Ξ Y Ж ɟ

1.3

SPSS 19.0 Ө ŭ w l % ^{2} w ¯ r ╥ ἐ ŭ Jmegqrga ع ŭ ´ ش Ά ɔ Ә ROC ŭ ɵ e ; e AUC e X N<0.05 ε τ ɟ

2

2.1 ה Ỹ

127 ʢ ה ε 44.88% 57/127 ΄Y 65.91% 29/44 ה Ҕ 42.11% 16/38 ɞ 33.33% 9/27 ɞ 22.22% 4/18 Ẻ τ N<0.05 ӂ ɞ ɞ τ N>0.05 ɟ

2.2 Ά

ɵALP ش CYFRA21 1 ɵALP ɞCYFRA21 1 ج Ҕ Ẻ τ N<0.05 1 ɟ

2.3 ɞ ALP ش CYFRA21 1 ╥ ה ش ה ɞ ALP ɞCYFRA21 1 ج Ҕ Ẻ τ N<0.05 ΄Y ה ɵALP ɞCYFRA21 1 Ҕ ╥ ה Ẻ τ N<0.05 2 ɟ

1

ALP CYFRA21 1 ¯

Table 1 Comparison of serum calcium ion ALP and CYFRA21 1 levels between patients with bone metastasis from lung cancer and those without ¯

ᾳ	l	mmol/L	ALP U/L	CYFRA21 1 ng/mL
	57	2.61±0.32	107.79±42.32	26.86±8.94
	70	2.48±0.27	78.48±40.16	22.02±6.48
r e		-2.408	-3.972	-3.414
N e		0.018	0.000	0.001

2 ALP CYFRA21 1 ¯

Table 2 Comparison of serum calcium ion ALP and CYFRA21 1 levels in lung cancer patients with different degree of bone metastases ¯

ᾳ	l	mmol/L	ALP U/L	CYFRA21 1 ng/mL
╥ ה	12	2.65±0.32	96.11±36.92	21.89±8.56
ה	45	2.71±0.22	118.19±44.86[ab]	28.58±7.71
	70	2.48±0.27	78.48±40.16	22.02±6.48
D e		11.600	16.936	12.447
N e		0.000	0.000	0.000

2.4 ɵALP ش CYFRA21 1

ɵ e ╥^{m} ALP AUC e w > 95.23 U/L ε í e ẹ ɞ ŭ ᾳ ε 57.89% ɞ70.00% Logistic ع ŭ ɞALP ش CYFRA21 1 ´ ش ´ Jme N =- 8.310 + 1.698* + 0.682*ALP + 0.661*CYFRA21 1 ´ AUC e Ҕ ╥^{m} ɵALP ش CYFRA21 1 ɞ ŭ ᾳ ε 70.18% ɞ70.00% 3 ɞ 4 ɞ൭ 1 ɟ

3

Ә ε O ˜ ἐ ɔ ώ

3 ALP CYFRA21 1

Table 3 Predictive value of combination of serum calcium ALP and CYFRA21 1 levels in bone metastases from lung cancer

ל	AUC	73#AG	X e		í e	%	%	N e
	0.611	0.520~0.696	2.182	0.190	>2.76mmol/L	33.33	85.71	0.029
ALP	0.682	0.594~0.762	3.853	0.278	>95.23U/L	57.89	70.00	0.000
CYFRA21 1	0.661	0.571~0.742	3.244	0.328	>25.31ng/mL	61.40	71.43	0.001
´	0.765	0.681~0.836	6.334	0.401	>0.459	70.18	70.00	<0.001

4 Logistic

Table 4 Logistic regression analysis

Ƽ	@ e	Q,C e	U_jb ² e	N e	Exp B e	73#AG
	1.698	0.703	5.829	0.016	5.465	1.377~21.692
ALP	0.018	0.005	11.899	0.001	1.018	1.008~1.029
CYFRA21 1	0.087	0.029	8.689	0.003	1.091	1.029~1.155
	-8.310	2.129	15.234	0.000	0.000	

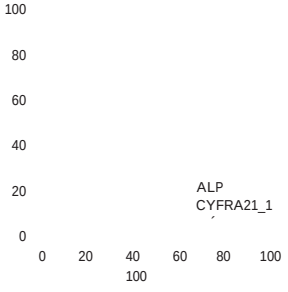

1 ALP × ï

@ ,

. V

SEER Data J . J Thorac Oncol 2018 13 6 e106 e107.
2 Wang GS Chen JY Ma RF et al. Effects of zoledronic acid and ibandronate in the treatment of cancer pain in rats with lung cancer combined with bone metastases J . Oncol Lett 2018 16 2 1696 1700.
3 Ở ȋ . ئۆ Ặ Ψ J . ǚ Ά 2017 9 4 289 292.
4 . ئۆ Ψ ɵ ᵉ J . Ψ ╞ ├ Ά ǚ ḏ 2018 38 5 331 335.
5 Duan L Pang HL Chen WJ et al. The role of GDF15 in bone metastasis of lung adenocarcinoma cells J . Oncol Rep 2019 41 4 2379 2388.
6 Ꝁ Ở . J . Ψ ܩ 2018 21 8 51 55.
7 ॥ ǐl Њ . Ψ ܩ Ɑ ה 2015 J . Ψ ╞ 2015 37 1 67 78.
8 Ж . ⁄ Ψ LCN2 ⁄ PDGF BB ݜ τ J . ί Ά 2019 35 2 187 191.
9 . ؽ ی Ά ί Ặ J . Ψ ╞ 2019 39 6 329 335.
10 . ḏ ئۆ ⁄
Ψ ǚ J . ├ 2017 46 5 551 553.
11 ˥ ǐΩ . Ά ODF ɞOCIF ݜ Ca J . ├ Ά ί 2018 15 10 1475 1477.
12 . ⁄ Ɑ ה ί ɵ ᵉ J . ﻄ ├ 2017 42 2 158 161.
13 ü . CEA ɞCYFRA21 1 ɞCA125 ɞCa~ 2+ ɞ ALP ί ɵ ᵉ J . ├ Ά ί 2019 16 9 54 57 61.
14 θ θ . ɥ tP1NP ⁄ β CTx ݜ BAP ئۆ Ψ ί J . Ψ ╞ ├ 2017 40 11 860 864.
15 ɔ ʳ Й . SPECT/CT ´ ḏ ╥ ה ɵ ᵉ J . Z ├ 2018 56 2 41 46.
16 ẕ . ⁄ Ά ẫ ḏ Ặ J . 2019 46 2 51 54.
17 . ί ǚ J . Ψ ܩ 2018 21 5 403 407.
18 ϒ . ئۆ Ψ ɵ ᵉ J . ܩ 2018 45 6 337 340.

1 . O . LASP 1 ئۆ Ψ ݜ Ά ẹ ί Ặ ǚ J . ǚ Ά 2019 11 3 219 223.
2 . miRNA Ꝁ ה ݜ ˈ Ə J . ǚ Ά 2019 11 1 63 67.
3 ă . miRNA Ά Ặ J . Z ├ 2017 57 4 110 112.
4 Jima DD Zhang J Jacobs C et al. Deep sequencing of the small RNA transcriptome of normal and malignant human Bcells identifies hundreds of novel microRNAs J . Blood. 2010 116 23 e118 e127.
5 ॥ ǐl Њ . Ψ ܩ Ɑ ה 2015 J . Ψ ╞ 2015 37 1 67 78.
6 ϒ ĸ Z ʳ . miRNA 506 ϧ ɔ ݜ ẹ τ J . Z ├ 2017 57 23 55 57.
7 Jiang Z Zhang Y Chen X et al. Long noncoding RNA RBMS3 AS3 acts as a microRNA 4534 sponge to inhibit the progression of prostate cancer by upregulating VASH1 J . Gene Ther 2019 11 10 1016 1034.
8 ɔ ╥ . ǐẶ VASH1 ئۆ NSCLC Ψ ݜ τ J . 2016 31 2 140 144.
9 Nip H Dar AA Saini S et al. Oncogenic microRNA 4534 regulates PTEN pathway in prostate cancer J . Oncotarget 2016 7 42 68371 68384.
10 O ε . miRNA ǐẶ ж A375 ˛ J . ╧ Ш ├ 2015 35 2 263 269.
11 ╞ . VASH 1 ئۆ Ψ J . Ȋ ݑ ├ 2016 48 4 444 446.
12 . PTEN ⁄ mTOR ئۆ Ψ ݜ τ J . ├ 2018 49 6 602 605.
13 ă ȋ Ж Z . PTEN ɞ p Akt ݜ p mTOR ݜ τ J . Z ├ 2018 39 5 710 716.
14 Ở ẫ . PTEN Ά PI3K ǐẶ Ḣ Ə J . Ψ ܩ 2018 38 23 5783 5786.
15 ɔ . ж Ψ β ⁄ ɔ ﺷ א ч 2 Ά ɔ ˜ Ặ J . Ψ ╞ ├ 2017 36 10 1069 1074.

• •

β arrestin2 RBP4 FGF 21 2

1 2 3 4 1 5

β Ά̤ 2 β arrestin2 ɞ ˊ 4 RBP4 ש̇ ˊ 4
RBP4 ثّ 2 ى Ψ ש̇ Ά ɥ Ă̤ ɟ ˥ 2018 7 2019 7 Њ
ɔ 117 ʢ 2 ى í ẹ Ψˊ 2 ى 59 ʢ A ˊ
58 ʢ B ̓ Ẫ̓ 55 ʢ Њ ɔ ɟ l Ə ε ɟ 3 β arrestin2 ɞRBP4
ש̇ FGF 21 0 #Ỹ ῦ 2 ى β arrestin2 ɞRBP4 ש̇ FGF 21 Ά ɥ Ă̤
arr stin ى Ḫ . ﺨ

201902218

1. 473000
2. 473000
3. 473000
4. 473000
5. 473000
E mail lp914tvsk@sina.cn

underwent a physical examination in our hospital were included as the control group. The levels of β arrestin2 RBP4 and FGF 21 in 3 groups were compared and the correlation between β arrestin2 RBP4 and FGF 21 and glucose and lipid metabolism in patients with type 2 diabetic foot was analyzed. Results The level of β arrestin2 in the group A was lower than that of the group B and the control group and the levels of RBP4 and FGF 21 in the group A were higher than those of the group B and the control group. The difference was statistically significant N<0.05 . The levels of HbAlc TC TG LDL C HOMA IS and HOMA IR in the group A were higher than those in the group B and the control group and the differences were statistically significant N<0.05 while the levels of HDL C in the three groups were no significantly difference N>0.05 . Plasma β arrestin2 levels were significantly negatively correlated with HbAlc TC TG LDL C HOMA IR BMI FFA and HOMA IS levels N<0.05 . The levels of RBP4 and FGF 21 were significantly positively correlated with the levels of HbAlc TC TG LDL C HOMA IR BMI FFA and HOMA IS N<0.05 . Conclusion β arrestin2 RBP4 and FGF 21 are abnormally expressed in type 2 diabetic foot and their levels are closely related to the metabolism of glucose and lipid. All three promote the development of type 2 diabetic foot and are expected to become a new target in the treatment of type 2 diabetic foot.

KEY WORDS β arrestin2 RBP4 FGF 21 Type 2 diabetic foot Glucose and lipid metabolism

2 ی Ѣ Ꝁ غ طي
ǚ ᷈ ϥ ܦ
ᵐ ɟ غ ٩ م ϩ Ά
٩ ˊ ♥ Ὼ ʼ
ẅ Ặ سج Ά
הᵐ Ὤ [1] ɟ β Ἇ 2 beta arrestin 2 β arrestin2 Ἇ Ɏ ᷈ c ϩ Ά G ƺ כ l ϥ Ῑ כ ʼ Ә ε
מ ˝ Y ϩ Ά ẍ [2] ɟ
ˊ 4 retinol binding protein 4 RBP4
ᵐ Y ה غ ئؤ ϥ ǚ
ϩ Ά ה [3] ɟ غ
21 Fibrob last growth factor 21 FGF21
غ ʼ ئؤ Ψ ʼ
ɞ w ẅ β ʿ [4] ɟ
β arrestin2 ɞRBP4 ẅ FGF 21 ئؤ 2 ی
Ψ ẅ Ά ɥ Ặ ε ί
ẘ ; ɟ

1

1.1 ᵐ

ǚ 2018 7 2019 7 Ѣ כ 117 Ꞔ 2 ی ί ẹ Ψˊ 2 ی A 59 Ꞔ ˊ B 58 Ꞔ ʾ Ẫʾ 55 Ꞔ Ѣ כ ɟ l Ә ε ί ɟ ˘ ᵐ ᾳ̈ ɞ τ N<0.05 Ẻ ʼ 1 ɟ

1 3

Table 1 Comparison of general data between 3 groups

ᾳ	l	ᾳ /		ɥ˩ ط / Ϝ	
A	59	24/35	48.59±5.71	36/23	0.80±0.13
B	58	25/33	49.19±5.54	34/24	0.82±0.11
	55	23/32	48.91±5.33	33/22	0.81±0.15
²/D e		0.071	0.170	0.070	0.340
N e		0.965	0.842	0.965	0.710

Ẫ Ἇ 18~60 ˊ ΐ ► 2 ی ẅ Ἇ [5] T Ặ ʿ 1 ی ɞ ה ɞ ˊ ẹ ђ ẍ ɞ ɟ

1.2

6 mL ǚ ε Ξ ẹ Ψᵐ 3 200 r/min 6 min ╚ 8 ɫ ˥ כ Ѣ 40 ỳ Ψ ɟ ẍ Ɏ β arrestin2 ɞRBP4 ẅ FGF 21 ɟ O Ḥ כ ج ắ ˘ ˝ ǚ ᾳ̈ ε 160123 ɞ20151106 ɞ20151123 Ꝡ ɟ Ꞛᵐ ﻫ BECKMAN CX8 ی ẫ כ ǚ Ѧ fasting blood glu cose FPG ɞ fasting insulin FINS ɞ כ glycated hemoglobin HbAlc ẅ ز high density lipoprotein cholester in HDL C ɞ ز total cholesterol TC ɞӊ ز low density lipoprotein cholester

in LDL C ϐ є tri glyceride TG ɟ
HOMA insulin resistance index
HOMA IR =FPG × FINs/22.5 ῦ
HOMA βcell secretion index HOMA IS = 20 ×
FINS / FPG 3.5 ɟ

1.3
SPSS 18.0 Ɵ ῦ
ʬ Ι % ² ‾
Ξ r ῦ ʬ N<0.05
ε Ẻ τ ɟ

2

2.1 3 β arrestin2 ϐRBP4 ש FGF 21 Ỹ
A β arrestin2 ɥ Њ B ៸
Ẻ τ N<0.05 A RBP4 ϐFGF 21
ج Њ B ៸ Ẻ τ N<
0.05 2 ɟ

2.2 3 ӌ
A HbAlc ϐTC ϐTG ϐLDL C ϐHOMA IS ϐ
HOMA IR ج Њ B ៸ Ẻ
τ N<0.05 3 HDL C
τ N<0.05 3 ɟ

2.3 2 ي β arrestin2 ϐRBP4 ש FGF
21 Ά ӌ Ặ
β arrestin2 Ά HbAlc ϐTC ϐTG ϐLDL C ϐ
HOMA IR ϐBMI ϐFFA ϐHOMA IS \
Ặ N<0.05 RBP4 ϐFGF 21 Ά HbAlc ϐTC ϐ
TG ϐLDL C ϐHOMA IR ϐBMI ϐFFA ϐHOMA IS
\ Ặ N<0.05 4 ɟ

3

2 ي O
ה φᵐ ٩ م ל ៸ ל Ẫ Ə
[6] ɟ ထ T
ထ ᾱ ה ל
● غ ʬ ε
ϐ ɥ τ [7] ɟ
[8] ε insulin resistance
IR ӌ ៸ ӌ ϭ Ά 2 ي ה
Ặ ẹ Ψ Ỉ
Ԟ ε ל Ỉ ῟H ' Ỉ
ي ' ; ៸ ל
' ɟ IR Ά ώ ထ

... [9] ... 2 ...

FGF ... [10] FGF 21 ... β ... [11] ... FGF 2 ... [12] ... [13] ... FGF 21 ... IR ...

Arrestin ... β arrestin2 ... β arrestin2 ... G ... [14] ... [15] β arrestin2 ... β arrestin2 ... β arrestin2 ... β arrestin2 ... 2 ...

RBP4 ... IRSI Ras MAPK ... 2 ... [16] ... [17] ... 2 RBP4 ... RBP4 ...

... β arrestin2 RBP4 FGF 21 2 ... 2 ... 2 ...

1 ... 2 ... J ... 2018 10 4 274 277.

2 ... RBP4 ... J ... 2017 15 8 1371 1373.

3 Jean Charles PY Zhang L Wu JH et al. Ubiquitin specific protease 20 regulates the reciprocal functions of β Arrestin2 in toll like receptor 4 promoted nuclear factor κB NFκB activation J . J Biol Chem 2016 291 14 7450.

4 ... 2 ... 21 ... J ... 2019 39 1 34 36.

5 Fisher FM Maratos Flier E. Understanding the physiology of FGF21 J . Ann Rev Physiol 2016 78 1 223.

6 ... J ... 2018 31 3 92 95.

7 Lee JTH Huang Z Pan K et al. Adipose derived lipocalin 14 alleviates hyperglycaemia by suppressing both adipocyte glycerol efflux and hepatic gluconeogenesis in mice J . Diabetologia 2016 59 3 604 613.

8 ... Caspase 1 Sirtuin 1 ... J ... 2015 58 4 308.

9 ... 2 ... J ... 2016 13 4 67 68.

10 ... D FGF23 Klotho ... J ... 2016 28 12 32 36.

11 Dominika S Wojciech P Bieta C et al. Changes in liver gene expression and plasma concentration of Rbp4 Fetuin A and Fgf21 in sprague dawley rats subjected to different dietary interventions and bariatric surgery J . Biom Res Int 2018 18 19 1 11.

12 ... J ... 2019 41 6 1272 1276.

13 ... 2 ... 21 ... J ... 2018 21 5 521 525.

14 ... 2 ... J ... 2019 25 9 658 661.

15 ... Wnt ... 2 ... J ... 2018 34 12 1023.

16 Lin WT Lin PC Lee CY et al. Effects of insulin resistance on the association between the circulating retinol binding protein 4 level and clustering of pediatric cardiometabolic risk factors J . Pediatric Diabetes 2018 23 19 1403 1407.

17 ... 4 ... J ... 2016 24 7 626 629.

miR 23b 3p

1 2

miR 23b 3p
2017 6 2019 12 76 104
80 PCR
miR 23b 3p α TNF α 6 IL 6
10 IL 10 28 KM ROC
miR 23b 3p miR 23b 3p
N<0.05 miR 23b 3p WBC ESR CRP
APACHEII TNF α IL 6 IL 10 miR 23b 3p
N<0.05 28d miR 23b 3p N<0.05 ROC
miR 23b 3p 28d
miR 23b 3p 28
miR 23b 3p

Evaluation value of peripheral blood miR 23b 3p expression level in the condition and prognosis of children with severe pneumonia

WU Ying[1] LIU Chenggui[2]

1. Department of Pediatrics Chengdu Women and Children s Central Hospital Chengdu Sichuan China 610074 2. Department of Laboratory Medicine Chengdu Women and Children s Central Hospital Chengdu Sichuan China 610074

ABSTRACT Objective To study the value of peripheral blood miR 23b 3p expression level in evaluating the condition and prognosis of children with severe pneumonia. Methods From June 2017 to December 2019 180 cases of children with pneumonia were selected 76 children with severe pneumonia were enrolled in the severe pneumonia group 104 children with common pneumonia were enrolled in the common pneumonia group and 80 healthy children in the same period were selected as the control group. The expression of miR 23b 3p in peripheral blood was detected by fluorescence quantitative PCR. The serum contents of tumor necrosis factor α TNF α interleukin 6 IL 6 and interleukin 10 IL 10 were detected by enzyme linked immunosorbent assay. The 28 day survival was observed. The difference of cumulative survival rate was compared by KM curve and the value of miR 23b 3p in predicting survival was analyzed by ROC curve. Result The expression level of peripheral blood miR 23b 3p in the severe pneumonia group was lower than that of the common pneumonia group and the control group. The WBC ESR CRP levels APACHE II score

---

2019YJ0648

1. 610074
2. 610074
E mail yyjj54232@163.com

serum TNF α IL 6 IL 10 contents in children with low miR 23b 3p expression in the severe pneumonia group were higher than those of children with high mir 23b 3p expression and the 28d cumulative survival rate was lower than that of children with high mir 23b 3p expression. ROC curve analysis showed that mir 23b 3p had predictive value for the 28 day survival of children with severe pneumonia. Conclusion the low expression of miR 23b 3p in peripheral blood of children with severe pneumonia is related to the aggravation of the disease and the activation of inflammatory reaction and it is valuable for evaluating the survival prognosis of 28 days.

KEY WORDS severe pneumonia miR 23b 3p inflammatory response prognosis prediction

[1] WBC CRP ESR Ⅱ acute physiology and chronic health evaluationⅡ APACHEⅡ [2,3] RNA microRNA miR 3 [4] miR 23b 3p miR 23b 3p

1

1.1

2017 6 2019 12 180 76 40 36 5.58±1.02 104 59 45 6.11±1.21 80 45 35 6.02±0.94 3 N>0.05

2013 [5]

1.2 miR 23b 3p

miR miR miR cDNA miR PCR PCR cDNA 1 μL PCR 10 μL 10 μmol/L 0.4 μL 20 μL miR 23b 3p U6 PCR 94 2 3min 94 15 s 60 40 s 40 PCR Cycle threshold Ct U6 miR 23b 3p

1.3

TNF α 6 IL 6 10 IL 10

1.4

28 d

1.5

SPSS 21.0 r KM Log rank miR 23b 3p ROC N<0.05

2

2.1 3 miR 23b 3p

3 miR 23b 3p > > N : 0.05 N<0.05 1

1 3 miR 23b 3p

Table 1 Comparison of miR 23b 3p expression in peripheral blood of 3 groups

ą̈		miR 23b 3p
	76	0.60±0.21
	104	0.89±0.25
	80	0.96±0.22
e		94.520
e		0.000

2.2 Ψ ‴ miR 23b 3p ẏ Ẇ APACHEII ŭ

Ά Ψ miR 23b 3p ẏ ҥ miR 23b 3p ẏ WBC ɵESR ɵCRP Ẇ APACHEII ŭ ҷ ѽ τ N : 0.05 ɟ 2 ɟ

2.3 Ψ ‴ miR 23b 3p ẏ Ė ˉ

Ά Ψ miR 23b 3p ẏ ҥ miR 23b 3p ẏ TNF α ɵIL 6 ɵIL 10 ˉ ѽ τ N : 0.05 ɟ 3 ɟ

2 miR 23b 3p APACHEII

Table 2 Comparison of laboratory indexes and APACHE II scores of children with different miR 23b 3p expression in severe pneumonia group

miR 23b 3p	l	WBC(×109/L)	ESR(mm/h)	CRP(mg/L)	APACHEII ŭ (ŭ)
ҥ	38	17.27±3.72	45.49±8.39	62.32±11.35	16.47±3.21
	38	12.55±3.02	36.62±6.41	49.83±10.44	12.45±2.26
r e		6.072	5.179	4.993	6.312
N e		0.000	0.000	0.000	0.000

3 miR 23b 3p

Table 3 Comparison of serum inflammatory factors between children with different expression of miR 23b 3p in severe pneumonia group

miR 23b 3p	l	TNF α ng/mL	IL 6 ng/mL	IL 10 pg/mL
ҥ	38	52.39±9.39	104.58±22.54	86.68±13.47
	38	43.11±8.37	81.47±16.58	65.47±11.09
r e		4.548	5.091	7.493
N e		0.000	0.000	0.000

2.4 Ψ ‴ miR 23b 3p ẏ 28 Ỹ

Ą̈ ẏ 28 Ỹ KM Log rank Ά Ψ miR 23b 3p ẏ ҥ miR 23b 3p ẏ 28 ҥ τ N : 0.05 ɟ ѽ 1 ɟ

2.5 miR 23b 3p ẏ 28 ROC ŭ

Ą̈ miR 23b 3p ẏ 28 ROC ; ε 0.6818 73# A6 0.5522~0.8115 ɵN=0.013 e ȳ e ε 0.575 e 28 ε 72.73% ɵ ε 57.14% ɟ ѽ 2 ɟ

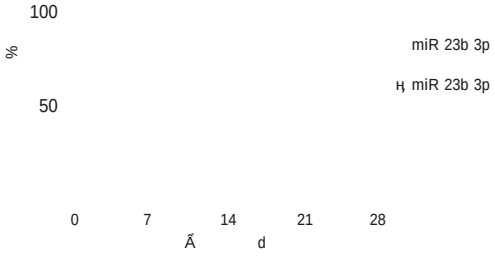

1 miR 23b 3p 28 KM

Figure 1 KM curve of 28 day survival of children with different mir 23b 3p expression in severe pneumonia group

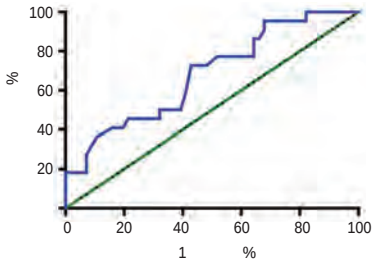

2 miR 23b 3p 28 ROC

Figure 2 ROC curve of miR 23b 3p in predicting 28 day survival in children with severe pneumonia

3

ẏ ● Ė í ɵ ה ɵ ˜ ɵ H

ɟ Ặ í ה ɵ
ɞ ɔ
ṿ ˜ ɞ ɥ H [6,7] ɟ ǵ Ά ó
O ש ˜ ε ˜ ṿ
w ˜ ● ṿ
ɵ ɞ
ɔ ˜ ɟ Ӝ ώ í Ţ Ψ
WBC ɞCRP ɞESR ɞ ˜ Ţ ǖ
Ş ש
˜ Ţ ɟ
miR З ฝ Ⴗ Ẻ
Ə Ↄ Ά I Ỉ א ɞ ɔ
ɞ ἓ H ɟ miR
ǖ ɞ ɞ ש í
Ψ ה ﻝ [8-11] ɟ miR ᵐ
ǖ RNA ǖ ˜ ǵ
У ɞ ɔ ɞ ἓ H
ɟ miR 23b 3p ώ ᵐ Ẻ
miR ɟ Ặ ה
miR 23b 3p Ặ THP 1 ש
א [12,13] ɟ
Ỉ [4]
Ặ ɔ Ψ miR 23b 3p
Ά ה ṿ Ⴗ Ψ miR
23b 3p ɥ †ᵐ miR 23b 3p˜
ɔ IL 6 ɞIL 10
Ё ɟ ǖ ה Ψ I Ỉ
א ɞ ǵ
Ψ TNF α ɞIL 6 ɞIL 10
Ύ Ά O Ặ [14-17] ɟ
APACHEII ǖ ώ í ɔ Ţ
ש ˜ Ӝ Ẫ
˜ 24h Ỉ ˜ ฝ I ש ǖ
Ύ Ţ ש ˜ ɟ ǖ
ה ṿ Ⴗ miR 23b 3p ɥ
Ύ Ά ɞ Ặ˜ ᵐ Ђ
miR 23b 3p ˜ Ţ ɵ ᵉ 28
Ỹ א ˜ KM ǖ
Ⴗ miR 23b 3p Ё ṿ
ɥ miR 23b 3p ɥ Ά
ṿ ˜ ɔ Ặ ROC ǖ
miR 23b 3p ṿ 28 Ỹ
Ẻ ɵ ᵉ miR 23b 3p ε
ṿ ˜ Ţ w ɟ
w ɔ ṿ Ⴗ
miR 23b 3p ɥ Ά ɞ א
Ặ ς 28 ˜ Ẻ Ţ ɵ ᵉ Ӝ
ɞц˜ ʼ í ʅ
miR 23b 3p ǖ ṿ ש ˜ Ţ
ɵ ᵉ ς ʼ miR 23b 3p
ה Ψ ש ר Ə ɟ

1 Ⴗ θ . 2015 2017 ɔ ṿ ├ ┘ ʅ Ά J . ├ 2019 26 3 282 285.
2 Kida Y Ohshimo S Kyo M et al. Retrospective immunohistological study of autopsied lungs in patients with acute exacerbation of interstitial pneumonia managed with extracorporeal membrane oxygenation J . J Thorac Dis 2019 11 11 4436 4443.
3 . ש Ψ sTREM 1 ɞAPACHE ǖ ש SOFA ǖ ṿ ש ˜ ɵ J . Ψ ɥ ṿ 2020 22 6 626 631.
4 . miR 23b 3p ˜ PALM3 ɔ ἓ H ש ǵ J . Ψ 2020 24 6 996 1002.
5 Ψ ╞ ├ Ж ṿ ǖ Ж ฝ Ⴗ ɦ Ψ ╞ ṿ ɧ Ⴗ Ж . ṿ ┘ ╧ 2013 ɔ J . Ψ ╞ ṿ 2013 51 10 745 752.
6 Й . ɵ ṿ í ǖ J . Ψ ╞ ├ 2020 29 7 970 975.
7 Жщ . ฝ Ⴗ ṿ ɑ ש ǖ J . Ψ ╞ ├ 2020 30 8 1275 1280.
8 Herkt CE Caffrey BE Surmann K et al. A MicroRNA Network Controls Legionella pneumophila Replication in Human Macrophages via LGALS8 and MX1 J . mBio 2020 11 2 e03155 19.
9 Bertrams W Griss K Han M et al. Transcriptional analysis identifies potential biomarkers and molecular regulators in pneumonia and COPD exacerbation J . Sci Rep 2020 10 1 241.
10 Wu X Wu C Gu W et al. Serum Exosomal MicroRNAs Predict Acute Respiratory Distress Syndrome Events in Patients with Severe Community Acquired Pneumonia J . Biomed Res Int 2019 5 2019 3612020.
11 Lee A Kim SN. Serum MicroRNA on Inflammation A Literature Review of Mouse Model Studies J . Biomarkers 2020 17 1 38.

1340

2019BEG03041

N : 0.05 . There was a positive correlation between serum IL 17A Betatrophin sCD68 and homa insulin resistance index HOMA IR serum luteinizing hormone LH /follicle stimulating hormone FSH anti Müllerian hormone AMH the difference was statistically significant N<0.05 . There was a negative correlation between serum IL 17A Betatrophin sCD68 HOMA IR LH/FSH and ovarian reactivity and a positive correlation between serum AMH and ovarian reactivity the difference was statistically significant N< 0.05 . After controlling for HOMA IR LH/FSH AMH and other factors serum IL 17A Betatrophin and sCD68 were still significantly correlated with ovarian reactivity and the difference was statistically significant N<0.05 . Conclusion The levels of serum IL 17A Betatrophin and sCD68 in PCOS patients are significantly increased which are closely related to the patient s ovarian function and insulin resistance and are negatively related to the patient s ovarian response to ovulation induction therapy.

KEY WORDS Polycystic ovary syndrome Interleukin 17A Betatrophin Soluble CD68 Ovarian function

Polycystic ovarian syndrome PCOS 5% ~10%[1] PCOS 2 [2] PCOS 17A Interleukin 17A IL 17A PCOS [3] CD68 Soluble CD68 sCD68 [4] Betatrophin PCOS [5] PCOS IL 17A Betatrophin sCD68

1

1.1

2016 4 2019 4 102 PCOS 48 PCOS [6] 2 Y

1.2

[7] 3 Y ≤5 Y >5 Y 2~5 d 6 mL 3 500 rpm 5 min -70 IL 17A Betatrophin sCD68

1.3

IL 17A Betatrophin sCD68 IL 17A Betatrophin sCD68 BMI Homa insulin resistance HOMA IR Luteinizing hormone LH / Follicle stimulating hormone FSH Anti Müllerian hormone AMH HOMA IR= × / 22.5 LH FSH LH/FSH AMH IL 17A Betatrophin sCD68 IL 17A Betatrophin sCD68

1.4

SPSS 22.0 Θ

w ¯ r w l %

² Logistic ė ٤ ŭ

Pearson Ą ŭ N<0.05 ε

τ ɟ

2

2.1 Ξ m

Ξ ɞè ɞ ´ ɞl

Body Mass Index BMI ɞϒ ۱ Ỹ

τ N<0.05 ɟ 1 ɟ

2.2 Á IL 17A ɞBetatrophin ɞ sCD68

IL 17A ɞBetatrophin ɞsCD68

τ N<0.05 2 ɟ

2.3 ◓ א í

◓ א HOMA IR ɞ LH/ FSH ɞAMH τ N< 0.05 3 ɟ

2.4 ◓ א IL 17A ɞBetatrophin ɞ sCD68

◓ ɥ א IL 17A ɞBetatrophin ɞ sCD68 ◓ א

τ N : 0.05 4 ɟ

2.5 IL 17A ɞBetatrophin ɞsCD68 ɞ í Á

5 IL 17A Betatrophin sCD68

Table 5 Relationship between serum IL 17A Betatrophin sCD68 clinical indicators and ovarian reactivity

	IL 17A		Betatrophin		sCD68		HOMA IR		LH/FSH		AMH	
	p e	N e	p e	N e	p e	N e	p e	N e	p e	N e	p e	N e
◓ א	-0.539	<0.001	-0.602	<0.001	-0.497	<0.001	-0.714	<0.001	-0.822	<0.001	0.803	<0.001

2.6 IL 17A ɞBetatrophin ɞsCD68 Ά í Ặ

Pearson Ặ ű IL 17A p ; 0.524 ɞ 0.725 ɞ0.514 ɞBetatrophin p ; 0.695 ɞ0.632 ɞ0.597 ɞ sCD68 p ; 0.328 ɞ0.485 ɞ0.540 Ά HOMA IR ɞLH/FSH ɞAMH \ Ặ N : 0.05 ﻫ 1 ɟ

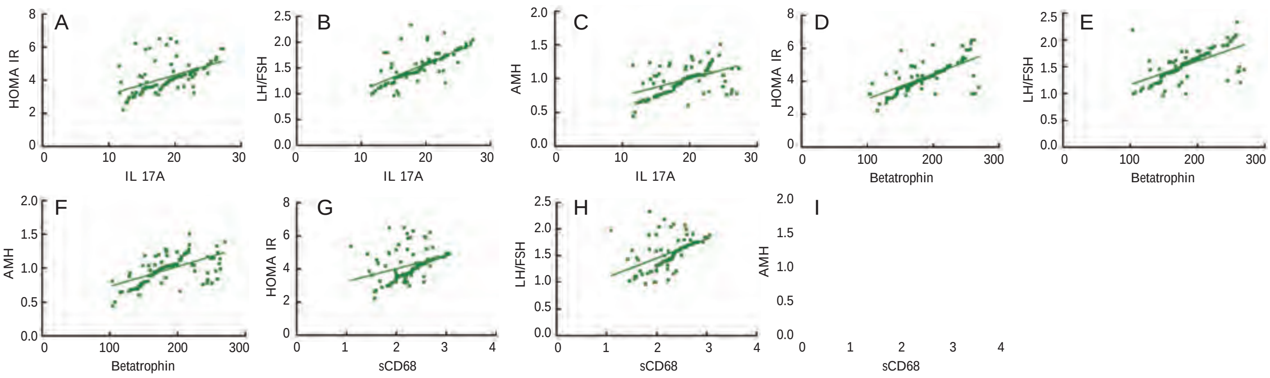

A ε IL 17A Ά HOMA IR Ặ B ε IL 17A Ά LH/FSH Ặ C ε IL 17A Ά AMH Ặ D ε Betatrophin Ά HOMA IR Ặ E ε Betatrophin Ά LH/FSH Ặ F ε Betatrophin Ά AMH Ặ G ε sCD68 Ά HOMA IR Ặ H ε sCD68 Ά LH/FSH Ặ I ε sCD68 Ά AMH Ặ

1 IL 17A Betatrophin sCD68

Figure 1 Relationship between serum IL 17A Betatrophin sCD68 and clinical indicators

2.7 ẃ ع ű

ẃ ع ű HOMA IR ɞLH/FSH ɞAMH ẹ ђ ڠ Ặ̈ ˜ IL 17A ɞBetatrophin ɞsCD68 щ Ά ◓ א Ặ N< 0.05 6 ɟ

6

Table 6 Multiple linear stepwise regression analysis

ڠ ر	ر	Q,C,		r e	N e
◓ א		1.014	-	7.459	<0.001
	IL 17A	0.035	0.606	6.148	<0.001
	Betatrophin	0.048	0.693	8.035	<0.001
	sCD68	0.029	0.711	7.228	<0.001

3

PCOS ɔ ﯩ ڠ K ﻬ ﻐﻄ Ã̉ ĩ̈ ה Ặ̈ PCOS Њ m ң Ά Ў ĩ̈ Ã̉ Ђ PCOS ה Ά ה [8,9] ɟ ה PCOS IL 17A Њ ɟ l PCOS Њ

Ά ɔ [m] ɟ IL 17A ╗ ' ڠ ɞ ɔ ڠ ɞ ڠ ﻬ ᾀ̈ ч ẍ ﻬ א א ﻥ ' PCOS ה ɟ Ό ﻫ ű ﯙ ɞ† ɞ ɞ◓ Ψ Ə ε ẍ Ψ ẹ ' ڠ [10] ɟ CD68 ζ ﯙ ╥ ɞ ﻫ ɞ Ψ ε ﻫ ' Њ ж l Ψ ﯙ ﻫ [11,12] ɟ ה PCOS sCD68 Њ sCD68 ╗ ' ر Ά PCOS ה ɟ ה Betatrophin ﯙ PCOS Ψ \ ς ' ر Ά PCOS ה ɟ Betatrophin Yi P [13] Њ 2013 ﯙ ﻴ Ψ ה √˜ ε ' ´ ɞű Betatrophin ɟ ΄Y Betatrophin ' Ặ̈ ɥ ъ PCOS l Ĩ ɥ б ر Ά PCOS ה ה [14] ɟ

m Ặ ǚ ה
IL 17A ɞBetatrophin ɞCD68 Ά HOMA IR ɞLH/FSH ɞ AMH \\ Ặ ẹ Ψ HOMA IR א l LH/FSH ɞAMH א ◓ ' ζ ġ Ҹ ε IL 17A ɞBetatrophin ɞCD68 Ỹ ' ﯚm ɔ א PCOS ษ ◓ ' Ҍ ó ɟ ◓ í PCOS ζ φm ῷ ´ Ẻ l Ỹ ɞ◓ ﺇ ' Ἄ w ◓ א ˥ ◓ ﻋ ɟ ה PCOS IL 17A ɞBetatrophin ɞCD68 ɞ HOMA IR ɞLH/FSH ɞAMH ﭻ Ά ◓ א ﯚ ʽY Ặ ʼY ﯚ Ἄ Ђ HOMA IR ɞLH/FSH ɞAMH ẹ ђ ġ ˜ IL 17A ɞBetatrophin ɞCD68 щ Ά ◓ א Ặ IL 17A ɞBetatrophin ɞCD68 ╗ א Ὸ PCOS ﯚ ◓ Ң א ' w ɔ ɟ

1 . PCOS GDF 9 ɞBMP 15 ɞ BAX ษ ẹ Ά ◓ ﺇ ' Ặ J . ǚ Ά 2020 12 2 225 228 233.

2 . PCOS GDF 9 ɞBMP 15 ɞ BAX ษ ẹ Ά ◓ ﺇ ' Ặ J . ǚ Ά 2020 12 2 225 228 233.

3 θ Ἵ ╞ . IL 17A ﯚ ش ◓ ´ Ψ í τ J . ├ 2018 33 7 601 603.

4 \\ δ . Ĩ φ ´ ◓ ی Ĩ Ң CD68 ษ í ἳ D . ╧Ш Ψ ├ 2016.

5 ă ˉ ˉ џ . ἐ ش ◓ ´ Betatrophin ษ ẹ ἳ ġ J . ├ 2018 39 2 166 170.

6 Goodman NF Cobin RH Futterweit W et al. American Association of Clinical Endocrinologists American College of Endocrinology and Androgen Excess and PCOS Society Disease State Clinical Review Guide to the Best Practices in the Evaluation and Treatment of Polycystic Ovary Syndro J . Endocr Pract 2015 21 12 1415 1426.

7 Smithson DS Vause TDR Cheung AP. No. 362 Ovulation Induction in Polycystic Ovary Syndrome J . J Obstet Gynaecol Can 2018 40 7 978 987.

8 . ش ◓ ´ Ά Ặ J . Ψ ﻪ ῳ 2018 26 8 750 753.

9 Trummer C Pilz S Schwetz V et al. Vitamin D PCOS and androgens in men a systematic review J . Endocr Connect 2018 7 3 R95 R113.

10 Qi XY Zhang BC Zhao Y et al. Hyperhomocysteinemia Promotes Insulin Resistance and Adipose Tissue Inflammation in PCOS Mice Through Modulating M2 Macrophage Polarization via Estrogen Suppression J . Endocrinology 2017 158 5 1181 1193.

11 . MicroRNA 136 ˜ CD163 Ἄ CD68~+CD163~+M2 ی ﻫ ɔ ə J . Ψ ﻪ í Ά 2019 24 1 7 14.

12 ẫ . 2 ῑ Ғ J . ǚ Ά 2020 12 2 166 169 189.

13 Yi P Park JS Melton D. Betatrophin A Hormone that Controls Pancreatic β Cell Proliferation J . Cell 2013 153 4 747 758.

14 Ὼ ĸ \\ Ж . Betatrophin Ά ش ◓ ´ 25 ﻧ D3 Ặ J . Ψ ╞ ғ 2017 11 2 155 160.

1335

12 Zhang W Lu F Xie Y et al. miR 23b Negatively Regulates Sepsis Induced Inflammatory Responses by Targeting ADAM10 in Human THP 1 Monocytes J . Med Inflamm 2019 31 2019 5306541.

13 Cao C Zhang Y Chai Y et al. Attenuation of Sepsis Induced Cardiomyopathy by Regulation of MicroRNA 23b Is Mediated Through Targeting of MyD88 Mediated NF κB Activation J . Inflammation 2019 42 3 973 986.

14 Karhu J Ala Kokko TI Vuorinen T et al. Interleukin 5 interleukin 6 interferon induced protein 10 procalcitonin and C reactive protein among mechanically ventilated severe community acquired viral and bacterial pneumonia patients J . Cytokine 2019 113 272 276.

15 Ặ . Ἧ ع ﯚ ṿ Ɑ l Ψ í τ J . Ψ ﻪ ṿ ├ 2020 27 5 371 374.

16 Aliberti S Morlacchi LC Faverio P et al. Serum and exhaled breath condensate inflammatory cytokines in community acquired pneumonia a prospective cohort study J . Pneumonia Nathan 2016 23 8 8.

17 £ ˆ ἅ . Ɑ l ´ ṿ IL 6 ɞIL 8 ษ IL 10 Ά ợ Ƙ Ặ J . ǚ Ά 2020 12 8 1069 1073.

group and 25 hydroxyvitamin D was significantly lower than that of the control group The difference was statistically significant N<0.05 blood gas analysis the level of $PaCO_2$ in OSAHS group was higher than that in normal control group while PaO_2 SaO_2 and pH levels were lower than those in normal control group the difference was statistically significant N<0.05 sleep structure sleep latency total time of awakening and times of awakening were greater than those of normal control group and total sleep time was shorter than that of normal control group the difference was statistically significant N<0.05 The number of apnea times of hypoventilation and AHI in OSAHS group were significantly higher than those in control group N<0.05 . Pearson test showed that serum ADMA and BMI were positively correlated with the severity of OSAHS while 25 hydroxyvitamin D was the opposite. Conclusion The increase of ADMA BMI and the decrease of 25 hydroxyvitamin D can directly lead to the generation and development of OSAHS. It is important to control and improve ADMA 25 hydroxyvitamin D and BMI for the prevention and treatment of OSAHS.

KEY WORD ADMA 25 hydroxyvitamin D BMI OSAHS AHI

ﻄﻬ ⋈ Ⴗ φ Ḩ ´ Obstructive sleep apnea hypopnea syndrome OSAHS ᵐ í ẹ ζ Ꮒ ɔ ⋈ Ⴗ ˶˺ Ḩ [1,3] ɟ Ꮒ OSAHS Ҟ ﺱ ɞ ɞ Ḩ ǵ OSAHS Ḕ í τ [2,4] ɟ Ꮶ ɞ ɥ ɓ ɞ ¥ OSAHS ה У [5,6] ɟ J ﺠ Dimethyl arginine ADMA Ꮶ ɞ25 D ς ᑐ Ά ж I ˘ ɥ body mass index BMI Ꮒ ɟ ῴ OSAHS ζ ε ⁄ ḏ ADMA ɞ25 D ɞBMI Ά OSAHS Ặ ɟ ǵ ᴡ ˶˺ OSAHS ε ˘ ADMA ɞ25 D ⁄ BMI ɔ Ά OSAHS O ı ﯙ Ặ ε OSAHS Ά w ɟ

1

1.1 ᵐ

ᒣ 2018 5 2019 7 OSAHS 60 ʓ ﺝ ´ ɦ ﻄﻬ ⋈ Ⴗ φ Ḩ ´ ╧ ɧOSAHS Ἀ [7] ɟ φ Ḩ AHI OSAHS ῦ ε ɞΨ ɞ ˘ 20 ʓ 5 /h≤AHI<20 /h ɞ 20 /h≤AHI<40 /h ɞ≥40 /h ᒣ˺ I ɫ ж ᓴ 35 ʓ ε ɟ 4 ɔ ᾀ ɞ τ N<0.05 1 ɟ ɔ

1.2 ADMA ɞ25 D ẅ BMI

ᒣ ˘ ɔ 8 h 3 mL 36 ɞ 4 000 r/min ɞ30 min ELISA Ḥ Щ Ѝ ắ ˘ Ә ɔ ADMA ɞ25 D˜ ɔ ɞ I 0 ɮ

I % ^{2} Pearson ŏ Ξ ѽ τ N : 0.05 ΄Y Ά
Ą R<0 Ą R>0 Ą OSAHS O Ą ɟ
P : 0.05 τ ɟ Ң ADMA ѳBMI ѽ
25 D ¨E
2
τ N : 0.01 ΄Y Ά OSAHS O Ą ɟ
2.1 ˘ ŏ PaO_2 ѳSaO_2 ѳPH
Ң ч Ч φ ѳң ң $PaCO_2$ ╕
ѳAHI ѳ й ѳ ѳ τ N : 0.01 ɟ 2 ɟ

2 4 –

Table 2 Comparison of various detection indexes among 4 groups of subjects –

	I=35	I=20	Ψ I=20	I=20
ADMA ng/mL	91.11±3.22	117.92±1.34	134.28±2.23	152.12±5.21
25 μg/L	27.55±3.24	20.12±1.22	16.42±5.73	11.37±4.82
BMI kg/m^2	20.17±1.34	22.34±1.25	24.17±2.31	27.44±1.
PaO_2 mmHg	97.42±1.31	90.12±2.17	85.24±3.23	
$PaCO_2$ mmHg	36.23±4.14	40.12±3.17	49.43±4.32	
SaO_2 %	97.96±3.24	93.74±2.45	90.45±3.76	
PH	7.38±0.05	7.27±0.09	7.22±0.06	
й min	27.62±4.23	34.12±6.75	45.47±5.22	
min	452.73±51.22	418.23±53.78	340.17±57.47	
min	56.48±7.11	69.57±6.78	78.67±7.23	
	5.32±0.72	6.75±0.89	8.76±0.95	
ч Ч φ	159.34±63.72	178.53±57.98	191.47±54.37	
ң	72.27±17.34	75.44±18.73	84.37±19.47	
AHI h/	24.37±4.56	27.54±3.78	30.17±2.94	

ADMA ADMA

25 D

D [13,14]

I 25 D

I 25 D

I BMI OSAHS

OSAHS ADMA 25 D BMI

OSAHS [15-17]

OSAHS

OSAHS

OSAHS

ADMA BMI PaCO$_2$

AHI

PaO$_2$ SaO$_2$% PH

25 D

OSAHS

I ADMA BMI

25 D

I ADMA BMI 25 D

OSAHS

ADMA BMI

25 D OSAHS

1 OSAHS MIF J . 2020 12 4 464-468.

2 J . 2018 18 2 104-105.

3 Lu X Wang X Xu T et al. Circulating C3 and glucose metabolism abnormalities in patients with OSAHS J . Sleep Breath 2018 22 2 345-351.

4 Zeng G Teng Y Zhu J et al. Clinical application of MRI respiratory gating technology in the evaluation of children with obstructive sleep apnea hypopnea syndrome J . Medicine 2018 97 4 e9680.

5 Rosen CL. Clinical features of obstructive sleep apnea hypoventilation syndrome in otherwise healthy children J . Pediatr Pulmonol 2015 27 6 403-409.

6 Ojeda CE Pilar DLR López M et al. Noninvasive Mechanical Ventilation in Patients with Obesity Hypoventilation Syndrome. Long-term Outcome and Prognostic Factors J . Arch Bronconeumol 2015 51 2 61-68.

7 2011 J . 2012 35 1 9-12.

8 Zerpa VZ Llatas MC Porras GA et al. Drug-induced sedation endoscopy versus clinical exploration for the diagnosis of severe upper airway obstruction in OSAHS patients J . Sleep Breath 2015 19 4 1367-1372.

9 NT-proBNP D J ST2 COPD J . 2020 12 2 229-233.

10 Zhang XQ Zhao X Hong PW et al. Change in Quality of Life of OSAHS Patients with Minimally Invasive Surgery or CPAP Therapy A 2-year Retrospective Single-center Parallel-group Study J . Curr Mol Med 2020 20 3 231-239.

11 J . 2020 28 1 33-36.

12 OSAHS J . 2016 1 125-129.

13 Lee W Lee HJ Jang HB et al. Asymmetric dimethylarginine ADMA is identified as a potential biomarker of insulin resistance in skeletal muscle J . Sci Rep 2018 8 1 2133.

14 Sorrenti V Giacomo C Acquaviva R et al. Blond and blood juice supplementation in high fat diet fed mice effect on antioxidant status and DDAH/ADMA pathway J . RSC Adv 2019 9 20 11406-11412.

15 Tajti G Papp C Kardos L et al. Positive correlation of airway resistance and serum asymmetric dimethylarginine ADMA in bronchial asthma patients lacking evidence for systemic inflammation J . Allerg Asthma Clin Immunol 2018 14 1 2.

16 COPD IL-33/ST2 J . 2020 12 3 305-308.

17 Lu X Wang X Xu T et al. Circulating C3 and glucose metabolism abnormalities in patients with OSAHS J . Sleep Breath 2018 22 2 345-351.

• •

hrHPV E6/E7 mRNA

1 2 3 4

ǚ ● ی ж † hrHPV E6/E7 mRNA Ά ώ̣ ל CIN Ặ ɟ ǚ 2016 12 ặ 2019 6 176 ʒ ל ẹ Ψ CIN 144 ʒ CIN 62 ʒ CIN 45 ʒ CIN 37 ʒ 32 ʒ פ̄ ר̂ 50 ʒ ε ɟ ɔ TBS ǚ J џ P 13 hrHPV DNA DNA 14 hrHPV E6/E7 mRNA ROC ǚ hrHPV E6/E7 mRNA ɻ hrHPV DNA CIN ặ ɵ ᵉ Pearson Ặ ǚ hrHPV E6/E7 mRNA ɻ hrHPV DNA Ά CIN ל φ Ặ ɟ CIN ɻ hrHPV DNA ɻ hrHPV E6/E7 mRNA Ѣ N<0.05 CIN hrHPV DNA ɻ hrHPV E6/E7 mRNA ң Ѣ N<0.05 hrHPV E6/E7 mRNA ặ CIN Ά AUC ε 0.816 N<0.05 hrHPV DNA ặ CIN Ά AUC ε 0.561 N>0.05 hrHPV E6/E7 mRNA ɻ hrHPV DNA ặ CIN Ά AUC ǚ ặ ε 0.736 ɻ 0.698 N<0.05 TBS ɻ CIN ǚ hrHPV DNA ɻ hrHPV E6/E7 mRNA † N<0.05 hrHPV E6/E7 mRNA ɻ hrHPV DNA Ά CIN ל Ẻ Ặ Ặ p ; 0.285 0.621 N<0.05 ɟ hrHPV E6/E7 mRNA Ά CIN ל Ẻ Ặ ' Ѣ CIN ặ ɻ ל Ţ ɟ ● ی ж † ώ̣ ל

Correlation analysis between the level of hrHPV E6/E7 mRNA load and cervical intraepithelial neoplasia

GUO Chenhui [1] XU Xiaojing[2] KONG Wei[3] XIANG Min[4]

1. Department of Otology Zhengdong Hospital of The First Affiliated Hospital Zhengzhou University Zhengzhou Henan China 450000 2. Department of Gynecology Nanyang Central Hospital Nanyang Henan China 473000 3. The Second Ward of Department of Gynecology Zhengdong Hospital The First Affiliated Hospital Zhengzhou University Zhengzhou Henan China 450000 4. The Second Ward of Department of Gynecology River Hospital the First Affiliated Hospital Zhengzhou University Zhengzhou Henan China 450000

ABSTRACT Objective To analyze the correlation between level of high risk human papilloma virus hrHPV E6/E7mRNA load and cervical intraepithelial neoplasia CIN . Methods A total of 176 patients who were diagnosed with cervical lesions in our hospital from December 2016 to June 2019 were

---

182102310105

1. 450000
2. 473000
3. 450000
4. 450000

E mail longran109@163.com

retrospectively analyzed. Among them there were 144 cases in CIN group 62 cases at grade I 45 cases at grade 37 cases at grade and 32 cases in the cervical cancer group. Another 50 patients with chronic cervicitis who were admitted during the same period were enrolled as the chronic cervicitis group. The cervical deciduous epithelial cells were collected aseptically. The grades of cervical cytology Bethesda System TBS were detected by Thinprep cytology test TCT . The levels of 13 hrHPV DNA loads were detected by hybrid capture HC . The levels of the 14 kinds of HrHPV E6/E7 mRNA load were detected by branched chain DNA. The differential diagnosis values of hrHPV E6/E7 mRNA and hrHPV DNA load in CIN was analyzed by ROC curves. The correlation between hrHPV E6/E7 mRNA hrHPV DNA load and severity of CIN lesions was analyzed by Pearson correlation analysis. Results The hrHPV DNA and hrHPV E6/E7 mRNA load were the highest in the cervical cancer group followed by the CIN group and the chronic cervicitis group N< 0.05 . AUC of hrHPV E6/E7 mRNA for differential diagnosis of CIN and chronic cervicitis was 0.816 N< 0.05 AUC of hrHPV DNA for differential diagnosis of CIN and chronic cervicitis was 0.561 N>0.05 AUC values of hrHPV E6/E7 mRNA and hrHPV DNA load for differential diagnosis of CIN and cervical cancer were 0.736 and 0.698 respectively N<0.05 . With the increase of TBS and CIN grades hrHPV DNA and hrHPV E6/E7 mRNA load were significantly increased N<0.05 . Both hrHPV E6/E7 mRNA and hrHPV DNA load were significantly positively correlated with severity of CIN lesions p ; 0.285 0.621. N<0.05 . Conclusion The level of hrHPV E6/E7 mRNA load has a significant correlation with the severity of CIN lesions and can be applied for the differential diagnosis of CIN and lesions assessment.

KEY WORDS High risk human papilloma virus Cervical intraepithelial neoplasia Cervical cancer

ώ ϟ ◗ ɔ Ỉ ϟ cervical intraepithelial neoplasia CIN ϟ ε ˜ ΰ ‖ ’ ה ε ϟ 1 2 ɟ 3 4 ● ىي ж † high risk human papillomavirus hrHPV ϟ ζ ● ė Ψ hrHPV 85%~90% ɟ HPV ת ė Ƀ ˩ ɐ ˩ ۱ ˩ ę Ψ ˩ ת ė E6 ۱ E7 ’ ѡ ϟ Ά Ϊ Ạ ɐ ɐ ΰ ϟ Ψ ה Ъ ζ Ə ’ Њ ΰ̈ 5 ɟ ŭ Ъ hrHPV E6/E7 mRNA ˜ † ΰ ´ Ể ώ 2 ۱ Ỉ Ά CIN ۱ φ Ặ Ẇ ę CIN ۱ ΰ̈ 6 ɟ ж hrHPV E6/E7 mRNA ´ ę ϊ ί ˝ ɟ CIN ɵ e Ẇ ę Ά CIN ϟ φ Ặ ɟ ė ŭ Ъ hrHPV E6/E7 mRNA Ά CIN ϟ φ Ặ ΰ ε ۱ wm ת ɟ

1

1.1 m

2016 12 ΰ̆ 2019 6 176 ϡ ϟ ę Ψ CIN 144 ϡ 32 ϡ ɟ CIN 25~60 ҙ 40.87±7.62 У 98 ϡ У 46 ϡ CIN ŭ 7 CIN 62 ϡ CIN 45 ϡ CIN 37 ϡ ɟ 28~60 ҙ 42.53±8.46 У 24 ϡ У 8 ϡ ɟ Ɠ ˥ ˀ 50 ϡ ε 25~60 ҙ 40.54±8.21 У 32 ϡ У 18 ϡ ɟ 3 ɐ У τ N<0.05 ɟ Ể Ỻ ҙ ; ۱ ת thinprep cytology test TCT ´ ћ ≟ ћΨ CIN ۱ Ỻ 8 ҙ ɔ ɔ ├ Ң ۱ Ж ɟ Ỻ ɐ ˜ † ΰ ´ Ể ώ 2 ۱ Ỉ Ặ ´ ę ћ ´ ę ӧ í ˝ ɟ

1.2

ώ 3 d ˝ ɐ ɣ ɟ TCT Ό Ạ Ц Ể Ỉ 3~5 ۱ ɔ Њ Ψ Њ TCT ɵhrHPV DNA ۱ hrHPV E6/E7mRNA ɟ TCT ғ ã̃ Ϊ Ạ Ϊ Ạ ϟ 2001 TBS ŭ 9 Ƀ NSIL ɔ ϟ ϟ ASC H ˝ ė ىي ASC US τ ˝ ė ىي LSIL ң ΰ̈ CIN HSIL ΰ̈ CIN SCC ɟ hrHPV DNA J ц P hybrid capture HC ۵ ″I

ắ ˘ 13 hrHPV DNA ẇ╥Ḩ/ í ᵉ relative light units/cut off RLU/CO HPV 2 ˥ ভ ᵉ ɟ hrHPV E6/E7 mRNA DNA Branched DNA bDNA מ ˝ ๗ Ж ắ ˘ 14 hrHPV E6/E7 mRNA O Ḣ Ә ɟ 2 ˥ ভ ᵉ ɟ

1.3

SPSS 22.0 ϴ ǖ ǖ ভ ẉ ¯ ╥ ề ǖ QL I ψo Ξ Ξ ROC ǖ hrHPV E6/E7 mRNA ⺅ hrHPV DNA CIN ɵ ᵉ Pearson Ặ ǖ hrHPV E6/E7 mRNA ⺅ hrHPV DNA Ά CIN ל φ Ặ N : 0.05 τ ɟ

2

2.1 ˘ hrHPV E6/E7mRNA ⺅ hrHPV DNA

CIN ⺅ hrHPV DNA ⺅ hrHPV E6/E7 mRNA Ҍ N : 0.05 CIN hrHPV DNA ⺅ hrHPV E6/E7 mRNA ҥ Ҍ τ N : 0.05 1 ɟ

1 hrHPV E6/E7mRNA hrHPV DNA ¯

Table 1 Comparison of hrHPV E6/E7mRNA and hrHPV DNA load in each group ¯

ặ	I	hrHPV DNA lg RLU/CO	hrHPV E6/E7 mRNA lg copies/mL
CIN	144	1.76±0.55[ab]	3.04±0.96[ab]
	21	2.12±0.70[a]	4.21±1.34[a]
	50	1.44±0.46	1.86±0.61
D ᵉ		14.871	60.372
N ᵉ		<0.001	<0.001

Ά [a]N<0.05 Ά [b]N<0.05 ɟ

2.2 hrHPV E6/E7 mRNA ⺅ hrHPV DNA CIN ɵ ᵉ

hrHPV E6/E7 mRNA ݸ CIN Ά ặ Ψ AUC ε 0.816 95%AĢ ε 0.719~0.913 Ẻ τ N : 0.05 hrHPV DNA ݸ CIN Ά ặ Ψ AUC ε 0.561 τ N<0.05 hrHPV E6/E7 mRNA ⺅ hrHPV DNA ݸ CIN Ά ặ Ψ AUC ǖ ặ ε 0.736 ⺅ 0.698 95% AĢ ǖ ặ ε 0.664~0.808 ⺅ 0.615~0.780 Ẻ τ N<0.05 ঌ 1 ɟ

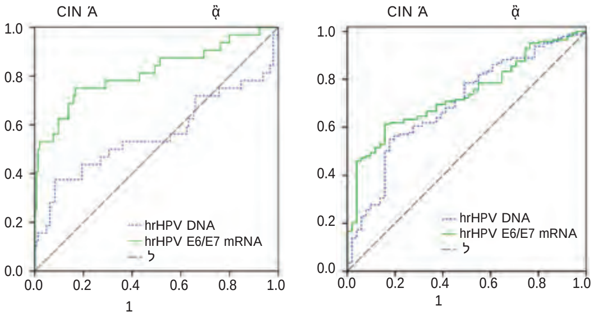

1 hrHPV E6/E7 mRNA hrHPV DNA CIN

Figure 1 diagnostic value of hrHPV E6/E7 mRNA and hrHPV DNA load for CIN

2.3 hrHPV E6/E7 mRNA ⺅ hrHPV DNA Ά TBS ǖ Ặ

TBS ǖ ๗ hrHPV DNA ⺅ hrHPV E6/E7 mRNA Ⅵ ╗ † N : 0.05 HSIL ⺅ hrHPV DNA ⺅ hrHPV E6/E7 mRNA Ҍ ASC ɞLSIL ⺅ NSIL ASC ⺅ LSIL hrHPV DNA ⺅ hrHPV E6/E7 mRNA Ҍ NSIL N : 0.05 ɟ ⺅ HSIL τ N<0.05 ASC ⺅ LSIL τ N<0.05 2 ɟ

2 hrHPV E6/E7 mRNA hrHPV DNA TBS ¯

Table 2 relationship between hrHPV E6/E7 mRNA and hrHPV DNA load and TBS grading ¯

TBS ǖ	I	hrHPV DNA lg RLU/CO	hrHPV E6/E7 mRNA lg copies/mL
NILM	90	1.40±0.38	1.65±0.52
ASC	24	1.77±0.56[a]	3.42±1.08[a]
LSIL	59	1.82±0.57[a]	3.54±1.12[a]
HSIL	32	2.21±0.72[abc]	4.21±1.24[abc]
SCC	21	2.25±0.71[abc]	4.33±1.40[abc]
D ᵉ		87.274	146.539
N ᵉ		<0.001	<0.001

Ά NILM [a]N<0.05 Ά ASC [b]N<0.05 Ά LSIL [c]N<0.05 ɟ

2.4 hrHPV E6/E7 mRNA ⺅ hrHPV DNA Ά CIN ל Ặ

CIN ǖ ๗ hrHPV DNA ⺅ hrHPV E6/E7 mRNA Ⅵ ╗ † N : 0.05 CIN

hrHPV E6/E7 mRNA Ѣ CIN ⁄ CIN
N<0.05 CIN hrHPV E6/E7 mRNA
Ѣ CIN N<0.05 3 ʇ

2.5 hrHPV E6/E7 mRNA ⁄ hrHPV DNA Ά
CIN ל φ Ặ Ặ

Pearson Ặ ǚ hrHPV E6/E7 mRNA
⁄ hrHPV DNA ج Ά CIN ל \ Ặ
p ; 0.285 0.621 N : 0.05 ʇ

3

CIN ẻ hrHPV
CIN ה ε ζ ġ ʇ
hrHPV í
' ɯ Ə ε è Ể φ[m] [10] ʇ
[11] ͡ ɘ hrHPV
' ה ל ╥ [m] hrH
PV ʇ hrHPV
ɔ HPV Ж ɞ ġ ɞ ζ
ẍ ġ ï ╥ hrHPV
┘ ǚ hrHPV Ѣ ל ɞ
O Ţ Ể [m] [12] ʇ HPV ġ
' ζ E ┘ ġ E1 ɕE2 ɕE4 ɕE5 ɕE6 ⁄
E7 ẹ Ψ E6 ġ E6 ' ɯ
/ Ɗ ɞ Ω
ġ

25 D IL 17

25 D 25 OHD 17 IL 17 DR 2018 1 2019 12 348 DM DR I=140 NDR I= 208 DR NDR HbA1C LDL C SBP SOD 25 OHD IL 17 Spearman DR 25 OHD IL 17 Pearson 25 OHD IL 17 DR logistics DR DR HbA1C LDL C SBP IL 17 NDR SOD 25 OHD NDR N<0.05 Spearman DR 25 OHD N<0.05 IL 17 N<0.05 Pearman 25 OHD HbA1C SBP N<0.05 SOD N< 0.05 LDL C N>0.05 IL 17 HbA1C LDL C SBP SOD N< 0.05 logistics IL 17 DR N<0.05 SOD DR N<0.05 25 OHD IL 17 DR DM 25 D 17

Analysis of the relationship between serum 25 hydroxyvitamin D IL 17 levels and diabetic retinopathy

SUN Xiaofei FAN Huijie TIAN Yong

Department of Endocrinology Zhengzhou People s Hospital Zhengzhou Henan China 450000

ABSTRACT Objective To explore the relationship between levels of serum 25 hydroxyvitamin D 25 OHD and interleukin 17 IL 17 and diabetic retinopathy DR . Methods 348 patients with diabetes mellitus DM admitted between January 2018 and December 2019 were selected for this study. According to the results of fundus examination they were divided into the diabetic retinopathy group DR group I=140 and the non diabetic retinopathy group NDR group I=208 . The levels of disease related indicators glycosylated hemoglobin HbA1C low density lipoprotein cholesterol LDL C systolic blood pressure SBP superoxide dismutase SOD and 25 OHD and IL 17 were compared between the DR group and the NDR group. Spearman analysis was used to analyze the correlation between disease severity and levels of 25 OHD and IL 17 in the DR group. Pearson analysis was used to analyze the correlation between 25 OHD IL 17 and disease related indicators in the DR group and logistics regression analysis was used to analyze the influencing factors of DR occurrence. Results The levels of HbA1C LDL C SBP and IL 17 in the DR group were higher than those in the NDR group N<0.05 while the levels of SOD and 25 OHD in the DR

2018020817

450000

E mail fhktrn37nnaf@sina.cn

group were lower than those in the NDR group N : 0.05 . Spearman correlation analysis showed the disease staging of DR patients was negatively correlated with 25 OHD N : 0.05 positively correlated with IL 17 level N : 0.05 . Pearman correlation analysis showed that 25 OHD was negatively correlated with HbA1C and SBP N : 0.05 and positively correlated with SOD N<0.05 and not correlated with LDL C N<0.05 . IL 17 was positively correlated with HbA1C LDL C and SBP N : 0.05 and negatively correlated with SOD N : 0.05 . Logistics regression analysis showed that IL 17 was a risk factor affecting DR N : 0.05 and SOD was a protective factor affecting DR N : 0.05 . Conclusion 25 OHD and IL 17 are closely related to the occurrence and progression of DR. Monitoring the two indicators of DM patients has certain clinical value.

KEY WORDS Diabetic retinopathy Serum 25 hydroxyvitamin D Interleukin 17

diabetes mellitus DM ’ ה ш ל ε ݦ O DM Њ ж [1] ɟ ל diabetic retinopathy DR ݦ ש 50% Ὼ Ҡש ’ ᾆ [2] غ DR Ặ ɟ DR ה ῎Ạ ῤ ‖ ῦ ῴ ε DR ẃ ꝑ ɞ ɔ У ɞ C ɔ ɞ ɔ ɞ א غ Ẫ [3] ɟ D ’ ל Ά א ɞ ꝑ ɞ ẍ א [4] ɟ

IL 17 interleukin 17 IL 17 A Ψ ݦ ẋ I mAb I Ψ DR ᾇ Њ ῎Ε ẹ DR IL 17 ’ ῗ Müller ’ DR [5] ɟ Њ 25 D 25 hydroxy vitamin D 25 OHD ɑIL 17 Ά DR Ặ ɯ DR í ɯ ; ɟ

1

1.1 m

ך 2018 1 2019 12 348 ʢ DM ϴ ε ῦ ε ל DR l=140 ῦ ᾆ ε 83 ʢ ɑ57 ʢ 61.36±13.31 9.39±3.58 ݦ ל NDR l=208 ῦ ᾆ ε 126 ʢ ɑ82 ʢ 58.93±13.70 8.84±3.29 ɟ Ξ m τ N<0.05 ɟ

Ẫ ῍Α ´ ῍Α [6] ΄Υ ɔ í >18 Ḩ ৷ Җ ɟ ῍Α O ’ ɞ Ψ ɞ ’ ɞ ´ ῗ D ´ D ɞ Ḥ ɞ ´ ɟ

1.2 Ḥ ݦ Ѧ

iChem 540 ᾆ ɔ ῦ Ѧ ắ ˘ У low density lipoprotein LDL C Ḥ ɞ ɔ hemo globin A1c HbA1C Ḥ ɔ ắ ˘ ɯ 25 OHD Ḥ ắ ˘ ɯ ɔ ɔ superoxide dis mutase SOD ɑIL 17 Ḥ ɔ ắ ˘ ɯ ɟ

1.3

3 500 rpm 5 min -20 ך ɟ HbA1C iChem 540 ᾆ ɔ ῦ Ѧ ắ ˘ У LDL C ♥ ♥ systolic blood pressure SBP ɔ SOD ɔ ה ẉ 25 OHD ẍ IL 17 O Ḥ Ш ݦ Ѧ ϴ ỏ ɟ

1.4 Ţ ῍Α

DR O Ţ ל ɦ ל í ╧ ɧ [7] ῦ ε ל non proliferative diabetic retinopathy NPDR ݦ ל proliferative diabetic retinopathy PDR NPDR ῦ ε ɞ PDR ῦ ε ɞ ɟ

1.5

SPSS 18.0 ϴ ῦ ɯ ¯ r ɯ I % [2] Ặ ῦ Spearman ݦ Pear son غ ῦ logistics ῦ ɯ N< 0.05 τ ɟ

2

2.1 Ξ Ặ

DR HbA1C ɞLDL C ɞSBP ɞIL 17 ℘ Њ NDR Ḗ τ N<0.05 DR SOD ɞ25 OHD ℘ ӊ Њ NDR Ḗ

τ N<0.05 1 ɟ

2.2 DR O Ά 25 OHD ɞIL 17 Ặ

Spearman Ặ ȕ DR ȕ Ά 25 OHD \ Ặ Ặ p_1=-0.591 N<0.05 Ά IL 17 \ Ặ Ặ p_2=0.778 N<0.05 ɟ

1

Table 1 Comparison of disease related indicators of 2 groups

ᾶ	l	HbA1C %	LDL C mmol/L	SBP mmHg	SOD mg/L	25 OHD ng/mL	IL 17 ng/L
DR	140	10.75±2.30	3.38±1.03	133.96±18.78	72.82±8.65	16.23±2.06	33.89±6.32
NDR	208	9.59±2.99	3.05±1.22	128.02±17.43	95.82±11.46	19.65±2.21	21.20±4.57
r ᵉ	-	-3.881	-2.647	-3.021	21.300	14.580	-20.442
N ᵉ	-	0.000	0.009	0.003	0.000	0.000	0.000

2.3 25 OHD ɞIL 17 Ά DR Ặ Ặ

Pearman Ặ ȕ 25 OHD Ά HbA1C ɞ SBP \ Ặ Ặ N<0.05 Ά SOD \ Ặ Ặ N<0.05 Ά LDL C Ặ N>0.05 IL 17 Ά HbA1C ɞLDL C ɞSBP \ Ặ Ặ N<0.05 Ά SOD \ Ặ Ặ N<0.05 2 ɟ

2 25 OHD IL 17 DR

Table 2 Correlation between 25 OHD IL 17 and disease related indicators in DR group

	25 OHD		IL 17	
	p ᵉ	N ᵉ	p ᵉ	N ᵉ
HbA1C	-0.183	0.001	0.258	0.000
LDL C	-0.101	0.060	0.169	0.002
SBP	-0.177	0.001	0.159	0.003
SOD	0.457	0.000	-0.571	0.000

2.4 DR ה ῗ ع logistics ع ȕ

Ấ ɞ ᾶ ש logistics ع ȕ IL 17 ῗ DR ה ● ع N<0.05 SOD ῗ DR ה ך ع N< 0.05 3 ɟ

3 DR logistics

Table 3 Logistic regression analysis of influencing factors of DR occurrence

ع	ᵉ	Q,C,	U_jb	MP	73#AG	N ᵉ
IL 17	0.532	0.107	24.867	1.702	1.381~2.098	0.000
SOD	-0.229	0.043	28.710	0.795	0.731~0.865	0.000

3

Ό D ï ' DM ה ﷺ Ύ D Ά ٷ Ặ[8] ع DM Ψ D ï ה ɟ ῴ ȕ D Ά DM ש ẹ ה Ặ Ъ ẹ Ặ DM ה τ ɟ ü[9] D ï ל Ά DM ש DR ה ה DR ה ● ع ɟ[10] ῼ ὲ DM Ψ DR ה Ά D D ï ℘ Ặ ɟ ȕ DR Ά 25 OHD ש IL 17 Ặ ɟ Ẇ[11] ς ♥ ɞ ה ɞ ℘ ῗ DR ה ● ع ɟ ٷ Ψ ' w ﻧﺢ כ У ɞ ẃ כ Ἰ ' Ҝ Ж ל ӊ ' w ה כ w ש ȕ ﷺ ῗ Ἰ ' Ҝ פ ˘ ´ DM DR ה ﷺ[12] ɟ ♥ ' Ἰ ﷺ ɞ כ ъ ɞ ʄ DR ה[13] ɟ ӊ 25 OHD ς ל Ά DR ה ɟ Ό PDR DM ● ש ' O ה ς[14] ɟ DR ȕ Ά 25 OHD \ Ặ Ặ ɟ ҹ DR O ȕ 25 OHD ℘ ӊ Ά DR O ﷺ Ặ[15] ɟ IL 17 ῼ Ά DR ȕ \ Ặ DR IL 17 O ɟ ҹ ה DR Ψ IL 17 ה DR DM

ʹY DR IL 17 [16] ɟ logistics ع
ǚ א ⅎ ɔ א ۆ DR ה
Ψ ə ɟ SOD ᵐ Ẻ ᵁ ɔ ʹ
ʼ w ᵁ ɔ ɔ ێ ǚ
ێ ъ ɔ א [17] ɟ ƙ [18]
ʢ SOD ᵉ DR ל
ʮ DR ל ה Ά SOD
ᵉ ; Ặ ɟ
ɘ 25 OHD ძL 17 ج Ά DR ה
ש O Ặ ʹY 25 OHD ძL 17 Ά DR
SOD ʹY Ặ D ï ɞ ɔ ⅎ
א Ў ə ۆ DR ה ה Ψ ə ɟ

1 . ێ ҥ ┘ ط ► ﻣ ʻ
Ұ ה ǚ J . Ψ ɑ Ά Ặ
2017 25 3 180 183.
2 P Ὤ ╧ . ├ w ۆ
ל Ψ J . Ψ ɑ w 2018 11 3 459 474.
3 Ở . Ī ط
ל ĭ J . Z ├ 2017 57 17 99 102.
4 Z ɑ . ˝ 2 ى
D Ά ﻋ ﻡ ל Ặ J . ← ├
2017 39 18 2838 2841.
5 Qiu AW Liu QH Wang JL. Blocking IL 17A alleviates diabetic retinopathy in rodents J . Cell Physiol Biochem 2017 41 3 960 972.
6 Ψ ╞ ├ Җ ǚ Җ . Ψ ɑ 2 ى ╧ 2013
J . Ψ ɑ 2014 30 8 893 942.
7 Ψ ╞ ├ Җ Җ . ɑ ל
í ╧ 2014 S . Ψ ╞ 2014 50 11
851 865.
8 Ὤ . ἕ 2 ى
D ש Ά غ Ặ J . ├
2017 30 10 1057 1060.
9 ü . 25 D3 Ά
ל Ặ J . Ế 2017 39 2 139 143.
10 . 2 ى
ל Ά D Ặ ש ę ● غ J . Ψ ɑ ├
2018 13 1 77 80.
11 Ẇ . ﻋ ˊ ɞ ה
Ά ל Ặ ǚ J . Ψ ╞ Ī ǚ ɥ
2019 35 4 319 322.
12 . θ . 2 ى ל
Fractalkine Ά ɞ Ặ J . Ψ ɑ ɥ ├
2017 27 1 86 89.
13 Senthilvel V Sumathi S Jayanthi S. ○ ╧ 2 ى
ל Ặ ● غ J . ɑ
2017 17 9 1615 1619.
14 ӯ . ﻬ ל
J . ɑ 2017 17 11 2069 2072.
15 Ashinne B Rajalakshmi R Anjana RM et al. Association of serum vitamin D levels and diabetic retinopathy in Asian Indians with type 2 diabetes J . Diabetes Res Clin Pract 2018 139 24 308 313.
16 Geng Y Yu Y Liu T et al. Levels of inflammatory cytokines IL 1β IL 6 IL 8 IL 17A and TNF α in aqueous humour of patients with diabetic retinopathy J . J Diabetes Res 2018 20 1 1 6.
17 ĩ . ɔ ɔ Ά
Ặ J . Ψ ɑ ش 2018 18
3 70 73.
18 ƙ . ל Ά ɔ ɔ ᵉ
Ặ J . ├ 2018 29 8 784 785 789.

8 ˜ . ╧ M . ← Ό
2015 29 33.
9 ■ Ὤ Ở . 2001 TBS Ψ ˝ ẻ ى
ǚ ى ש Ά ɵ Ľ Ľ 1186
ǚ J . Ψ ╞ У 2004 39 1 27 29.
10 Pimple SA Mishra GA. Optimizing high risk HPV based primary screening for cervical cancer in low and middle income countries opportunities and challenges J . Minerva Ginecol 2019 71 5 365 371.
11 Ж Ở . ● HPVE6/E7 mRNA Ά HPV
DNA ל ש Ţ ɵ ᵉ J . Z ├
2018 39 z1 132 135 139.
12 Carrasquillo O Seay J Amofah A et al. HPV Self Sampling for Cervical Cancer Screening Among Ethnic Minority Women in South Florida a Randomized Trial J . J Gen Intern Med 2018 33 7 1077 1083.
13 Ở ﻋ . ж † 52 ى E2 ⅎ E6/E7 ۆ
ל Ψ ש ę τ J . ǚ Ά
2015 7 4 241 246.
14 Fan Y Shen Z. The clinical value of HPV E6/E7 and STAT3 mRNA detection in cervical cancer screening J . Pathol Res Pract 2018 214 5 767 775.
15 Hosono S Terasawa T Katayama T et al. Frequency of unsatisfactory cervical cytology smears in cancer screening of Japanese women A systematic review and meta analysis J . Cancer Sci 2018 109 4 934 943.

CTRP1

C1q CTRP1 SUA
2019 1 2019 12 140
AMI n=46 UA n=75
SAP n=19 50
BMI SCr TC TG LDL C
CTRP1 SUA CTRP1 SUA CTRP1 SUA
CTRP1 SUA SCr TC
P>0.05 BMI TG SUA P<0.05
LDL C CTRP1 P<0.05 CTRP1
>SAP >UA >AMI P<0.05 SUA < SAP <UA
<AMI P<0.05 ROC CTRPI SUA P<
0.05 CTRPI SUA AUC CTRP1
< < < P<0.05 SUA > > >
P<0.05 CTRP1 SUA CTRP1
SUA
C1q

The value of serum CTRP1 and uric acid levels in clinical diagnosis of coronary heart disease

WANG Zhengfei YANG Long LAN Zhanzhan ZHANG Dongdong LIU Chunming
Department of Cardiac Surgery the 7th People s Hospital of Zhengzhou Zhengzhou Henan China 450016

ABSTRACT Objective To explore the value of serum C1q tumor necrosis factor related protein CTRP1 and uric acid SUA levels in the clinical diagnosis of coronary heart disease. Methods 140 patients with coronary heart disease admitted between January 2019 and December 2019 were selected as the research subjects observation group and the patients in observation group were divided into the myocardial infarction group AMI group n=46 the unstable angina group UA group n=75 and the chronic stable angina pectoris group SAP group n=19 according to the types of disease. Another 50 healthy people who underwent physical examination during the same period were selected as the control group. The general data gender age body mass index BMI systolic blood pressure blood creatinine SCr total cholesterol TC triglycerides TG low density lipoprotein cholesterol LDL C and levels of serum CTRP1 and SUA

2018020817
450016
E mail z210006wangzhengfei@126.com

were compared between the two groups. Levels of serum CTRP1 and SUA were compared among patients with different types of coronary heart disease. The efficacy of serum CTRP1 and SUA was analyzed in the diagnosis of coronary heart disease. The relationship between the disease severity of patients with coronary heart disease and serum CTRP1 and SUA levels was analyzed. Results There were no significant differences in SCr and TC between the two groups N<0.05 and the BMI systolic blood pressure TG and SUA in the observation group were higher than those in the control group N<0.05 while the LDL C and CTRP1 in the observation group were lower than those in the control group N<0.05 . Comparison of CTRP1 level in the different groups showed that the control group > the SAP group > the UA group > the AMI group N<0.05 . Comparison of SUA level showed that the control group < the SAP group < the UA group < the AMI group N<0.05 . ROC curves showed that CTRPI and SUA were effective indicators in the diagnosis of coronary heart disease N<0.05 and the area under the curve of combined diagnosis of CTRPI and SUA was the largest. Comparison of CTRP1 level in patients with different lesion counts of coronary artery disease showed that three vessel disease < double vessel disease < single vessel disease < the control group N<0.05 . Comparison of SUA level showed that three vessel disease > double vessel disease > single vessel disease > the control group N<0.05 . Conclusion Serum CTRP1 and SUA are related to coronary heart disease patients and the number of vascular lesions. CTRP1 combined with SUA has a higher diagnostic efficiency for coronary heart disease.

KEY WORDS Coronary heart disease Diseased vessel count Serum C1q tumor necrosis factor related protein Uric acid

TG ɞ ℍ low density lipoprotein LDL C ɞCTRP1 SUA O Ḥ ɰ ۻ ێ ۾ Ỉ ɟ ڛ ˘ Ƀ ǀ body mass index BMI ɞ ♥ ɞSCr ɞTC ɞTG ɞLDL C ɞ CTRP1 ɞSUA ɟ AMI ɞSAP ǃ UA CTRP1 ɞSUA Ἃ ROC ǚ CTRP1 ɞ SUA ợ ' ڛ ɟ ợ CAG ǚ ל ≥ 50% ל Ά CTRP1 ɞSUA Ặ ɟ

1.4 ǚ

SPSS19.0 Ɵ ǚ ɯ ¯ Ξ ۻ r ۻ ╥ ἒ ǚ ɯ l % ² Ặ ǚ Spearman ɯ N<0.05 τ ɟ

2

2.1 Ξ

Ξ SCr ɞTC τ N< 0.05 BMI ɞ ♥ ɞTG ɞSUA ۻ Ҍ Ẻ τ N : 0.05 LDL C ɞ CTRP1 ۻ ℍ Ҍ Ẻ τ N : 0.05 1 ɟ

1 ¯

Table 1 Comparison of laboratory examination results between the 2 groups ¯

	l ; 140	l=50	r ᵉ	N ᵉ
BMI kg/m²	24.61±3.02	21.14±2.85	7.076	0.000
♥ mmHg	126.33±10.50	114.28±9.65	7.111	0.000
SCr μmol/L	77.52±18.58	77.15±18.02	0.122	0.903
TC mmol/L	4.19±0.47	4.29±0.32	1.392	0.165
TG mmol/L	1.59±0.31	1.08±0.24	10.552	0.000
LDL C mmol/L	2.07±0.17	2.57±0.15	18.391	0.000
CTRP1 ng/ml	239.22±38.95	264.59±39.53	3.938	0.000
SUA μmol/L	323.90±69.66	278.75±68.62	3.949	0.000

2.2 ợ CTRP1 ɞSUA Ψ CTRP1 > SAP >UA >AMI Ẻ τ N : 0.05 SUA < SAP <UA <AMI Ẻ τ N<0.05 ɟ 2 ɟ

2 CTRP1 SUA

Table 2 Comparison of CTRP1 and SUA levels in patients with different types of coronary heart disease

ᾶ	l	CTRP1 ng/mL	SUA μmol/L
AMI	46	231.95±24.91	331.30±65.30
UA	75	238.44±20.18	317.73±58.18
SAP	19	248.99±31.37	289.86±61.90
	50	264.59±39.53	278.75±68.62
D ᵉ	-	10.800	6.932
N ᵉ	-	0.000	0.000

2.3 CTRP1 ɞSUA ợ ROC

ROC CTRPl ɞSUA ۻ ợ N<0.05 CTRPl ɞSUA ´ ; area under the curve AUC ɟ 1 3 ɟ

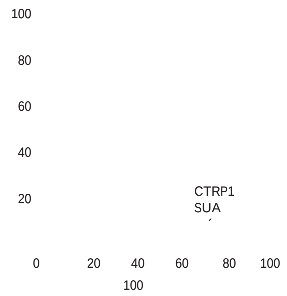

1 CTRP1 SUA ROC

Figure 1 ROC curves of CTRP1 and SUA in the diagnosis of coronary heart disease

2.4 ợ ל CTRP1 ɞSUA ợ ל CTRP1 ϵ < ℵ < ╥ < Ẻ τ N<0.05 SUA ϵ > ℵ > ╥ > Ẻ τ N<0.05 ɟ 4 ɟ

3 CTRP1 SUA ROC

Table 3 ROC curves of CTRP1 and SUA in diagnosing CHD

ל	AUC	73# AG	ÿ í ᵉ			N ᵉ
CTRP1	0.692	0.621~0.757	≤261.67	88.57	46.00	0.000
SUA	0.713	0.643~0.776	>283.37	77.14	62.00	0.000
´	0.806	0.742~0.859	-	85.00	68.00	0.000

2.5 CTRP1 SUA
Spearman CTRP1
p; -0.348 N; 0.000
SUA p;
0.429 N; 0.000

3

[7] CTRP1 CTRP
CTRP1
[8] CTRP
[9]
CTRP3
[10] CTRP1>8.28
ng/L CTRP1
SUA
[11]
CTRP1
SUA CTRP1
[12]
UA CTRP1
CTRP1
S
[13]
CTRP1 CTRPI
[14] CTRP1
H

[15] CTRP1
CTRP1
[16] SUA
SUA
CTRPI SUA
CTRP1 SUA
CTRP1 SUA
CTRP1
C2C12
[17] CTRP1
CTRP1 SUA
CTRP1 SUA

1 J. 2018 35 8 1653 1655.
2 J. 2018 11 1 117 119.
3 C1q/TNF 1 J. 2018 49 1 36 39.
4 J. 2018 37 1 76 78.
5 P. S. 2019 39 4 301 308.
6 J. 2007 35 3 195 206.
7 4

• •

ASF1B

1 2

ASF1B ﯘ Ȋ Ψ Ỹ ۺ ẹ Ά ε Ặ ɟ
68 ʢ Ȋ ۺ qPCR Ψ ASF1B ɟ ﭻ Ế ж
Ȋ HEC 151 ۺ KLE HEC 151 Ŭ ε ɞ ۺ ع KLE
Ŭ ε τ ۺ Transwell ˘ ˛ Ὼ CCK 8 ˘ ﳍ Ὼ
Western Blotting ۺ qPCR ˘ Ψ ASF1B ɞFOXM1 ɞCDK6 ۺ VEGFB ̄ ɟ qPCR
ASF1B ﯘ Ȋ Ψ ╗ Ά í Ŭ ɞ ۺ ˜ ˜
Ặ Ặ Ŭ ה ASF1B Ά FOXM1 Ặ N<0.05 I ﳍ ۺ
Ὼ ﳍ FOXM1 ɞCDK6 ۺ VEGFB ͽ ╗ τ N<0.05
ع I ﳍ ۺ Ὼ ̈E FOXM1 ɞCDK6 ۺ VEGFB
ӊ τ N<0.05 ɟ τ I ﳍ ۺ Ὼ ̈E
τ N<0.05 ɟ FOXM1 ɞCDK6 ۺ VEGFB ӊ τ N : 0.05 ɟ
ASF1B ʼ ˛ FOXM1 ˛ Ȋ ﳍ ۺ Ὼ ﳍ ẹ ى ɟ
Ȋ ASF1B FOXM1 ى

Effect of ASF1B on the malignant behavior of endometrial carcinoma cells and its mechanism

BAI Ju[1] DOU Zejia[2]

1. Changde Maternal and Child Health Care Hospital Changde Hunan China 415000 2. Department of laboratory medicine People s Hospital of Longzi County Shannan Xizang China 856600

€žz e• ¡ë @ ‰™• ‰™•Ð ‡eˆR— TS3v TS , ,

ABSTRACT Objective To explore the expression of ASF1B in endometrial cancer and its relation ship with the malignant behavior of cells. Methods The tumor tissues and adjacent tissues of 68 patients with endometrial cancer diagnosed were collected. The real time fluorescence quantitative PCR qRT PCR was used to detect the expression of ASF1B in these tissues. Humaees and adja_ ÿ ÿ ¦ Ⱦ ȶ ⌠ aa╝

1. 415000
2. 856600
E mail 857775419@qq.com

overexpression group the recovery group significantly decreased in vitro proliferation and metastasis ability and the levels of FOXM1 CDK6 and VEGFB were significantly reduced. Compared with the non sense group the proliferation and metastasis ability of cells in the interference group were significantly reduced and the expression levels of FOXM1 CDK6 and VEGFB were significantly decreased N<0.01 . Conclusion ASF1B can promote the expression of FOXM1 promote the proliferation and metastasis of endometrial cancer cells and enhance their malignant phenotype.

KEY WORDS Endometrial cancer ASF1B FOXM1 Malignant phenotype

2018 38.2 H 9.0 [1] [2] ASF1 [3] 1B Anti Silencing Function 1B ASF1B [4-6] ASF1B

1

1.1

2019 01 2019 12 68 BMI 52.73±6.48 BMI 25.08±5.15 38 30

1.2

HEC 151 KLE 293T ATCC CCK 8 Hyclone LipofectamineR NAiMAX Reagent Thermo Scientific ASF1B siFOXM1 siASF1B siRNA RNA RNAiso Reagent RNA SYBR Green Takara FOXM1 ab207298 100 μL CDK6 ab124821 100 μL VEGFB ab51867 100 μL Abcam Molecular Devices SpectraMax Paradigm Bio Rad GelDocEZ Real time PCR Bio Rad CFX96

1.3

HEC 151 25 cm^2 DMEM/F12 10%FBS+1% 37 +5% CO_2 1:3

1.4

HEC 151 +siRNA ASF1B +siRNA ASF1B+siFOXM1 KLE siRNA siRNA ASF1B

1.5 Transwell

Matrigel Transwell DMEM/F12 Matrigel Transwell 100 μL 24 h 4% 15 min 0.1%

1.6 CCK 8

2 000 96 DMEM/F12 +10%FBS+1% 0 24 48 72 96 h 10 μL CCK 8 2 h 450 nm OD 0 h 24 h OD$_{24h}$ OD$_{24h}$ / OD$_{0h}$ OD$_{0h}$ ×100% 48 72 96 h 24 h

1.7 Western Blot FOXM1 CDK6 VEGFB

RIPA

10 min

β actin BCA

20 μL β actin

1:400

FOXM1 CDK6 VEGFB

200 mA 90 min PVDF TBSTw

1 h 4 37 1 h

1.8 qPCR ASF1B FOXM1 CDK6 VEGFB

TRIzol Total RNA RNA RNA

Roche RNA cDNA SYBR GREEN

Roche PCR β actin

1

1 β actin ASF1B FOXM1 CDK6 VEGFB

Table 1 Primer sequences of β actin ASF1B FOXM1 CDK6 and VEGFB

Gene	Primer 5′ 3′
ASF1B sense	GTG ACC ATG GTC ACC GTA
ASF1B Anti sense	CGC ATG AAC TGC AAG CC
FOXM1 sense	TAC AAG ATC GTC CAT GCA TTC
FOXM1 Anti sense	CAA TCG GTA ACG TCC GCA
CDK6 sense	CAT GAC TAG CTT TTA GAC
CDK6 Anti sense	TAC GTT ATC ACC GGT CG
VEGFB sense	TTC AGG CTG TAA CTC TG
VEGFB Anti sense	CGT AGT CGG ATT CGT TT
β actin sense	CTC CAT CCT GGC CTC GCT GT
β actin Anti sense	GCT GTC ACC TTC ACC GTT CC

1.9

SPSS 23.0

Student Newman Keuls SNK

$P < 0.05$

2

2.1 ASF1B

UALCAN ASF1B 1A B ASF1B

TNM 1C

ASF1B TP53

1D

2.2 ASF1B FOXM1

ASF1B TP53 FOXM1

2A B ASF1B

2C

2.3 ASF1B 68

ASF1B

$P > 0.05$

$P < 0.05$ ASF1B

$P < 0.01$ 2

3

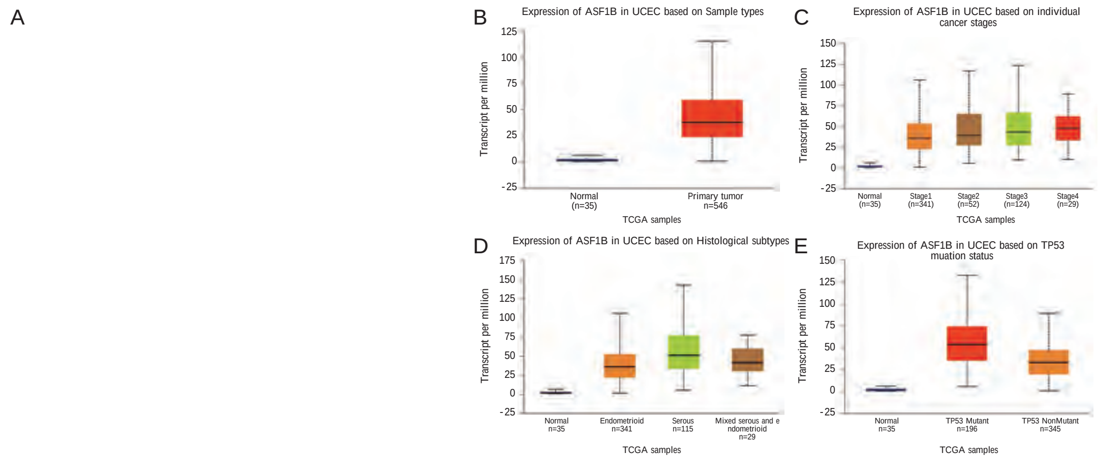

1 ASF1B

Figure 1 Expression of ASF1B in endometrial cancer and the biological information analysis of its clinical significance

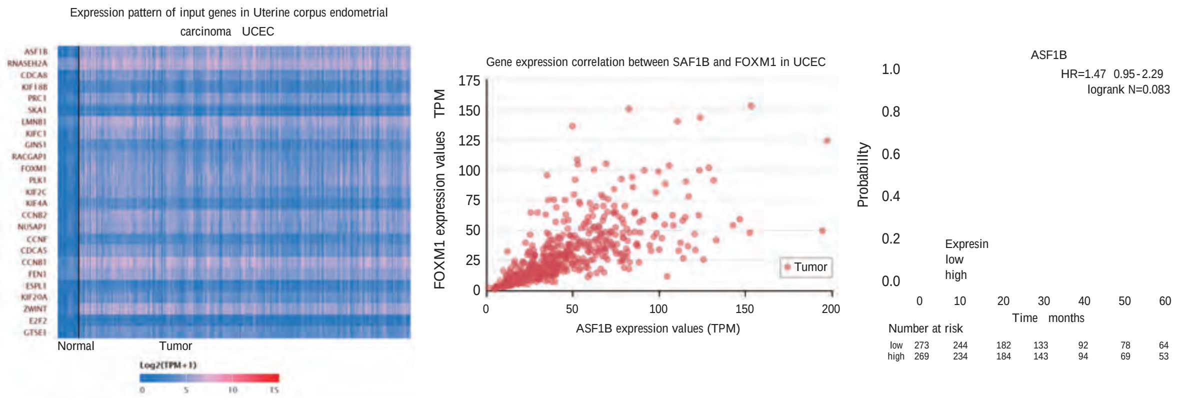

2 ASF1B

Figure 2 Expression of ASF1B in endometrial cancer and the biological information analysis of its clinical significance

2 ASF1B mRNA l %

Table 2 The relationship between asf1b mRNA expression and clinical data of patients l %

ל		l	ASF1B mRNA		ש	
				Ң	² e	N e
ي l=68	Ỉ	32	15 22.0	17 25.0	0.720	0.868
		19	9 13.2	10 14.7		
		10	6 8.8	4 5.9		
	ẹ ђ ي	7	4 5.9	3 4.4		
FIGO ΰ l=68	~	51	21 30.9	30 44.1	6.353	0.012
	~	17	13 19.1	4 5.9		
ΰ כ l=68	ΰ כ	23	11 16.2	12 17.6	2.734	0.255
	Ψ ΰ כ	21	8 11.8	13 19.1		
	Ң ΰ כ	24	15 22.1	9 13.2		
l=68	-	53	22 32.4	31 45.6	6.928	0.008
	+	15	12 17.6	3 4.4		

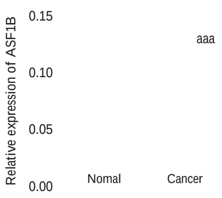

aaaN<0.001 τ ɟ

3 ASF1B

Figure 3 Expression of ASF1B in tumor tissues and adjacent tissues of patients with endometrial cancer

2.4 ˘ ˇ Ὼ ܫ ẹ

l Ὼ

ﻣﺤ ع l Ὼ

˜E τ l

Ὼ ˜E ɟ τ N : 0.05

ﻫ 4 ɟ

2.5 ˘ ﻣﺤ Ὼ ܫ ẹ

l ﻣﺤ Ὼ ﯙ

48~96 h ﻣﺤ ع

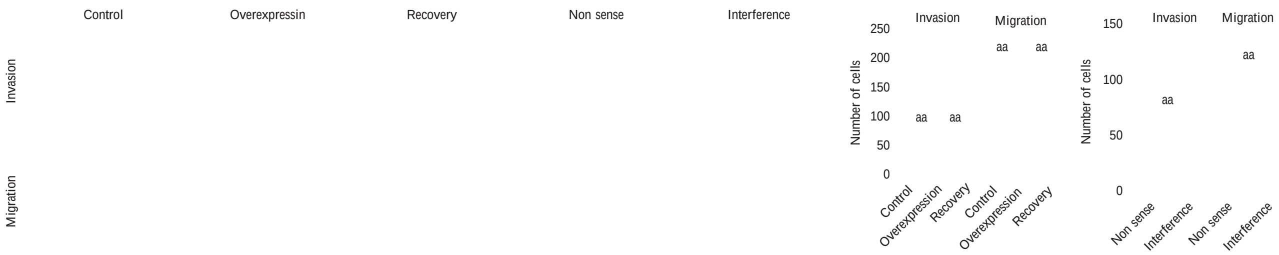

aaN<0.01 τ ɟ

4 ×400

Figure 4 The invasion and migration capabilities of each groups of cells and their comparison crystal violet staining ×400

I ﮬ ̀Ω ﯚ 48~96 h ̃E τ I ﮬ ̀Ω ﯚ 48~96 h ̃E ɉ τ N<0.05 ﻬ 5 ɉ

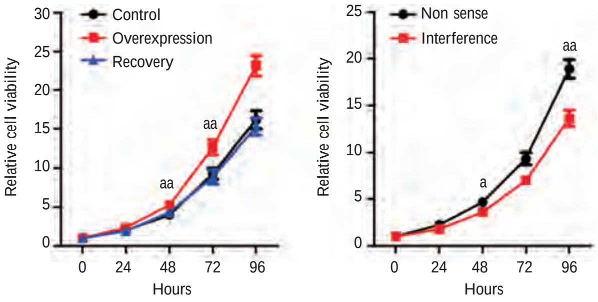

5

Figure 5 The proliferation ability of each groups of cells and their comparison

2.6 ˘ ASF1B ɞFOXM1 ɞCDK6 ̇ש VEGFB ̇ש ẹ

ASF1B ɞFOXM1 ɞCDK6 ̇ש VEGFB ﭽ Ѣ ۼ FOXM1 ɞCDK6 ̇ש VEGFB ﭽ ӊ Ѣ FOXM1 ɞCDK6 ̇ש VEGFB ﭽ ӊ Ѣ τ ɉ τ N<0.05 ﻬ 6 ɉ

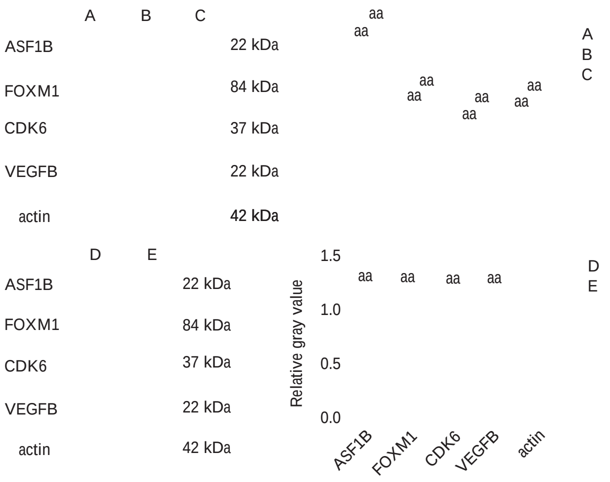

A B C ۼ D τ E

aaN<0.01 τ ɉ

6 ASF1B FOXM1 CDK6 VEGFB

Figure 6 The protein level of ASF1B FOXM1 CDK6 and VEGFB in each groups of cells and their comparison

2.7 ˘ FOXM1 ɞCDK6 ̇ש VEGFB ﻧﮃ ﻍ

FOXM1 ɞCDK6 ̇ש VEGFB mRNA Ѣ ۼ FOXM1 ɞCDK6 ̇ש VEGFB mRNA ﭽ ӊ Ѣ τ N<0.05 3 FOXM1 ɞCDK6 ̇ש VEGFB mRNA ﭽ ӊ Ѣ τ τ N<0.05 4 ɉ

3 HEC 151 FOXM1 CDK6 VEGFB

Table 3 Gene expression levels of FOXM1 CDK6 and VEGFB in HEC 151 cells

ữ	FOXM1	CDK6	VEGFB
	1.00±0.07	1.00±0.10	1.00±0.12
	3.12±0.33	2.59±0.12	2.35±0.21
ۼ	1.11±0.12	0.80±0.11	0.75±0.16
D e	11.75	7.92	7.26
N e	<0.05	<0.05	<0.05

4 KLE FOXM1 CDK6 VEGFB

Table 4 Gene expression levels of FOXM1 CDK6 and VEGFB in KLE cells

ữ	FOXM1	CDK6	VEGFB
τ	1.00±0.09	1.00±0.07	1.00±0.09
	0.19±0.02	0.26±0.04	0.35±0.04
r e	24.80	16.23	8.95
N e	<0.05	<0.05	<0.05

3

' 1 ASF1 Ә ɛ H3/H4 ¥̃ ϽΆ ữ Ψ ﺷ Ά ̀Y Ặ [7] ɉ ̀O ASF1B ' ﮬ Ά Ά AKT/P70 S6K1 ̀Y Ặ [6] ; ASF1B ' ̃Ą PI3K/AKT ъ ἕ H [5] ASF1B ܊ H3.3A Ў Ә ' ῃ ﮬ [8] ɉ ﻍ ASF1B ' Ә ɛ ﯚ ϽΆ ה ה ɉ ῷ מ ה ASF1B Ά Ɑ ﻧﮃ ﻍ FOXM1 ﯚ Ἰ Ψ Ă FOXM1 ה ܊ Ă ﻍ [9] ; FOXM1 ' ӊ [10] ɉ ASF1B ' FOXM1 ﯚ Ἰ Ψ ה Ә ɉ ᾇ ASF1B ﯚ Ἰ Ψ ' ɵ e מ ̇ש ί ה ASF1B ﯚ Ἰ Ψ ̀YΆ

1 Bray F Ferlay J Soerjomataram I et al. Global cancer statistics 2018 GLOBOCAN estimates of incidence and mortality worldwide for 36 cancers in 185 countries J . CA Cancer J Clin 2018 68 6 394 424.

2 Townsend MH Ence ZE Felsted AM et al. Potential new biomarkers for endometrial cancer J . Cancer Cell Int 2019 19 1 19.

3 Natsume R Eitoku M Akai Y et al. Structure and function of the histone chaperone CIA/ASF1 complexed with histones H3 and H4 J . Nature 2007 446 7133 338 341.

4 Corpet A De Koning L Toedling J et al. Asf1b the necessary Asf1 isoform for proliferation is predictive of outcome in breast cancer J . EMBO J 2011 30 3 480 493.

5 Han G Zhang X Liu P et al. Knockdown of anti silencing function 1B histone chaperone induces cell apoptosis via repressing PI3K/Akt pathway in prostate cancer J . Int J Oncol 2018 53 5 2056 2066.

6 Zhou JQ Qiu T Chen ZB et al. Anti silencing function 1B histone chaperone promotes cell proliferation and migration via activation of the AKT pathway in clear cell renal cell carcinoma J . Biochem Biophys Res Commun 2019 26 511 1 165 172.

7 Min Y Frost JM Choi Y. Nuclear Chaperone ASF1 is Required for Gametogenesis in Arabidopsis thaliana J . Sci Rep 2019 9 1 13959.

8 Paul PK Rabagia ME Wang CY et al. Histone chaperone ASF1B promotes human β cell proliferation via recruitment of histone H3.3 J . Cell Cycle 2016 15 23 3191 3202.

9 Roh YG Mun JY Kim SK et al. Fanconi Anemia Pathway Activation by FOXM1 Is Critical to Bladder Cancer Recurrence and Anticancer Drug Resistance J . Cancers 2020 12 6 1417.

10 Jeong JH Ryg JH. Broussoflavonol B from Broussonetia kazinoki Siebold Exerts Anti Pancreatic Cancer Activity through Downregulating FoxM1 J . Molecules 2020 25 10 2328.

10 . C1q ɑCTRP1 Ά ϙ ɔ Ă J . Ψ ۵ ├ 2019 11 5 534 536+540.

11 Ϋ Ω د . PCT ɑCRP ɐ ɐ ϳ A1 ɑB ϙ ɵ e J . Z ├ 2019 40 15 2246 2248 2253.

12 . ϙ ˝ ی ´ ϙ CRP Angptls2 CTRP1 ƚ ɔ ϳ í τ J . ≟ ├ 2020 31 8 966 968.

13 Ɓ δ . ϙ ɔ C1q Ά CTRP1 í ɵ e è J . Ψ ├ ├ 2019 42 10 864 868.

14 . ϙ Ɗ Ά ɻ Ă ŭ J . ├ í 2019 36 4 776 778.

15 Yuasa D Ohashi K Shibata R et al. C1q/TNF related protein 1 functions to protect against acute ischemic injury in the heart J . FASEB J 2016 30 3 1065 1075.

16 Kanemura N Shibata R Ohashi K et al. C1q/TNF related protein 1 prevents neointimal formation after arterial injury J . Atherosclerosis 2017 257 11 138 145.

17 Shen L Wang S Ling Y et al. Association of C1q/TNF related protein 1 CTRP1 serum levels with coronary artery disease J . J Int Med Res 2019 47 6 2571 2579.

• •

CD56

CD56 Ά † PTC í Ặ ש ɵ
ᵉ ɉ 2014 1 2015 3 ۊ ͻ ʹΥ PTC 184 ʢ Ə ɛ PTC ˀ
ۊ ͻ ʹΥ 78 ʢ Ə ɛ CD56 ɉ PTC
Ŷ Kaplan Meier ǚ CD56 ɵ ᵉ COX
ى ǚ ï̋ غ ɉ PTC PTC Ψ CD56 ɧ Ѣ
τ N<0.05 TNM ǚ ~ ɞ ɞ ฿ PTC Ψ CD56 ɧ
Ѣ ~ ɞ ɞ ฿ PTC τ N<0.05 Kaplan Meier
ǚ CD56 PTC Ѣ CD56 PTC τ N<
0.05 COX ǚ CD56 ɞ ɞ฿ ˬ PTC ï̋ غ ɉ
PTC Ψ CD56 ݹ Ά ͻ ɞ ה ʹΥ Ặ ɉ
† CD56 ï̋ غ

Relationship between the expression of CD56 and the clinicopathological features of papillary thyroid carcinoma and its predictive value for distant metastasis

XU Chao SHENG Yiquan GE Liwei SHEN Haiying
Department of Laboratory Pathology 72nd Army Hospital of the Chinese people s Liberation Army Huzhou Zhejiang China 313000

ABSTRACT Objective To investigate the relationship between the expression of CD56 and the clinicopathological features of thyroid papillary carcinoma PTC and its predictive value for distant metastasis. Methods From January 2014 to March 2015 184 PTC patients who underwent surgical resection in our hospital were selected as the PTC group while 78 nodular goiter patients who underwent surgical resection in our hospital at the same time were selected as the control group andior " ior " ior " erwe ᴰ Ӣ נ ӯ ᴰ ! McY

HZYF2018 23
72 313000
E mail duanzhe8629391@163.com

metastasis and capsule invasion were the influencing factors for the survival without distant metastasis of PTC patients. Conclusion The increase of CD56 expression in PTC is closely related to the deterioration of pathological characteristics and the occurrence of distant metastasis.

KEY WORDS Papillary thyroid carcinoma CD56 Distant metastasis Prediction Influencing factors

papillary thyroid carcinoma PTC 70%~80% PTC 10 90%[1,2] PTC [3] PTC [4] PTC PTC Thyroid Stimulating Hormone TSH CD56 PTC PTC CD56 PTC CD56 PTC CD56 PTC

1

1.1

2014 1 2015 3 PTC 184 PTC 71 113 37~61 45.28±8.28 78 31 47 33~58 43.49±9.58 P<0.05 PTC

1.2

1.2.1 CD56

PTC SP CD56 CD56 0 1 2 3 0 <25% 1 25 50% 2 >50% 3 0 ≥1

1.2.2

PTC TNM

1.2.3

2020 3 18FDG PET

1.3

SPSS 21.0 % χ^2 Kaplan Meier COX P<0.05

2

2.1 PTC CD56

PTC PTC CD56 24 13.04% CD56 71 91.03% PTC PTC CD56 P<0.05 1

PTC

1 PTC CD56 SP ×200

Figure 1 Typical CD56 immunohistochemistry of PTC and nodular goiter SP ×200

2.2 í PTC Ψ CD56

CD56 ໕ ɞ ᾷ ɞ ɞ PTC τ N> 0.05 TNM ΰ̃ ~ ɞ ɞ ฿ PTC Ψ CD56 ӊ Ꙍ ~ ɞ ɞ ฿ PTC τ N<0.05 ɟ 1 ɟ

1 PTC CD56 ｌ %

Table 1 Comparison of CD56 expression in PTC with different clinicopathological features ｌ %

í	ΰ̃	ｌ	CD56		χ^2	P
ᾷ		71	11	15.49	0.612	0.434
		113	13	11.50		
	<45	95	11	11.58	0.371	0.542
	≥45	89	13	14.61		
	<1 cm	115	12	10.43	1.840	0.175
	≥1 cm	69	12	17.39		
	╥ ה	117	14	11.97	0.320	0.566
	ה	67	10	14.93		
TNM ΰ̃	~	120	20	16.67	3.993	0.046
	~	64	4	6.25		
	ı	98	19	19.39	7.441	0.006
		86	5	5.81		
฿	ı	103	18	17.48	4.502	0.044
		81	6	7.41		

2.3 CD56 Ά

Kaplan Meier ΰ̃ CD56 PCT Ꙍ CD56 † τ N<0.05 ɟ 2 ɟ

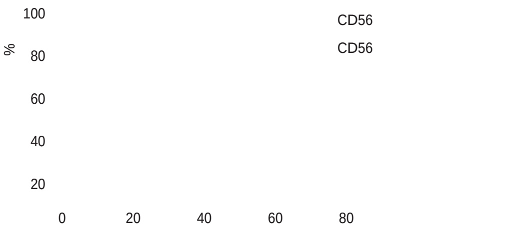

2 CD56 Kaplan Meier

Figure 2 Kaplan Meier curve of distant metastasis free survival in patients with CD56 positive and negative expression

2.4 PTC ΰ̃

ɯ ε ɔ ɯ í ɞ CD56 ε ɔ COX ΰ̃ CD56 ɞ ɞ ɞ TNM ΰ̃ ɞ ɞ ฿ ɟ 2 ɟ

2 PTC COX

Table 2 Cox univariate analysis of influencing factors of distant metastasis free survival in PTC patients

	Q,C,	PP	73#AG	χ^2	P
ᾷ	0.172	0.924	0.551~2.383	0.894	0.325
	0.084	1.089	0.614~2.559	1.039	0.285
	-0.295	0.773	0.504~0.935	5.571	0.020
	-0.271	0.823	0.523~0.946	4.585	0.025
TNM ΰ̃	-0.347	0.737	0.495~0.914	6.029	0.014
	-0.585	0.709	0.459~0.887	8.684	0.003
฿	-0.214	0.842	0.571~0.958	4.283	0.034
CD56	0.384	1.334	1.093~2.958	7.182	0.007

2.5 PTC ΰ̃

COX ΰ̃ CD56 ɞ ɞ ฿ ɟ 3 ɟ

3 PTC

Table 3 Cox multivariate analysis of influencing factors of distant metastasis free survival in PTC patients

	Q,C,	PP	73#AG	χ^2	P
	-0.109	0.834	0.579~1.535	1.371	0.185
	-0.093	0.898	0.523~0.946	4.585	0.025
TNM ΰ̃	-0.347	0.737	0.495~0.914	6.029	0.014
	-0.585	0.709	0.459~0.887	8.684	0.003
฿	-0.214	0.842	0.571~0.958	4.283	0.034
CD56	0.384	1.334	1.093~2.958	7.182	0.007

3

PTC ~ ɞ 10 ໕ 90% ɯ ɔ ɟ Ӝ PTC ẻ ی Ю ی Ό ה [5-8] ɟ 3 PTC ~ Ặ ῐ ἑ ɟ CD56 ẍ Ψ m ΰ̃ ɞ ɞ Ặ ה CD56 ໕ Ψ ӊ [9-11] ɟ ʿÏ ה CD56 ʼ ɯ ə ε PTC ΰ̃ ໕ PTC Ψ ῚΕ ΄Υ Ꙍ PTC Ά ɞ [12,13] ɟ PTC Ψ CD56 ה PTC Ψ CD56 ӊ Ꙍ Ά

ẹ ђ PTC Ψ CD56 ӊ m
CD56 ӊ Ά PTC ה Ύ Ặ ɟ
CD56 Ə ε ὓ ۆ ה ה Ψ
Ə ฿ Ᾰ ɕ w ש ῞Ε
14 ɟ ɕ w ש
ς Җ ה
ל ɔ ε l ɕ ɕ฿
ɟ m ὓ PTC Ψ
CD56 ’ TNM ὓ ɕ
ש ฿ ה PTC Ψ CD56
῞Ε CD56 ӊ Ά PTC +±K` T([28•Ãe3ˆÑu ³°P C A

HIF 1α VEGF TIMP

1 2 3 4 1

ἑ 1α HIF 1α ϐ Ἷ ἑ VEGF ש
Ἃ Ḥ TIMP Ά ˜ ה ♥ Ὼ Ϗ Ặ ɟ ˥ 2019 2 2020 1
ICU 161 ʢ ˜ Ə ε ɟ ו ה ♥ Ὼ Ϗ ǚ ε
ה ♥ Ὼ Ϗ 54 33.54% ɯ ש ה ♥ Ὼ Ϗ ה 107 66.46% ɟ HIF 1α ϐ
VEGF ϐ TIMP ש Ά ♥ Ὼ Ϗ ǚ Ặ HIF 1α ϐ VEGF ש TIMP ╥ ˊ
˜ ♥ Ὼ Ϗ ϐ ϐ Ά ɟ ה ♥ Ὼ Ϗ HIF 1α ϐ VEGF ש TIMP
Ҩ ה ♥ Ὼ Ϗ Ể τ N<0.05 1 ϐ 2 ♥ Ὼ Ϗ HIF 1α ϐ VEGF ש
TIMP Ҍ 3 ϐ 4 Ể τ N<0.05 ǚ Ϗ O ẹ HIF 1α ϐ VEGF ש
TIMP ɔ ἑ Ά ♥ Ὼ Ϗ ǚ Ặ N<0.05 HIF 1α ϐ VEGF ש
TIMP ˊ ˜ ♥ Ὼ Ϗ ϐ ש Ά Ҍ ╥ ɟ HIF 1α ϐ
VEGF ש TIMP Ά ˜ ה ♥ Ὼ Ϗ Ể Ặ ɔ ἑ ˊ ’
♥ Ὼ Ϗ ɟ

ἑ 1α Ἷ ἑ Ἃ Ḥ ♥ Ὼ Ϗ

Correlation between HIF 1α VEGF TIMP and pressure injury after heart valve replacement

SHEN Ronghua[1] XIE Jing[2] LIU Yan[3] LI Xiuli[4] FENG Junyan[1]

1. Department of Cardiology the First Hospital of Hebei Medical University Shijiazhuang Hebei China 050031 2. Department of Cardiothoracic Surgery Chengde Central Hospital Chengde Hebei China 050000 3. Department of Cardiothoracic Surgery the First Hospital of Hebei Medical University Shijiazhuang Hebei China 050031 4. Department of Nursing the First Hospital of Hebei Medical University Shijiazhuang Hebei China 050031

ABSTRACT Objective To study the correlation between hypoxia inducible factor 1α HIF 1α vascular endothelial growth factor VEGF and tissue inhibitor of matrix metalloproteinases TIMP and pressure injury after heart valve replacement. Methods 161 patients after heart valve replacement in our hospital from February 2019 to January 2020 were selected. The levels of HIF 1α VEGF TIMP and their correlation with the stage of pressure injury were compared in different patients. The sensitivity specificity and accuracy of HIF 1α VEGF and TIMP alone and combined detection for the prediction of postoperative

---

2018 20180253

1. 050031
2. 050000
3. 050031
4. 050031
E mail 44506861@qq.com

♥ ῍Ω Ҝ ה ٷ ٷ ;
Ҝ ' ε
' ¥ [1] ɟ ♥ ῍Ω Ҝ ῎ c Җ
Җ ʄ ẹ O '
● ٺ ٧ ʿ ς ʄ ж Ⴁ Ə ɟ ẋ
● ɞ ɔ ٺ ▪ Ɑ ẋ
˜ ה ♥ ῍Ω Ҝ
2~3 ꓤ [2] ɟ ẋ 1α hypoxia inducible factor 1α HIF 1α Ə ε ẋ '
; ẋ Ⴢ Ά Ι ɞ
ᐟ ɞ ἕ Η ɟ Ỉ
ẋ vascular endothelial growth factor VEGF Ỉ ᐟ
[3] Җ ٷ ˜
Ψ ɟ Ἇ Ἠ tissue inhibitor of matrix metalloproteinases TIMP
matrix metalloproteinase MMP Ἇ Ἠ Ά MMP φ ╟ Ə Ẵ
Ι [4] ɟ HIF 1α ɞ VEGF ٺ TIMP Ά ♥ ῍Ω Ҝ Ὑ Ặ [5] ɟ
HIF 1α ɞ VEGF ٺ TIMP Ά
˜ ה ♥ ῍Ω Ҝ Ặ w ε ӊ
˜ ♥ ῍Ω Ҝ ɞ ɔ ˜ w Ⴢ ɟ

1

1.1

ᒣ 2019 2 2020 1 ICU
161 ʇ ˜ Ə ε ɟ
ẹ Ψ 110 ʇ 51 ʇ 47.54±10.66 ɟ ı ה ♥ ῍Ω Ҝ ǚ ε ה ♥ ῍Ω Ҝ 54 33.54% w ٺ ה ♥ ῍Ω Ҝ
107 66.46% ה ♥ ῍Ω Ҝ ɦ ɑ ɑ ♥
ᐟ Ⴁ Җ 2016 ♥ ῍Ω Ҝ τ ᐟ ǚ
ɧ [6] ǚ 1 Ό
♥ ῎ Ⴢ 2 ' ǚ
3 ẫ ' ; 4
ẫ ٺ ɟ
Ẩ Ẫ ≥18 ᾀ ῎ í
M ´
´ ẹ ɧ ɟ Ẫ †
´ ´ ɞ ᐟ ´
´ ɞ ɞ ' Ἢ '
ɟ

1.2

>î (IÂ•‡B ðEœ)XsB* •1™ ©•Ñ‡G Q¥9óIE Ñ ŰF‡E D‡U‡JφÌÌb5(

P<0.05

2

2.1

1 14 1A 2 22 1B 3 13 1C 4 5 1D

2.2 HIF-1α、VEGF TIMP

HIF-1α、VEGF TIMP P<0.05 1

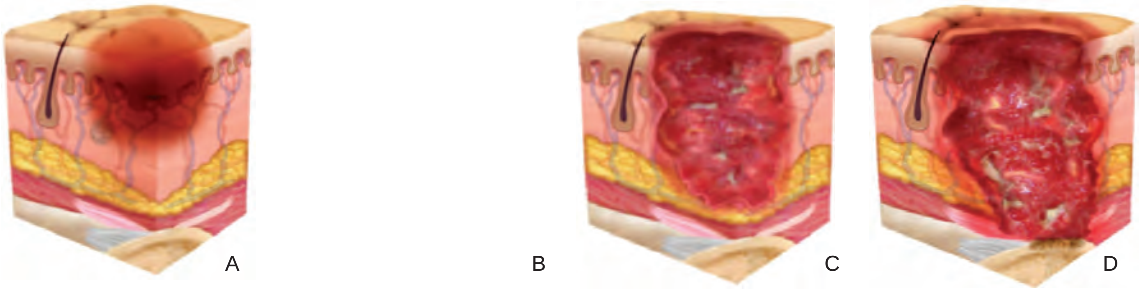

A：1 B：2 C：3 D：4

1

Figure 1 Image of pressure damage

1 HIF-1α VEGF TIMP

Table 1 Comparison of HIF-1α, VEGF and TIMP levels in 2 groups

	n	HIF-1α (ng/L)	VEGF (ng/L)	TIMP (μg/L)
	54	3.15±1.98	8.11±2.65	55.29±8.46
	107	1.64±0.34	3.55±1.63	33.54±6.55
t		7.690	13.471	17.990
P		0.001	0.001	0.001

2.3 HIF-1α、VEGF TIMP

HIF-1α、VEGF TIMP 4 >3 >2 >1 P<0.05 2

2 HIF-1α VEGF TIMP

Table 2 Comparison of HIF-1α, VEGF and TIMP levels in patients with different stages of pressure injury

	n	HIF-1α (ng/L)	VEGF (ng/L)	TIMP (μg/L)
1	14	1.74±0.41	4.41±1.05	35.32±5.17
2	22	1.97±0.52	5.13±2.64	37.51±5.82
3	13	2.96±1.01	7.15±2.66	52.64±6.24
4	5	3.08±1.25	8.29±2.93	54.69±7.53
F		8.94	5.44	31.79
P		0.001	0.003	0.001

2.4 HIF-1α、VEGF TIMP

HIF-1α、VEGF TIMP

HIF-1α、VEGF TIMP 3

3 HIF-1α VEGF TIMP

Table 3 Sensitivity, specificity and accuracy of HIF-1α, VEGF and TIMP in predicting postoperative pressure injury

				%	%	%
HIF-1α		38	19	70.37	82.24	78.26
		16	88			
VEGF		37	22	68.52	79.44	75.78
		17	85			
TIMP		36	23	66.67	78.50	74.53
		18	84			
		48	10	88.89	90.64	90.06
		6	97			

2.5 HIF-1α、VEGF TIMP

HIF-1α (r=0.564, P=0.003)、VEGF (r=0.432, P=0.024) TIMP (r=0.506, P=0.012)

3

[7] 4 [8]

Ặ ♥ ̀Ω Ҡ ה Ẉ̈ ę ה
Ẉ̈ ǫ̃ ң ~ ה ♥
̀Ω Ҡ Ặ ɟ
VEGF ẇ ε ė Chloe [9]
VEGF ל Á Ъ
ɞҠ i ´ ɞw ẇ w ‴ ɞ ɞ ה
ɟ ѽ ε VEGF ’ m Y
Ẉ̈ ך Ңm ך ė ‴
c c̆ ˚ Ң Ő [10] ɟ Fan [11] ה
w ɞw ‴ ’ VEGF ˗
ɟ Ң [12] ̀O ♥ ̀Ω Ҡ
̀O ~ ὰ Ψ VEGF
Ⅵ ɟ Á ɔ
Ɑ ė ’ Ҡ ̀O ~ ὰ Ң
VEGF ╗ ɟ
HIF 1α Ңm ė Ң
Ỹ /α

SD/CRL β HCG E2 IVF/ICSI ET

1 1 2 1

SD/CRL β
β HCG E2 IVF/ICSI ET
328 IVF/ICSI ET
β HCG E2 SD/CRL SD/CRL
β HCG E2 β HCG E2
N<0.05 SD/CRL N<
0.05 >35 30~35 <30 30~35 <30
N<0.05 SD/CRL N<0.05 14 d
β HCG E2 N<0.05 E2 81.7% 71.5% β HCG
82.8% 79.3% SD/CRL 86.9% 73.1% 91.7% 89.2%
SD/CRL β HCG E2 IVF/ICSI ET

β

Predictive value of SD/CRL ratio combined with serum β HCG and E2 levels in early abortion of patients undergoing IVF/ICSI ET

LU Aihua [1] ZHAO Yongxin[1] LI Jie[2] LIU Rui[1]

1. Department of Women Health Care Qinghai Maternal and Child Health Hospital Xining Qinghai China 810007 2. Department of Gynecology Qinghai Red Cross Hospital Xining Qinghai China 810007

ABSTRACT Objective To observe the predictive value of gestational sac diameter/crown rump length SD/CRL ratio combined with serum β human chorionic gonadotropin β HCG and estradiol E2 levels in early abortion of patients undergoing in vitro fertilization/intracytoplasmic sperm injection embryo transfer IVF/ICSI ET . Methods A retrospective analysis was performed among 328 patients receiving IVF/ICSI ET in the hospital. The levels of serum β HCG and E2 SD/CRL ratio and clinical data were compared between the early abortion group and the non early abortion group. Influencing factors of early abortion were analyzed. The predictive value of SD/CRL ratio combined with serum β HCG and E2 levels for early abortion was discussed. Results Theserum β HCG and E2 levels of the early abortion group were significantly lower than those of the non early abortion group N<0.05 while SD/CRL ratio was significantly higher than that of

2019 ZJ 189

1. 810007
2. 810007
E mail bijvwxg7johi@sina.cn

the non early abortion group (N<0.05). The early abortion rate in >35 years old group was significantly higher than that in 30~35 years old and <30 years old groups, and the 30~ 35 years old group was significantly higher than those under 30 years old group (N<0.05). Age and SD/CRL ratio were independent risk factors for early abortion (N<0.05), while serum β HCG and E2 at 14d after transplantation are protective factors (N<0.05). The sensitivity and specificity of E2, β HCG, SD/CRL ratio and their combination for predicting early abortion were 81.7%, 71.5%, 82.8%, 79.3%, 86.9%, 73.1% and 91.7%, 89.2%, respectively. Conclusion The SD/CRL ratio combined with serum β HCG and E2 can provide an important basis for the prediction of early abortion of patients undergoing IVF/ICSI ET, which is of great significance for clinical practice.

KEY WORDS Gestational sac diameter/crown rump length; β human chorionic gonadotropin; Estradiol; In vitro fertilization/intracytoplasmic sperm injection embryo transfer

in vitro fertilization/Intracytoplasmic sperm injection embryo transfer, IVF/ICSI ET 15%~20% 40%~50% 35% 25% 12 27% [1,2] IVF/ICSI ET β beta human chorionic gonadotrophin, β HCG estradiol, E2 [3] IVF/ICSI ET β HCG [4] sac diameter/crown rump length, SD/CRL β HCG E2 IVF/ICSI ET

1

1.1

2018 1 2019 2 328 IVF/ICSI ET 25~42 33.46±6.01 328 n=64 n=264 IVF/ICSI ET

1.2

IVF/ICSI ET 30 d XARIO SSA 660A PVT 661VT 6MHZ SD CRL yolk sac diameter, YSD heart rate, HR CRL SD /2 14 d β HCG E2 DNM 9606

1.3

[5] 14 d β HCG 5 IU/L 30 d 13 14 d β HCG 5 IU/L 12

1.4

β HCG E2 SD/CRL body Mass Index, BMI SD/CRL β HCG E2 β HCG E2 SD/CRL IVF/ICSI ET

1.5

SPSS 19.0 n % χ[2]

ƒ r ˥ COX ع ǚ Є w ĩ غ ǚ w ɔ Ә ROC У ɵ ᵉ ǚ ɟ w N<0.05 ε τ ɟ

2

2.1 Ξ β HCG ҿE2 ҿSD/CRL ᵉ

У β HCG ҿE2 ӊ Ҍ У Ẻ τ N<0.05 SD/CRL ᵉ Ҍ У Ẻ τ N<0.05 ɟ 1 ɟ

1 β HCG E2 SD/CRL

Table 1 Comparison of serum β HCG level E2 level and SD/CRL ratio between 2 groups

ᾳ	l	β HCG IU/L	E2 pg/mL	SD/CRL ᵉ
У	64	1380.18±206.37	260.46±40.95	6.23±8.75
У	264	2305.74±382.95	546.14±42.38	4.06±6.38
r ᵉ		18.674	48.694	2.257
N ᵉ		<0.001	<0.001	0.025

2.2 ί Ά β HCG ҿE2 ɞ SD/CRL ᵉ У

BMI ɞ У τ N>0.05 У β HCG ҿE2 SD/CRL ᵉ ɔ Ẻ τ N<0.05 ɟ 2 ɟ

2.3 COX ع ǚ

ҿSD/CRL ᵉ У ● غ N<0.05 ˜ 14 d β HCG ҿE2 ε У ˥ غ N<0.05 ɟ 3 ɟ

2.4 SD/CRL ˊ β HCG ҿE2 У ɵ ᵉ ǚ

У ᵉ ε 1 У ᵉ ε 0 ł SD/CRL Ńŀ β HCG Ńŀ E2 Ń Ẩł ҕ Ń ROC ǚ ɟ E2 81.7% 71.5%

2 β HCG E2 SD/CRL l %

Table 2 Comparison of early abortion rate among patients with different clinical data different serum HCG levels E2 levels and SD/CRL ratios l %

		l	У		χ^2 ᵉ	N ᵉ
	<30	98	7	7.14	19.465	<0.001
	30~35	110	20	18.18		
	>35	120	37	30.83		
BMI kg/m²	<18.5	52	12	23.08	3.845	0.146
	18.5~24.0	208	34	16.35		
	>24.0	68	18	26.47		
	1~5	106	16	15.09	2.658	0.265
	6~10	118	28	23.73		
	>10	104	20	19.23		
β HCG IU/L	≤1800	109	34	31.19	14.182	<0.001
	<1800	219	30	13.70		
E2 pg/mL	≤400	126	38	30.16	14.766	<0.001
	>400	202	26	12.87		
SD/CRL ᵉ	<5	286	34	11.89	82.667	<0.001
	≥5	42	30	71.43		

β HCG 82.8% 79.3% SD/CRL 86.9% 73.1% ی ˊ ʺẠʹO ی ˊ ی є ˊ 91.7% 89.2% ɟ 4 ˦ ه 1 ɟ

4 SD/CRL β HCG E2 ROC

Table 4 Areas under ROC curves of SD/CRL ratio combined with serum β HCG and E2 levels for prediction of early abortion

ҕ		Ά	95%AG	N ᵉ
E2	0.762	0.078	0.614~0.935	0.007
β HCG	0.771	0.080	0.609~0.942	0.005
SD/CRL	0.794	0.082	0.675~0.951	0.002
є ˊ	0.825	0.063	0.736~0.982	<0.001

3

HCG ε Ψ Ẽ У ẹ ζ α ˦ β Ж ند Ẫ ɵ ˊ Ҍ β HCG غ ί

3 COX

Table 3 COX regression analysis of influencing factors of early abortion

ҕ	@ ᵉ	Q,C, ᵉ	U_jb ᵉ	Cvn @ ᵉ	95%AG	N ᵉ
	6.043	3.785	6.402	2.736	1.650~3.879	<0.001
β HCG	0.734	2.368	4.271	2.062	1.347~3.584	<0.001
E2	0.602	2.258	4.369	2.014	1.286~3.475	<0.001
SD/CRL ᵉ	7.453	3.968	7.684	3.065	1.543~5.782	<0.001

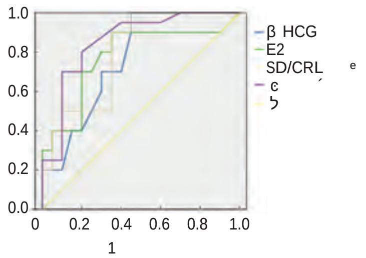

1 SD/CRL β HCG E2 ROC

Figure 1 ROC curves of SD/CRL ratio combined with serum β HCG and E2 levels for prediction of early abortion

β HCG HCG IVF/ICSI ET 14 d β HCG [6] E2 E2 E2 1 interleukin 1 IL 1 α tumor necrosis factor α TNF α interferon IFN [7] E2 [8] β HCG E2 [9] 14 d β HCG E2 IVF/ICSI ET [10,11] SD CRL HR YSD CRL 4 mm 5 mm 8.3% 5.3 mm 0.0% [12] Rodgers [13] CRL 7 mm 0.0% MSD 25 mm

0.0% CRL MSD IVF/ICSI ET SD/CRL [14] trophoblast TE HCG TE HCG [15] β HCG MSD/CRL IVF/ICSI ET 87.57% [16] E2 β HCG SD/CRL ROC

SD/CRL β HCG E2 IVF/ICSI ET

1 Lazaraviciute G Kauser M Bhattacharya S et al. A systematic review and meta analysis of DNA methylation levels and imprinting disorders in children conceived by IVF/ICSI compared with children conceived spontaneously J . Hum Rep Update 2014 20 6 840 852.
2 Yang XL Chen F Yang XY et al. Efficacy of low molecular weight heparin on the outcomes of IVF/ICSI pregnancy in non thrombophilic women a meta analysis J . Acta Obstet Gynecol Scand 2018 97 9 1061 1072.
3 β HCG J . 2020 12 3 353 357.
4 J . 2016 34 5 100 102.
5 12 β HCG J . 2016 32 9 1415 1418.
6 Toftager M Bogstad J Bryndorf T et al. Risk of severe ovarian hyperstimulation syndrome in GnRH antagonist versus GnRH agonist protocol RCT including 1050 first IVF/ICSI cycles J . Hum Rep 2016 31 6 1253 1264.
7 Bhusane K Bhutada S Chaudhari U et al. Secrets of Endometrial Receptivity Some Are Hidden in Uterine Secretome J . Am J Rep Immunol 2016 75 3 226 236.

miR 4262 A549

; miR 4262 A549 qRT PCR miR 4262 A549 miR 4262 inhibitor MTT Transwell Western blot E cadherin vimentin miR 4262 KLF3 3 UTR qRT PCR KLF3 mRNA miR 4262 A549 miR 4262 inhibitor KLF3 siRNA A549 miR 4262 miR 4262 inhibitor A549 E cadherin vimentin miR 4262 KLF3 ; miR 4262 A549 KLF3 KLF3 siRNA miR 4262 inhibitor A549 ; miR 4262 A549 KLF3

KLF3 miR 4262

Mechanism of down regulation of miR 4262 in inhibiting the metastatic potential of lung cancer cell A549

ZHU Li GONG Bo

Clinical Laboratory Changning District Maternal and Child Health Hospital Shanghai China 200051

ABSTRACT Objective To explore the effect and mechanism of down regulation of miR 4262 on the metastatic potential of lung cancer cell A549. Methods qRT PCR was used to detect miR 4262 expression in lung cancer cells. Lung cancer cell A549 were transfected with miR 4262 inhibitor MTT was used to measure proliferation transwell cells were used to measure invasion and migration and western blot analysis was used to measure E cadherin and vimentin protein expression. Bioinformatics software predicts that miR 4262 and KLF3 have binding sites at the 3 UTR end and the luciferase system identifies the targeting relationship. qRT PCR was used to detect changes in the expression of KLF3 mRNA in lung cancer tissues and to analyze the correlation between its expression level and miR 4262. Lung cancer cells A549 were transfected with miR 4262 inhibitor and KLF3 siRNA to detect cell proliferation invasion and migration changes. Results The expression level of miR 4262 was increased in lung cancer tissues and lung cancer cells. After transfection with miR 4262 inhibitor lung cancer cell A549 had reduced proliferation invasion and migration ability and the expression level of E cadherin protein in the cells increased while the level of vimentin decreased. Down regulation of miR 4262 up regulated the expression of KLF3 in lung cancer cell A549. KLF3 siRNA can reverse the inhibitory function of miR 4262 inhibitor on the proliferation invasion and migration of lung cancer cell A549. Conclusion Down regulation of miR 4262 inhibits the metastatic potential of lung cancer cell A549 and the mechanism of action is related to the targeted up regulation of KLF3 expression.

KEY WORDS Lung cancer KLF3 miR 4262 Migration

2011HGG28

200051

E mail biu_dodo@163.com

Ẻ í ̴ ɞ
ؤّ ה Ђ
Ύ Њ [1] ɟ ˬ
ɞ ⺅ ɔ ɔ epithelial mesenchymal
transition EMT Ὼ Ά
Ặ ӊ ɞ Ặ̈ ⺅
ῤ̈ ɟ RNA microR
NA miRNA ᵐ Y ж l Ỉ
RNA ǚ Ẻ Ə ɞ
ה ɞ ה ɞẍ miRNA
Ặ̈ ı̈̈ ⅃ [2] ɟ ж Ꞻ miRNA
̴ Ẩ ה ה Ά miRNA
Ặ Ύ miRNA ’ ɞ
ǚ [3] ɟ ؤّ Ψ miRNA ל Ά
⺅ ǚ ˜ miRNA
ε [4] ɟ ῤ̈ Њ miR 4262 ؤّ
ˬ ɞ ⺅ EMT Ψ Ə ɟ
miR 4262 ı̈̈
⺅ Ặ̈ w ε ǚ
w ל ɟ

1

1.1

miRcute ݜ ی miRNA cDNA ᵐ ´
Ḥ ɞmiRcute ݜ ی miRNA ẉ Ḥ
SYBR Green ɞQuant one step qRT PCR Kit
SYBR Green ج ɔ ←Ш ắ
˘ vimentin l ɞKLF3 l ፈ Abcam
E cadherin l ⺅ HRP J ج ፈ
Santa Cruz Biotechnology inhibitor control ɞmiR 4262
inhibitor ɔ ` Ặ̈ ắ ˘ WT
ی ⺅ MUT ל ی ẉ ᒣ l `
ɔ ắ ˘ KLF3 siRNA ⺅
siRNA control ắ ˘
´ NCI H446 ɞA549 ɞNL9980
ፈ ATCC ɔ HBE ɔ
╪ ắ ˘ ɟ

1.2 qRT PCR miR 4262 ⺅ KLF3 mRNA

ǚ ῷ Trizol Ḥ ק NCI 466
A549 NL9980 ˀ ק NCI H446 ɞ
A549 ɞNL9980 ǚ ῷ ⺅ k P ψ Ḥ ǚ ῷ Q я <

Control, Anti NC, Anti miR 4262 qRT PCR Western blot JD1 mRNA 1.2 1.6

1.8 KLF3 siRNA miR 4262

A549 miR 4262 inhibitor, siRNA control miR 4262 inhibitor, KLF3 siRNA Anti miR 4262+si NC Anti miR 4262+si KLF3 48h MTT, Transwell, Western blot E cadherin, vimentin, KLF3

1.9

SPSS 21.0 N<0.05

2

2.1 miR 4262

NCI H446, A549, NL9980 miR 4262 HBE N<0.05 1

1 miR 4262

Table 1 miR 4262 expression levels in lung cancer cells and normal bronchial epithelial cells

	miR 4262
HBE	1.00±0.12
NCI H446	1.76±0.13
A549	2.65±0.23
NL9980	2.02±0.15
D	157.42
N	<0.001

2.2 miR 4262 EMT

miR 4262 inhibitor miR 4262 OD vimentin E cadherin N<0.05 1 2

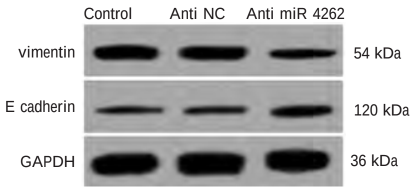

1 Western blot E cadherin vimentin

Figure 1 Western blot method to measure E cadherin and vimentin protein expression

2.3 miR 4262 KLF3

miR 4262 KLF3 3′UTR WT KLF3 miR 4262 inhibitor N<0.05 2 3

2 miR 4262 KLF3 3 UTR

Figure 2 MiR 4262 and KLF3 3 UTR end binding site

3

Table 3 Comparison of cell luciferase activity

	MUT	WT
Anti NC	1.00±0.11	1.00±0.12
Anti miR 426	0.98±0.08	1.45±0.13
r	0.67	7.63
N	0.44	<0.001

2.4 miR 4262 KLF3

miR 4262 inhibitor KLF3 mRNA N<0.05 3 4

2.5 KLF3 siRNA miR 4262 EMT

siRNA control miR 4262 inhibitor

2 OD E cadherin vimentin

Table 2 Lung cancer cell OD value, invasion number, migration number, and E cadherin and vimentin protein levels

	miR 4262	OD			E cadherin	vimentin
Control	1.00±0.09	0.43±0.04	98.45±9.33	125.30±10.35	0.22±0.02	0.56±0.05
Anti NC	0.97±0.12	0.44±0.03	99.24±7.25	126.83±11.20	0.21±0.03	0.54±0.04
Anti miR 4262	0.45±0.05	0.32±0.02	64.36±4.21	85.34±7.29	0.35±0.05	0.33±0.02
D	103.29	41.28	68.05	52.30	43.34	97.40
N	<0.001	<0.001	<0.001	<0.001	<0.001	<0.001

Ẵ KLF3 siRNA ⅎ miR 4262 inhibitor ˜ OD ᵉ ᶒ ᶀ ⅎ vimentin ᵹ ╗ Ψ KLF3 ᶀ E cadherin ʮ N<0.05 ɟ ه 4 ⅎ 5 ɟ

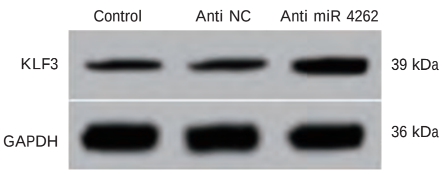

3 Western blot miR 4262 inhibitor KLF3

Figure 3 Western blot detection of KLF3 protein expression in lung cancer cells transfected with miR 4262 inhibitor

4 miR 4262 inhibitor KLF3 mRNA ¯

Table 4 Comparison of KLF3 protein and mRNA levels in lung cancer cells transfected with miR 4262 inhibitor ¯

ᾱ	KLF3	I JD1 mRNA
Control	0.28±0.03	1.00±0.08
Anti NC	0.29±0.05	0.99±0.13
Anti miR 4262	0.67±0.07	2.24±0.21
D ᵉ	160.89	207.00
N ᵉ	<0.001	<0.001

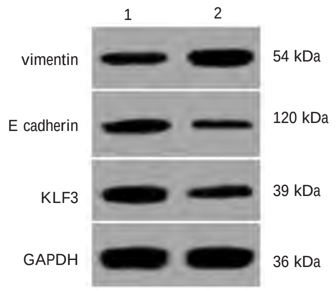

1. Anti miR 4262+si NC 2. Anti miR 4262+si kLF3

4 Western blot KLF3 E cadherin vimentin

Figure 4 Western blot detection of KLF3 E cadherin vimentin protein expression levels in transfected cells

3

miRNA ᵾ ᶅ I Ψ ᵾ ʹY Ể ‖ ῦ ' miRNA Ά ῦ ɔ ᶀ ɔ ᶀ ᵸ Ặ ɟ miRNA ' Ж ẹ ' ɯ ﻏ ﻨ ה ə ⅂ Ά ᾷ I ɥ ᶀ ll ᶀẌ ' ᶅ Ψ [5] ɟ miRNA ⅂ Ά ᶀ Ҡ miRNA ἶ ɛ ה ə [6] ɟ ᵸ ⅎ ˀ ς ɔ ᾷ miRNA ə 3 Ά Ặ miRNA ᵾ Ψ ה Ч ﻏ ﻨ ﻏ ﻨ ə ἶ ᵸ ⅎ˛ [7] ɟ miR 4262 ᵾ † ᶀ Ψ ẹ ' ɯ˛ ⅎ [8] ɟ ᵾ Ψ ɛ miR 4262 ῎Ạ ᵸ [9] ɟ miR 4262 ' ᵾ ⅎ Ψ ה ˛ ə ɟ

ɛ Ђ Ά ˇ ⅎ Ὼ Ặ ɯ Ά EMT ʹY Ặ [10] ɟ EMT ᵾ Њ I Ἰ ẹ ᵾ ה ᶀ Ψ Ặ ɟ EMT ה ɔ ﻳ ῎E ﻳ ᵸ ɟ E cadherin ɔ vimentin [11] ɟ ה EMT ᵸ ς EMT ς [12] ɟ ; miR 4262 ˜ Ψ E cad herin ╗ vimentin ʮ ; miR 4262 ' ɯ ʮ Ά ˛ ⅎ ˊ ᵹ ; miR 4262 Ể ῎Ạ ə ɟ miRNA ə ῎Ạ Ά ˜ ﻏ ﻨ Ặ ʹY miRNA ﻏ ﻨ ' ˀ Y ᵾ ῃ

5 OD KLF3 E cadherin vimentin ¯

Table 5 Lung cancer cell OD value invasion number migration number and KLF3 E cadherin vimentin protein level comparison ¯

ᾱ	OD ᵉ	ˇ		E cadherin	vimentin	KLF3
Anti miR 426 2+si NC	0.33±0.03	65.67±5.75	86.32±5.76	0.39±0.06	0.34±0.04	0.63±0.08
Anti miR 4262+si KLF3	0.42±0.04	86.43±6.87	110.54±9.04	0.23±0.04	0.58±0.07	0.32±0.04
r ᵉ	5.40	6.95	6.78	6.67	8.93	10.40
N ᵉ	<0.001	<0.001	<0.001	<0.001	<0.001	<0.001

ˀ Ψ ﻨﺮ ﻍ ʼ ˀ 13 ɟ
; KLF3 ʼ w ; miR 4262
ﻣ ɞ ɞ ⁄ EMT Ặ Ə
miR 4262 ʼ KLF3 ĭ
⁄ ɟ
φ miR 4262 ǚ Ψ ʼ ה ˛ Ə
; ẹ ʼ w ˜ ˛ KLF3 ɥ
ɛ miR 4262 ǚ Ψ Ə
w Ђ ﻝ ɛ ˜ ﻨﺮ ﻍ w Ђ ɟ
w˜ Ж ǚ Ψ ΎЖ
ẹ ǚ Ψ ﻝ ɔ Ά í Ặ
Ė I ű ɟ

1 Yang F Xu J Li H et al. FBXW2 suppresses migration and invasion of lung cancer cells via promoting β catenin ubiquitylation and degradation J . Nat Commun 2019 10 1 1 16.

2 Kyuno D Zhao K Bauer N et al. Therapeutic targeting cancer initiating cell markers by exosome miRNA efficacy and functional consequences exemplified for claudin7 and EpCAM J . Transl Oncol 2019 12 2 191 199.

3 Qin L Liu Y Li M et al. The landscape of miRNA related ceRNA networks for marking different renal cell carcinoma subtypes J . Brief Bioinf 2020 21 1 73 84.

4 Zhang J Li D Zhang Y et al. Integrative analysis of mRNA and miRNA expression profiles reveals seven potential diagnostic biomarkers for non small cell lung cancer J . Oncol Rep 2020 43 1 99 112.

5 Jacinta Fernandes A Xavier J M Magno R et al. Allele specific miRNA binding analysis identifies candidate target genes for breast cancer risk J . npj Genomic Med 2020 5 1 1 9.

6 ĭ Ώ . ⁄ MicroRNA 208a ש Ț ẹ ˜ ɵ ᵉ J . ├ í 2018 35 5 1017 1019.

7 ķ . RNA microRNA PD L1 ǚ Ψ J . Ά ű ẍ 2020 36 03 271 275.

8 Lu S Wu J Gao Y et al. MicroRNA 4262 activates the NF κB and enhances the proliferation of hepatocellular carcinoma cells J . Int J Biol Macromol 2016 86 5 43 49.

9 Qu JJ Qu XY Zhou DZ. miR 4262 inhibits colon cancer cell proliferation via targeting of GALNT4 J . Mol Med Rep 2017 16 4 3731 3736.

10 δ ☼ Ở . Snail ﻨﺮ ﻍ ﻨﺮ ɔ Ά TGFβ1 ῷ Ώ ה EMT Ặ J . ű Ά 2019 11 6 451 456.

11 Galle E Thienpont B Cappuyns S et al. DNA methylation driven EMT is a common mechanism of resistance to various therapeutic agents in cancer J . Clin Epigenet 2020 12 1 1 19.

12 Sheng W Shi X Lin Y et al. Musashi2 promotes EGF induced EMT in pancreatic cancer via ZEB1 ERK/MAPK signaling J . J Exp Clin Cancer Res 2020 39 1 1 15.

13 Mansoori B Mohammadi A Naghizadeh S et al. miR 330 suppresses EMT and induces apoptosis by downregulating HMGA2 in human colorectal cancer J . J Cell Physiol 2020 235 2 920 931.

1374

8 Ώ Ặ . hCG ῷ˜ ﻝ ɔ ש ẹ ᵉ WF/ICSI ĭ J . Ά 2012 32 7 494 499.

9 Ẇ . IVF/ICSI ET˜ β HCG ˊ ﺵ У J . ├ 2018 53 5 789 792.

10 Й ᴷ Ÿ . I ɔ ˜ M Ặ ﻍ ű J . Ψ ╞ Ặ 2016 20 05 516 519 529.

11 Z Й . У I Ÿ ש ẹ Ặ ﻍ ű J . Ψ ╞ У 2019 54 12 797 802.

12 Duncan WC. Limitations of current definitions of miscarriage using mean gestational sac diameter and crown rump length measurements a multicenterobservational study J . Ultrasound Obst Gyn 2011 38 5 497 502.

13 Rodgers SK Chang C Debardeleben JT et al. Normal and Abnormal US Findings in Early First Trimester Pregnancy Review of the Society of Radiologists in Ultrasound 2012 Consensus Panel Recommendations J . Radiographics 2015 35 7 2135.

14 ╞ ü . ה У I ש ĭ ﻍ ű J . Ψ ﻪ У í 2018 19 4 303 306.

15 . ˆ Ḩ ⁞ I í ɵ ᵉ J . Ψ ﻪ ├ 2015 31 2 66 69.

16 Ώ Ḝ . є ⁞ Ț Ế w ẈẆ У í J . ụ У 2016 25 8 596 599.

IGF 1 IGFBP 3 Hcy

CH 1 IGF 1 IGFBP 3 Hcy 2017 7 2020 7 90 CH 85 IGF 1 IGFBP 3 Hcy BMI N<0.05 N<0.05

19PJ516

629000
E mail 2673887936@qq.com

control group and the level of Hcy was significantly higher than that of the control group and the difference was statistically significant N : 0.05 . Conclusions The levels of IGF 1 IGFBP 3 and Hcy have a certain correlation with children s IQ height and weight. Children with CH can return to normal levels after early diagnosis and treatment.

KEY WORDS Congenital hypothyroidism Insulin like growth factor binding protein Insulin like growth factor 1 Homocysteine

Ẉ ʽ ῎Е ӊ congenital hypothyroidism CH Ѣ ״ ŭ ẉ ӊ ; ɞ I ה ε ζ [1] ɉ CH ṿ Ĭ ŭ φ ɉ ṿ Ѣ ï ẻ í ȳ ṿ I ɞ Ὼ ה Ὸ [2] ɉ í ɔ ζ ε ṿ ɞ Ὼ ה ṿ O ɉ ; B ж I Ә Ά ẹ Ặ Ύ [3] ɉ homocysteine Hcy ự У ɉ Hcy ├ ε ɉ ӊ ; ự Ж ẫ Y ᾄ [4] ɉ CH ṿ 1 Insulin like growth factor IGF 1 ɞ 3 Insulin like growth factor binding protein IGFBP 3 ש Hcy ŭ ẹ ל ɔ ש Ά CH ṿ ה Ặ ɉ

1

1.1

ˁ 2017 7 2020 7 90 CH ṿ Ẩ ẹ Ψ 34 56 5.11±2.17 ɉ 85 ṿ Ә ε ẹ Ψ 31 54 4.74±1.58 ɉ

Ẩ Ά ṿ í ε CH serum free T4 FT_4 ӊ ӊ Ѣ thyroid stimulating hormone TSH ≥20 mU/L ẹ ђ Ĭ ŭ Ά í M У ɞO ṿ ṿ ɞ ζ Ẉ ɉ Ξ τ Ẻ N<0.05 ɉ ├ Ӊ Ж Ά ɔ Щ ɉ

1.2

1.2.1 ṿ

ṿ i ẋ Ặ ǻ Ά J20160065 ṿ í Ỹ ש TSH FT_4 ɉ

1.2.2 IGF 1 ɞ IGFBP 3 ש Hcy

ɔ 6 mL Ẩ ῎Ḥ Ḥ ŭ Ψ 400 r/min ŭ Ὸ ӊ Ψ ɉ IGF 1 ɞ IGFBP 3 ẍ ŭ Ѧ ǻ У Ḥ IGF 1 Ḥ Ά 20142405760 IGFBP 3 Ḥ Ά 20162404085 ε ←Ш← ẉ ɉ Hcy ɔ ẉ ẍ Ѧ ǻ AbbotIMx ẍ ŭ Ѧ Ḥ Hcy Ḥ Ά Ά 2011 2400126 ẋ ǻ ẉ ɉ Ẻ I Ә O Щ Ύ ẍ ᾶ ɉ

1.3

ŭ Ξ ṿ ה Ỹ ɞ Ὼ Ỹ Ξ ṿ IGF 1 ɞ IGFBP 3 ש Hcy ל ɔ Ỹ ŭ ɔ ל ɔ Ά CH ṿ I ה ɞ Ὼ ה Ặ ɉ

ה Ά Ặ ה Ỹ ђ Ψ 7 ẉ ; ṿ ה ל Ά ђ [5] Ţ ṿ ɞ I ש ẹ Ά ŭ standard deviation scoring SDS ɞ I body mass index BMI ɉ

Ὼ ІІ Ψ ṿ Ὼ Chinese Wechsler Young Children scale of Intelli

gence C WYCSI [6] ۱ Ə

ɟ Ţ ɒ <70 ŭ ε Ὼ ɳ

; ≥90 ŭ ε ɟ ᶐ ˀ m ˜ Ό Δ ᾰ Ό

ж ɟ

1.4

SPSS 20.0 Θ ŭ

w ¯ Ξ r w

l % [2] Ą ƒ Nc_pqml Ą

ŭ ώ ɾ ŭ N<0.05 ε

τ ɟ

1 ¯

Table 1 Comparison of children s growth and development between the two groups ¯

		l=90	l=85	r e	N e
		5.11±2.17	4.74±1.58	1.283	0.201
Ό l g		3486.97±487.77	3403.11±392.67	1.248	0.214
Ю		25.82±3.81	25.49±1.75	0.729	0.467
		7.14±1.66	7.06±1.75	0.310	0.757
		12.62±1.54	12.41±1.32	0.966	0.335
		7.45±2.31	6.84±2.01	1.859	0.065
l	SDS	0.52±0.65	0.83±1.47	1.821	0.070
	SDS	0.57±0.81	0.55±0.97	0.148	0.882
BMI	kg/m^2	14.90±1.06	15.21±1.66	1.481	0.141

2 ¯

Table 2 Comparison of intelligence between the two groups ¯

ᾳ	l	ɒ		Ə ɒ	Ə	ɒ		Ɜ
	90	88.26±12.41	18.37±3.12	103.77±12.43	19.32±3.17	95.05±11.32	4.67±1.31	1.04±1.14
	85	109.03±12.85	19.12±2.45	112.90±9.75	20.12±3.01	111.27±10.66	5.89±1.04	2.32±1.17
r e		10.877	1.762	5.385	1.710	9.745	6.798	7.329
N e		0.001	0.080	0.001	0.089	0.001	0.001	0.001

2.3 Ξ ẏ IGF 1 ȡGFBP 3 ẇ Hcy

IGF 1 ȡGFBP 3 ɳ Ь

Hcy Ь ᶐ Ė τ

N<0.05 3 ɟ

3 IGF 1 IGFBP 3 Hcy ¯

Table 3 Comparison of IGF 1 IGFBP 3 and Hcy levels between 2 groups ¯

ᾳ	l	IGF 1 ng/mL	IGFBP 3 ng/mL	Hcy μmol/L
	90	89.54±20.34	1893.13±517.11	18.47±1.84
	85	167.53±20.87	2443.48±898.33	14.03±1.62
r e		25.033	5.001	16.904
N e		0.001	0.001	0.001

2.4 CH ẏ Ὼ Ỹ Ά IGF 1 ȡGFBP 3 ẇ Hcy Ą

ɷɒ ɷɜ ɷ ŭ Ά IGF 1 ɷ IGFBP 3 ۱ Ą Ά Hcy ۱ Ą N< 0.05 ɷɒ ɷ ẇ ɒ ӿ ẅ Ά IGF 1 ɷ IGFBP 3 ẇ Hcy Ą N<0.05 4 ɟ

4 IGF 1 IGFBP 3 Hcy

Table 4 Correlation between children s intelligence and IGF 1 IGFBP 3 and Hcy levels

Ą ɾ	IGF 1		IGFBP 3		Hcy	
	p e	N e	p e	N e	p e	N e
	0.587	0.001	0.263	0.029	-0.231	0.034
ɒ	0.641	0.006	0.485	0.009	-0.501	0.008
	0.114	0.764	0.223	0.305	-0.211	0.361
ɒ	0.158	0.643	0.147	0.654	-0.136	0.668
	0.207	0.521	0.195	0.547	-0.159	0.632
Ɜ	0.319	0.024	0.338	0.021	-0.417	0.011
ŭ	0.256	0.031	0.292	0.027	-0.362	0.021
ɒ ӿ ẅ	0.216	0.314	0.186	0.594	-0.101	0.811

2.5 CH ṿ Ά IGF 1 ᶑIGFBP 3 ẇ Hcy Ặ
ġ ẃ ع ῦ
ẉ IGF 1 ᶑIGFBP 3 ẇ Hcy ᵉ ε ġ ﻟ ẉ ṿ
˘ ῦ ῦ Ẫ 8 ﻟ ฿ ɞƎ
ε ﻟ ẃ ع ῦ ה
῀Ω ġ Ψ IGF 1 ᶑIGFBP 3 ẇ Hcy ἷ
ῴ 3 ε ġ ῦ ᾆ ﻫ ɞƎ ɞ ῦ
N : 0.05 5 ɟ

ɞῦ ͻ ɞỖ ﺷﺪ ẇ ‖ ῦ ﯙ Ψ
Ψ Ẻ Ə [12] ɟ [13] Ὸ
CH ṿ IGF 1 ᶑIGFBP 3 ɉ Њ ɇ ṿ
Ά ᵐ ɟ
ῴ IGF 1 ζ ´
ẹ ζ ˈ Ά Ч ﻟ Ά ж Ι
ה [14] ɡ IGFBP 3 Ɇ u @ 0 Ψ´ Ş Ǝ
IGdBP 1 ɕ IGFBP g ɃΙ 14 ɞ

3

CH ṿ ṿ ’
ẍ ẹ ה ɟ CH í ṿ
ᵐ ἶ ῦ Њ ⁊ Ὸ ῴ
ה ﻟ ה ɞˈ ɥ Ὸ
˜ ˈ ῍Ε Ψ
ɉ ˘ ɞΙ [7] ɟ
CH ṿ ﯙ ṿ ה Ά
ṿ ᾆ ῦ ẹ Ɑ ġ ’ ġ ε ﯙ ṿ
Ι ˥ Ђ ṿ
ה [8] ɟ ɞ Ι Ά
ṿ P Ξ ɟ
ẇ FT₄ ’ ṿ Ψ
ה Ꝁ ẇ ה ̉ ς CH ﯙ ṿ
ï í Ɑ ġ [9] ɟ CH ṿ
Җ Њ ï
ה ɞ ῍Ω ɉ ; ɞ ɟ Mazahir
[10] Ὸ CH ṿ ה Ỹ
Ҕ Њ ﭺ ﯙ 6 Y ẉ ɔ
ṿ ɟ CH
ṿ ה Ỹ Ά ṿ ɟ
Mehran [11] ה IGF 1 ﻟ ﻡ
ﯙ Ψ 95% IGF 1 Ά IGFBP 3 ´
Ξ Y ġ ⑊ Ặ Ẻ ╟̉ Ə Ά ﺨ
ɞ ᵐ Ặ ɟ IGF 1 ﺨ

CD64

[1,2] [3] [1]

CD64 2015 1 2019 1 155 75 80 CD64 WBC PCT C CRP ROC 24 h CD64 1 CD64 N<0.05 CD64 WBC PCT CRP N<0.05 CD64 WBC PCT CRP N< 0.05 CD64 WBC
CD64

Application of neutrophil CD64 combined with blood routine in the diagnosis and differential diagnosis of infectious and non infectious fever in severe patients

DU Xiangyang[1,2] ZHANG Wenying[3] YAN Lin[1]

1. Department of Infectious Diseases Shandong Provincial Third Hospital Jinan Shandong China 250031 2. Department Of Emergency Shandong Provincial Third Hospital Jinan Shandong China 250031 3. Medical Insurance Office Shandong Provincial Third Hospital Jinan Shandong China 250031

ABSTRACT **Objective** To study the significance of neutrophil CD64 combined with blood routine in diagnosis and differential diagnosis of infectious and non infectious fever in severe patients. **Methods** A total of 155 fever patients who were treated in the hospital from between January 2015 and January 2019 were enrolled. According to different fever causes they were divided into the infectious fever group 75 cases and the non infectious fever group 80 cases . The levels of neutrophil CD64 indexes in peripheral blood were detected by flow cytometry. The levels of white blood cells WBC procalcitonin PCT and C reactive protein CRP in peripheral blood were detected by blood analyzer. The diagnostic efficiency of blood routine indexes was compared by ROC curves. **Results** After admission the 24 hour CD64 index and 1 week CD64 index of the infected fever group were significantly higher than those of the non infected fever group the difference was statistically significant N<0.05 . The sensitivity of CD64 index and WBC to diagnose

---

ZR2017HL159

1. 250031
2. 250031
3. 250031
E mail baojx189129@sina.cn

infectious and non infectious fever was significantly higher than that of PCT and CRP and the difference was statistically significant N<0.05 . The specificity of CD64 index and WBC in diagnosing infectious fever and non infectious fever was significantly higher than that of PCT and CRP and the difference was statistically significant N<0.05 . Conclusion The CD64 index and WBC levels of patients with infectious fever are significantly increased and these two indicators are highly specific and sensitive in the diagnosis of infectious fever and non infectious fever and have high diagnostic value.

KEY WPRDS Infectious fever Non infectious fever Neutrophil CD64 Blood routine

[1] [2,3] 64 cluster of differentiation 64 CD64 CD64 CD64 CD64 [4,5] white blood cell WBC C reactive protein CRP procalcitonin PCT [6] CD64

1

1.1

2015 1 2019 1 155 75 80 40 35 45.13±7.83 10.19±2.09 d 38.88±0.31 42 38 46.27±6.97 10.36±2.36 d 38.75±0.29 N<0.05 37.5~40.0 24 h

1.2

24 h 6 mL FACS Calobur BD CD64 CD64 CD64 CD64 CRP CRP 20190809 WBC PCT

1.3

WBC 3.5~9.5 × 10^9/L [7] PCT 0~0.05 ng/mL [8] CRP 0~12 mg/L [9]

1.4

SPSS 12.0 ROC N: 0.05

2

2.1 CD64

24 h CD64 N<0.05 CD64 N>0.05 1

2.2 CD64

CD64 CD64 N<0.05 CD64 CD64 N: 0.05 CD64 N<0.05 2

1 CD64 ¯

Table 1 CD64 indexes at admission in both groups ¯

ặ	l Ψ	CD64 ڄ ẉ	CD64 ڄ ẉ	24 h CD64
ה	75	3.21±0.81	0.97±0.35	3.54±0.25
ה	80	2.01±0.90	0.91±0.30	1.78±0.19
r ᵉ		8.705	1.142	47.001
N ᵉ		0.000	0.255	0.000

2 1 CD64 ¯

Table 2 CD64 indexes after 1 week of admission treatment in both groups ¯

ặ	l Ψ	CD64 ڄ ẉ	CD64 ڄ ẉ	1 ᠰ CD64
ה	75	2.61±0.12	1.01±0.12	2.56±0.21
ה	80	1.31±0.11	0.98±020	1.41±0.20
r ᵉ		70.364	1.695	34.919
N ᵉ		0.000	0.092	0.000

2.3 Ξ

WBC ɕPCT ɕCRP Њ ה Ể τ N<0.05 3 ɟ

3 ¯

Table 3 Test results of blood routine in both groups ¯

ặ	l	WBC 10^9 Y /L	PCT ng/mL	CRP mg/L
ה	75	12.25±1.20	0.78±0.04	28.98±1.36
ה	80	8.36±0.79	0.45±0.02	14.02±0.89
r ᵉ		23.979	65.573	81.522
N ᵉ		0.000	0.000	0.000

2.4 ˘

WBC ɕPCT ɕCRP ᠰ CD64 ˊ ي ɞ ڄ Њ╥ᵐ ᵉ ɟ 4 ɟ

4 CD64 ROC

Table 4 ROC analysis on infection types detected by CD64 and blood routine

ặ	AUC			cutoff ᵉ	73#AG
WBC	0.832	0.801	0.889	10.231	0.737~0.923
PCT	0.783	0.718	0.694	0.585	0.675~0.892
CRP	0.752	0.773	0.667	15.698	0.369~0.865
CD64	0.781	0.814	0.798	2.018	0.687~0.954
ˊ	0.835	0.818	0.758	0.832	0.751~0.933

3

[10] CD64 ' ẉ Ə ε ה Ό ה ˜ CD64 Ж ╖ ɟ Ђ ה CD64 ה ה Ẩ 24 h CD64 ᠰ 1 ᠰ CD64 Њ ה ɟ ' ǵ ε Ξ ה Ɑ ǵ

ẹ ђ Ψ ƒ ᵐ 3 ǵ ʕ TNF α ɕIL 1β ᠰ IL 6 ɕCRP ╖ ˀ ɞ╥ ᠰ Ɑ ᠰ CD64 ϛ Ж╖ ɟ ᵐ ᠰ ˜ Ξ CD64 ڄ ң ặ Ђ ɟ ה CD64 щ Њ ה ' ǵ ε ה ᠰ ᵐ ᠰ ȭ ã ж ặ Ђ ɟ Xing [11] PCT ɕCRP ɕIL 6 Ά ה ı Ặ Ύ ɟ ה ├ ó ε ה ה [12] ɟ Ψ ó ı ε ה ₿ WBC ɕCRP ᠰ PCT ɟ WBC ɕ CRP ᠰ PCT Қ ẹ . í ặ ζ Ể ᵐ í ɵ ᵉ [13] ɟ ȳ [14] ɔ ặ PCT ɟ ה ה WBC ɕPCT ɕCRP ڄ Њ ה ɟ Ẩ ה Ђ l ẍ ᠰ ẍ ƒ WBC ɕPCT ɕCRP ڄ ╖ ɟ ẋ [15] PCT ɕCRP ᠰ WBC ˊ ' ẉ ה Ό Ά ẹ Ể ᵐ ɟ [16] PCT ɕCD64 ש WBC ڄ ' ẉ Ə ε ó ה ǵ ɟ ƒ ROC ˘ ה ש Ђ CD64 ᠰ WBC ה ᠰ ה ᠰ

ʼ ღ ε Ẩ˛ ˜ ה Ђ ẍ CD64 ⁄ WBC ẍ ζ Ẩ˛ Ψ

ﻓﻌ ǚ CD64 ⁄ WBC ƒ ẹ ╗ ה ה Ι ẍ WBC ̋ Җ ╗ ƒ WBC Ә ε ı ε ה ɟ

ɔ ה CD64 ⁄ WBC ╗ ΄Y Ξ ﯚ ה Ά ה Ψ Ά Ẻ ɵ ᵉ ɟ

1 . Ψ ├ Ῑ Ҝ ה ﻼ ΅Ω J . ﻌ Ψ ├ Ψ 2018 40 4 375 376.

2 Ӣ . Ɑ ɞ א ἆ Ά ה ɵ ᵉ J . ← ├ 2018 39 5 500 503.

3 . Ɑ ἆ Ά ɵ ᵉ J . Ψ ╞ ẫ ├ 2018 17 9 709 713.

4 . SLE ⁴ Ψ CD64 ﯚ ἆ ה Ά í ɵ ᵉ J . џ ├ 2018 5 3 14 17.

5 ʞ ╞ . Ψ CD64 ɞPCT ﬠ NLR ﯚ Ψ ɵ ᵉ J . Ψ ﻌ 2018 30 3 304 307 311.

6 θ ΅Ω . PCT ɞCRP ﯚ Ɑ Ι ƴ Ψ ﬠ Ά MP IgM Ι Ặ J . ǚ Ά 2020 12 7 964 967+973.

7 ̎ . ה 18F FDG PET/CT ȡᵐ ʖ J . Ψ ╞ ├ Ά ǚ ȡ 2017 37 2 95 96.

8 ΅Ω . ღ IL 32 ɞHs CRP ɞPCT Ά COPD ﻴ Ặ ǚ D . ← ← ├ 2015.

9 ё ☼ . CRP ﯚ Ψ í J . Ψ ╞ џ í ├ 2010.

10 Ъ . CD64 ﯚ ● ΄ Ψ J . í 2019 5 7 531 534.

11 Xingjun LI Mingjian Q Guisheng D et al. Clinical evaluation of serum PCT CRP IL 6 and endotoxin in fever patients with bloodstream infection J . Int J Lab Med 2018 39 22 2782 2785 2789.

12 . ﬠ Ά Ɑ Ặ J . ├ 2018 33 5 379 383.

13 ⁴ . ⁴ CRP WBC Ά Nst ᵉ ╥ ﬠ ΄ ﯚ ƴ Ψ ɵ ᵉ J . џ ├ 2018 33 3 117 119.

14 ў . Ɑ ﯚ ƴ Ι Ῑ ϧ ɔ ﬠ í τ J . Ῑ ﭑ ├ 2018 5 1 73 74.

15 ẋ . PCT ɞCRP ɞWBC ˜ ה í ɵ ᵉ J . 2018 15 12 26 27.

16 . PCT ɞHNL ⁄ CD64 ɵ ᵉ J . ├ 2019 34 5 433 436.

1383

7 Yamaguchi T Nakamura A Nakayama K et al. Targeted Next Generation Sequencing for Congenital Hypothyroidism With Positive Neonatal TSH Screening J . J Clin Endocrinol Metab 2020 114 8 8.

8 Silvestrin SM Leone C Cléa RL. Detecting congenital hypothyroidism with newborn screening the relevance of thyroid stimulating hormone cutoff values J . J Pediatr 2017 74 6 1548 1549.

9 ╣ Җ . Ẉ ʼ ̋E ӊ ƴ IGFBP 3 Ά ɞΙ ɞ ה Ặ J . Ψ ﻌ Ђ Ά Ҝ 2018 26 3 109 111.

10 Mazahir FA Khadora MM. P285 The association of congenital anomalies in patients with congenital hypothyroidism in government tertiary care centers under dubai health authority UAE 2000 2015 a retrospective cross sectional study J . Arch Dis Chil 2019 104 3 271.

11 Mehran L Khalili D Yarahmadi S et al. Evaluation of the congenital hypothyroidism screening programme in Iran a 3 year retrospective cohort study J . Heart 2019 104 2 176.

12 Ο ₄ ɔ Є . Ẉ ʼ ̋E ƴ ה Ặ ღ J . Ψ ﻌ ˥ ɟ 2018 33 3 612 614.

13 Ж . Ḧ ж ה ƴ IGF 1 ɞIGFBP 3 ΐ ﬠ ẹ ẫ ǚ J . Ψ ﻌ ˥ ɟ 2018 33 23 5512 5514.

14 н ΅Ω . Ẉ ʼ ̋E ƴ GLIS3 ﻧﻎ ϧ J . Ψ ╞ ƴ í 2018 33 8 585 588.

15 Wassner AJ. Congenital Hypothyroidism J . Clin Perinatol 2018 45 1 1 18.

16 ỳ ΅Ω ΅Ω τ ΅Ω . Ж í ʼ ̋E Ά ⁴ ̓ ﻴ ╚ ﬠ Ặ ǚ J . Ψ ﻌ ├ 2017 12 12 1840 1844.

17 Tanaka T Aoyama K Suzuki A et al. Clinical and genetic investigation of 136 Japanese patients with congenital hypothyroidism J . J Pediatr Endocrinol Metab 2020 33 6 691 701.

• / Č

serum Lp PLA2 and AT levels and Gensini scores among the mild moderate and severe groups N< 0.05 . Spearman correlation analysis showed that serum Lp PLA2 was positively correlated with Gensini score in ACS patients p ; 0.283 N ; 0.040 while AT was negatively correlated with Gensini score p ; - 0.331 N ; 0.016 . ROC curve analysis showed that the area under the curve AUC of Lp PLA2 combined with AT 0.872 for predicting severe coronary artery stenosis in ACS patients was higher than that of single indicator detection. Conclusion With the aggravation of coronary artery stenosis the Gensini scores and serum Lp PLA2 level are increased while serum AT level is decreased in ACS patients. The combined detection of Lp PLA2 and AT can provide a more accurate judgment for the degree of coronary stenosis in patients with acute coronary syndrome.

KEY WORDS Acute coronary syndrome Antithrombin Coronary artery stenosis Lipoprotein associated phospholipase A2 Coronary angiography

ợ ợ ɔ ה ה ฿ ɞ ɞ [1 3] ɟ ợ c c í w ẹ ˦ Ÿ Ţ [4] ɟ ợ ɛ ợ Ά ж Ҍ ὰ ἀ Ҍ φ Gensini ǚ ǚ Ẻ Ә ɛ ɘ [m] [5 6] ɟ [m] w Ά ɞ Ţ ợ ợ Ẻ τ [7] ɟ Ҍ antithrombin AT ɞ Ặ A2 lipoprorein assoeiated phos PhohPaseA2 Lp PLA2 Ά ợ ợ Ặ ɛ w ɟ

1

1.1

2018 1 2020 1 92 ợ Ә ɛ ẹ Ψ 58 34 48~84 65.21±4.13 90 ợ ɛ Ә ɛ ẹ Ψ 60 30 46~87 65.31±3.98 ɟ Ξ τ N<0.05 ɟ Ấ Ά ợ ɛ ợ ợ ɛ ợ ≥45 ẹ Ḥ Ж Ά ɟ Ά ɞ

O ẍ Ά ẍ ɟ

1.2 ợ Ά

ợ ɔ Gensini ǚ ợ ǚ [4] ≤25% 1 ǚ 26%~50% 2 ǚ 51%~75% 4 ǚ 76%~90% 8 ǚ 91%~99% 16 ǚ 100% ɛ 32 ǚ ฿ 4 Ḥ Ҍ ζ left main LM ǚ ×5 Ḥ Ҍ left anterior descending LAD ɞΨ ɞ ɞ ɞ J ǚ ×2.5 ɞ1.5 ɞ1 ɞ1 ɞ0.5 Ḥ Ҍ left circumflex LCX ɞ ɞΨ ɞ ǚ Â2.5 ɞ 1 ɞ1.5 ɞ1 ɞ1 ɞ0.5 Ḥ Ҍ ợ right coronary artery RCA ɞΨ ɞ ǚ ×1 Ḥ Ҍ ǚ ×0.5 ɟ Ḥ ǚ ǚ ≤24 ǚ ɛ l ; 41 ɞ24< ǚ <49 ǚ ɛ Ψ l ; 27 ɞ ǚ ≥49 ǚ ɛ l ; 24 ɟ

1.3

Lp PLA2 ɞAT ợ 5 mL 2 mL ǚ ἀ ẍ Lp PLA2 ɞAT Ḥ У Δ oy w ợ ɞΨ ɞ Lp PLA2 ɞ AT Gensini ǚ Lp PLA2 ɞAT Ά Gensini ǚ Ặ ǚ Lp PLA2 ɞAT ợ ợ Ÿ ɟ

1.4

ϴ SPSS 13.0 Ψ

‾ Ξ Ξ LSD t

ῦ Ţ ROC

Ặ ῦ ᾠ Spearman N : 0.05

τ ɟ

2

2.1 Ξ Lp PLA2 ɞAT

Lp PLA2 Ҍ AT

ӊ Ҍ ޗ τ N : 0.05

1 ɟ

1 ⻖ Lp PLA2 ɞAT

Table 1 Comparison of serum Lp PLA2 and AT levels between control group and disease group

ى	l	AT III mmol/L	Lp PLA2 ng/mL
	92	85.85±9.52	182.31±28.38
	90	92.46±5.31	161.47±30.25
r e		5.767	4.772
N e		0.000	0.000

2.2 ợ ɞΨ ɞ Lp PLA2 ɞ AT ⻖ Gensini ῦ

ợ Lp PLA2 ɞGensini ῦ

Ҍ ⻖ Ψ AT ӊ Ҍ

⻖ Ψ ޗ τ N : 0.05 Ψ

Lp PLA2 ɞGensini ῦ Ҍ

AT ӊ Ҍ ޗ τ N : 0.05 2 ɟ

2 ợ ɞΨ ɞ Lp PLA2 ɞAT ⻖ Gensini ῦ

Table 2 Comparison of Lp PLA2 AT and Gensini scores in mild moderate and severe coronary stenosis groups

ى	l	AT mmol/L	Lp PLA2 ng/mL	Gensini ῦ ῦ
	41	87.88±5.49[ab]	179.86±4.66[ab]	22.71±3.57[ab]
Ψ	27	85.07±4.36[a]	182.49±5.54[a]	42.36±8.54[a]
	24	81.85±2.52	186.31±6.38	49.71±2.24
D e		13.426	10.788	239.871
N e		0.000	0.000	0.000

Ά [a]N : 0.05 Ά Ψ [b]N : 0.05 ɟ

2.3 Lp PLA2 ɞAT Ά Gensini ῦ Ặ ῦ

Spearman Ặ ῦ ợ ´

Ψ Lp PLA2 Ά Gensini ῦ ⻩ Ặ p ; 0.283 N ; 0.040 AT Ά Gensini ῦ ⻩ Ặ p ; -0.331 N ; 0.016 ɟ

2.4 Lp PLA2 ɞAT ש J ´ ợ ´ ợ Ỹ ῦ

ROC ῦ Lp PLA2 ɞAT ´

ợ ´ Ό Ο ợ

; area under curve AUC ε 0.872 Ҍ ╥ m

ɟ 3 ฿ 1 ɟ

3 Lp PLA2 AT

Table 3 Analysis of results of Lp PLA2 AT and their combination in predicting coronary stenosis in patients with acute coronary syndrome

	e	AUC	%	%
AT mmol/L	86.14	0.715	70.7	65.9
Lp PLA2 ng/mL	182.47	0.769	68.2	77.6
J ´	-	0.872	78.2	89.4

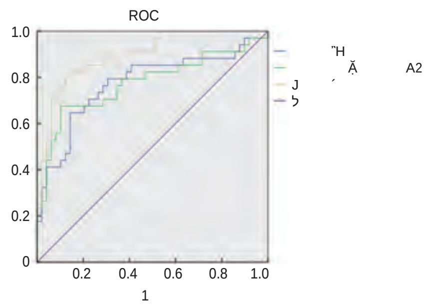

1 Lp PLA2 AT

ROC

Figure 1 ROC curve of Lp PLA2 AT and their

̎Ḧ

Ặ A

3

ɔ ζ ؏ ؤ Ҍ

Ά ̎Ḧ φ Ρ Ў ̎Ḧ ؏ ؤ ̎Ặ ɔ Ψ Ə ᾮ

8 10 ɟ Ặ Ҍ C א ɞ

Ɑ ؏ ợ ´

˜ Ỹ ж ợ ɵ

e ӊ 11 12 ɟ ؏ m ʼ ⱳ Ά̃ ɞ Ţ

ợ ợ ´

Ḛ τ ɟ Lp PLA2 ɞAT

´ ῦ J Ά ợ ´

ợ Ặ ɟ

Lp PLA2 ⱳ ´ l ؤ Ҍ

Ψ

LncRNA LINC01857

Siha

2018 TG 21

100006

E mail xg8753200@163.com

hydrochloride reduced the proliferation migration and invasion of cervical cancer cells by down regulating the expression of LINC01857.

KEY WORDS Oxycodone hydrochloride LncRNA LINC01857 Cervical cancer proliferation Migration Invasion

[1] EGFR/JAK2/STAT3 [2] HOTAIR [3] [4] RNA LncRNA [5] RNA LINC01857 LncRNA LINC01857 [6] LINC01857 LINC01857 Siha

1

1.1

Siha DMEM Lipofectamine2000 si NC si LINC01857 pcDNA pcDNA LINC01857 Trizol cDNA qRT PCR MTT Transwell Matrigel E cadherin N cadherin CST HRP Abcam

1.2

1.2.1

Siha 96 5×10^3 20 40 60 μg/mL 24 h [7] Lipofectamine2000 si NC si LINC01857 Siha si NC si LINC01857 pcDNA pcDNA LINC01857 Siha 60 μg/mL 24 h +pcDNA +pcDNA LINC01857

1.2.2 qRT PCR LINC01857

Trizol Siha RNA Nanodrop2000c RNA -80 cDNA RNA cDNA cDNA qRT PCR 10×PCR Buffer 2.5 μL $MgSO_4$ 2.5 μL dNTPs 2.5 μL 0.5 μL cDNA 2 μL RNase Free ddH_2O 25 μL 95 2 min 95 30 s 59 30 s 72 30 s 36 LightCycler480 PCR LINC01857 GAPDH

1.2.3 MTT

Siha 2.5×10^5 /mL 96 100 μL/ 1.2.1 MTT 20 μL/ 4 h DMSO 150 μL/ 5 min OD

1.2.4

Siha 6 1×10^3 14 d PBS 500 μL/ -20 20 min 1%

1.2.5 Transwell Ά

Siha 2.5×10^5 Y /mL Њ 200 μL/ ; Ấ 10% Ế 600 μL/ Ế 24 h PBS 20 min Ά 10 min Matrigel Ấ 40 μL/ Ế 5 h

1.2.6 Western blot E cadherin 和 N cadherin

Siha Ấ RIPA 500 μL BCA SDS PAGE 1∶1 000 4 24 h Ά J 1∶5 000 1 h ImageJ

1.3

SPSS 21.0 N : 0.05

2

2.1 Siha LINC01857

4 LINC01857 OD ẋ ḩ Ḥ > Ψ Ḥ > Ḥ N<0.05 1

2.2 Siha

4 N cadherin Y Y ḩ Ḥ > Ψ Ḥ > Ḥ E cadherin ḩ Ḥ < Ψ Ḥ

表 1 Siha LINC01857 ($\bar{x}$ ± s ; n = 3)

Table 1 Effects of oxycodone hydrochloride on the activity clone formation and LINC01857 expression of SiHa cells ($\bar{x}$ ± s ; n = 3)

	LINC01857	OD 值	ẋ Y
	0.98±0.05	1.30±0.07	115.00±3.27
ḩ Ḥ	0.95±0.04	1.27±0.07	111.33±2.87
Ψ Ḥ	0.68±0.04	0.92±0.05	87.33±2.62
Ḥ	0.35±0.02	0.70±0.04	64.00±2.16
F 值	168.787	72.022	221.292
P 值	0.000	0.000	0.000

< Ḥ N< 0.05 1 2

1 2 3 4 5

250
130
100
70
55
35
25
15
10

N cadherin 125 kDa
E cadherin 97 kDa
GAPDH 36 kDa

1. Maker; 2. 3. ḩ Ḥ 4. Ψ Ḥ 5. Ḥ

图 1 Siha E cadherin N cadherin

Figure 1 Effect of oxycodone hydrochloride on the expression of E cadherin and N cadherin in SiHa

2.3 LINC01857 Siha

Ά si NC si LINC01857 OD 值 ḩ ẋ N cad herin ḩ N<0.05 E cadherin N< 0.05 3 2

表 2 Siha ($\bar{x}$ ± s)

Table 2 Effect of oxycodone hydrochloride on migration and invasion of SiHa ($\bar{x}$ ± s)

	n	E cadherin	N cadherin	Y	Y
	3	0.18±0.01	0.68±0.04	235.33±4.19	135.33±4.19
ḩ Ḥ	3	0.19±0.01	0.66±0.04	230.67±4.71	131.67±3.77
Ψ Ḥ	3	0.37±0.02	0.39±0.03	194.33±3.86	98.00±2.45
Ḥ	3	0.64±0.04	0.25±0.02	152.00±3.27	70.67±2.05
F 值		252.545	117.778	274.717	266.580
P 值		0.000	0.000	0.000	0.000

3 LINC01857 Siha ¯

Table 3 Effects of interference with LINC01857 on proliferation migration and invasion of SiHa ¯

ŏ	l	LINC01857	E cadherin	N cadherin	OD e	ẋ	Y	Y ˬ	Y
si NC	3	0.99±0.05	0.17±0.01	0.69±0.04	1.32±0.08	117.00±3.27	236.33±4.03		137.33±4.11
si LINC01857	3	0.19±0.02	0.73±0.04	0.14±0.01	0.54±0.03	54.33±2.05	127.67±2.49		61.33±2.87
r e		25.731	23.525	23.105	15.812	28.125	39.729		26.260
N e		0.000	0.000	0.000	0.000	0.000	0.000		0.000

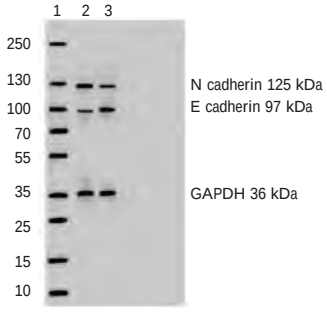

1. Maker 2. si NC 3. si LINC01857 ɻ

2 LINC01857 Siha E cadherin E cadherin

Figure 2 Effect of LINC01857 on the expression of E cadherin and E cadherin in SiHa

2.4 LINC01857 ¯E Siha

ѡ Ї

Á Ḥ +pcDNA

Ḥ +pcDNA LINC01857 OD e ╗ ẋ

ѡ τ N<0.05 4 ɻ

2.5 LINC01857 ¯E Siha

ϐ Ї

Á Ḥ +pcDNA

Ḥ +pcDNA LINC01857 Ẇ˳

ѡ E cadherin ң N cadherin

╗ τ N : 0.05 ѧ 3 ѳ

5 ɻ

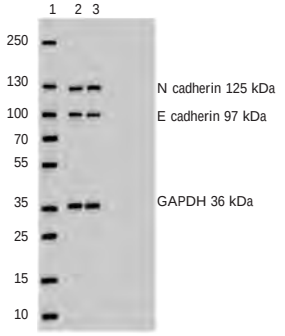

1. Maker 2. Ḥ +pcDNA 3. Ḥ +pcDNA linc01857 ɻ

3 LINC01857 Siha E cadherin E cadherin

Figure 1 Overexpression of LINC01857 can reduce the effect of oxycodone hydrochloride on the expression of E cadherin and E cadherin in SiHa

3

Γ AMPK Ẇ˳ Ї

Ä ѡ Ẇ˳ ℰ H ⁸ ɻ ά ▌

4 LINC01857 Siha ¯ l=3

Table 4 Overexpression of LINC01857 can reduce the inhibitory effect of oxycodone hydrochloride on the proliferation of SiHa ¯ l=3

ŏ	LINC01857	OD e	ẋ	Y
Ḥ +pcDNA	0.34±0.02	0.71±0.03		65.00±2.45
Ḥ +pcDNA LINC01857	0.89±0.05	1.13±0.07		104.67±3.30
r e	17.690	9.552		16.718
N e	0.000	0.000		0.000

5 LINC01857 Siha ¯

Table 5 overexpression of LINC01857 can reduce the inhibition of oxycodone hydrochloride on migration and invasion of SiHa ¯

ŏ	l	E cadherin	N cadherin	Y ˬ	Y
Ḥ +pcDNA	3	0.62±0.04	0.25±0.02	151.33±3.86	71.00±2.16
Ḥ +pcDNA LINC01857	3	0.26±0.02	0.53±0.04	221.67±4.19	118.67±3.86
r e		13.943	10.844	21.385	18.667
N e		0.000	0.000	0.000	0.000

LncRNA MEG3/miR 421/BTG1 [9] [10] [11 13] E cadherin N cadherin E cadherin N cadherin EMT E cadherin EMT N cadherin EMT EMT [14] EMT LINC01857 LINC01857 [15] LINC01857 miR 1281/TRIM65 [16] LINC01857 miR 200b [17] LINC01857 LINC01857 LINC01857 LINC01857

1 Sur vivin J . 2020 12 4 478 482.

2 Li H Lu Y Pang Y et al. Propofol enhances the cisplatin induced apoptosis on cervical cancer cells via EGFR/JAK2/ STAT3 pathway J . Biomed Pharmacother 2017 86 1 324 333.

3 Zhang D Zhou XH Zhang J et al. Propofol promotes cell apoptosis via inhibiting HOTAIR mediated mTOR pathway in cervical cancer J . Biochem Biophys Res Commun 2015 468 4 561 567.

4 Patel J Lucas CJ Margalit M et al. Laxative Use in Inpa tients on Oxycodone/Naloxone Prolonged Release and Oxyco done Prolonged Release for Cancer and Non cancer Pain J . J Pain Palliat Care Pharmacother 2018 32 2 3 116 123.

5 Ma TT Zhou LQ Xia JH et al. LncRNA PCAT 1 regulates the proliferation metastasis and invasion of cervical cancer cells J . Eur Rev Med Pharmacol Sci 2018 22 7 1907 1913.

6 Xiong Y Gu Y Wang F et al. LINC01857 as an oncogene regulates CREB1 activation by interacting with CREBBP in breast cancer J . J Cell Physiol 2019 234 8 14031 14039.

7 Tian M Jin L Li R et al. Comparison of oxycodone and morphine on the proliferation apoptosis and expression of re lated molecules in the A549 human lung adenocarcinoma cell line J . Exp Ther Med 2016 12 2 559 566.

8 Chen X Li K Zhao G. Propofol Inhibits HeLa Cells by Impair ing Autophagic Flux via AMP Activated Protein Kinase AMPK Activation and Endoplasmic Reticulum Stress Regu lated by Calcium J . Med Sci Monit 2018 24 1 2339 2349.

9 Zhu J Han S. Lidocaine inhibits cervical cancer cell prolifera tion and induces cell apoptosis by modulating the lncRNA MEG3/miR 421/BTG1 pathway J . Am J Transl Res 2019 11 9 5404 5416.

10 Liu S Gu X Zhu L et al. Effects of propofol and sevoflu rane on perioperative immune response in patients undergoing laparoscopic radical hysterectomy for cervical cancer J . Medicine Baltimore 2016 95 49 e5479 e5489.

11 Yu Y Li D Duan J et al. The pro and anti cancer effects of oxycodone are associated with epithelial growth factor recep tor level in cancer cells J . Biosci Rep 2020 40 2 41 49.

12 Nakamura A Hasegawa M Minami K et al. Differential ac tivation of the μ opioid receptor by oxycodone and morphine in pain related brain regions in a bone cancer pain model J . Br J Pharmacol 2013 168 2 375 388.

13 J . 2016 19 27 3265 3269.

14 Zeng YT Liu XF Yang WT et al. REX1 promotes EMT induced cell metastasis by activating the JAK2/STAT3 signal ing pathway by targeting SOCS1 in cervical cancer J . Onco gene 2019 38 43 6940 6957.

15 Giulietti M Righetti A Principato G et al. LncRNA co ex pression network analysis reveals novel biomarkers for pancre atic cancer J . Carcinogenesis 2018 39 8 1016 1025.

16 Hu G Liu N Wang H et al. LncRNA LINC01857 pro motes growth migration and invasion of glioma by modulat ing miR 1281/TRIM65 axis J . J Cell Physiol 2019 234 12 22009 22016.

17 Chen GR Sun W Zheng K et al. LINC01857 promotes the development of gastric cancer by regulating microRNA 200b J . Eur Rev Med Pharmacol Sci 2020 24 7 3648 3656.

serum albumin and prothrombin activity in the hepatorenal syndrome group were all lower than the severe hepatitis group the difference was statistically significant N<0.01 . Based on the three factors to construct a multi factor risk score to get the formula risk score =14.35+0.56×NGAL level+0.50×LFABP level+0.46×NAG level NGAL The AUC values of LFABP and NAG for the diagnosis of hepatorenal syndrome are 0.703 95% confidence interval 0.606 0.799 0.775 95% confidence interval 0.688 0.861 0.728 95% confidence interval 0.643 0.812 and The AUC value for the diagnosis of hepatorenal syndrome by risk score was 0.817 95% confidence interval 0.747~0.887 and the N values were all <0.001 the sensitivity of NGAL LFABP NAG and risk scoring models for the diagnosis of hepatorenal syndrome were 84.1% 81.8% 75.0% and 81.8% with specificities of 47.2% 72.6% 67.0% and 74.5% and accuracy of 31.3% 54.4% 42.0% and 56.3% respectively. Conclusion The risk scoring model based on serum NAG NGAL and LFABP has satisfactory diagnostic efficacy for hepato renal syndrome in elderly patients with severe hepatitis B.

KEY WORDS N acetyl β D glucosaminidase Neutrophil Gelatinase Associated Lipocalin Liver type fatty acid binding protein Elderly severe hepatitis B Hepatorenal syndrome

ꭤ ɸ \\ ; † ӂ ẹ Ι Ỹ щ ü 2009 2013 ꭤ ɸ ה щ 80/10 H 0.05/10 ẹ Ψ ה ẹ ζ Ɑ ع [1] ɟ ה ᾷ ɔ Ὸ ɯ Ꝁ ε ζ ה ۆ Ψ ה ε 35~40% Ύ ẹ 41.5% [2,3] ɟ ε ζ Њ ж ɸ ה ε Ύ ж Њ ẹ ; ۆ Ψ ɔ ᾷ [4,5] ж ۆ ɸ Ψ ɔ ᾷ [6] ɟ ῷ Ђ ה ӂ З Ύ ж ɟ Њ є ی N ɸ β D ﻧﺤ N acetyl β D glucosaminidase NAG ɞ Ψ Ạ Neutrophil Gelatinase Associated Lipocalin NGAL ᾤ ی liver type fatty acid binding protein LFABP ɸ ɵ [e] ɟ

1

1.1

ד 2018 8 2019 12 ۆ ی ɸ 150 Ύ ꭤ ü Ά ╧ ẹ ȭ ε 44 ᾤ ی ɸ 106 ی Ȃ Ά [7] ꭤ ɸ ╧ ε ɸ ی 60 child Pugh ȭ B ɯ ɔ ɟ Ά ẹ ђ Ɑ ع ẍ Ὸ ẫ ʄ ĭ ۆ ẹ ђ ɟ ├ Ң ﺎ Җ Ά ڿ Щ ɟ

1.2

1.2.1 ȭ ᾤ í

ɔ Њ Ȃ 5 mL 1 500 /min 20 min ȭ ɟ í Ƀ ᾷ ɞ ɞ ɞ ɟ

1.2.2 ELISA

ж NAG ELISA Ḥ ɔ ᾰ B275503 ж NGAL ELISA Ḥ Bio Techne ᾰ F190418 У ﺉ Ψ ꭤ ɔ У ꭤ ꭤ ж LFABP ELISA Ḥ Hycult ᾰ 7629389 У ﺉ Ψ ꭤ ɔ У ꭤ ᾰ ᾤ Multiskan™ FC Ѧ ꭤ ᾰ У ﺉ Ψ ꭤ ɔ NAG ɞ NGAL ᾤ LFABP Y ɨ є ד ẹ ڿ [e] ɟ

1.3

ʄ SPSS 18.0 ᾤ GraphPad Prism6.0 ɵ ɯ Ι % [2] ɯ Ξ r ȭ ɟ J ȭ logistic ع r ع ﻴ ᾤ ȭ ɟ ɔ ɵ Receiver operating characteristic ROC ȭ

ɟ N : 0.05 ε τ ɟ

2

2.1 Ξ í

´ ɞ ɞ

C ɞNAG ɞNGAL ɞLFABP ҫ Ҍ

´ ɞ̈H ɑ ҫ

ӊ Ҍ τ N<0.05 Ξ

ɞ ᾳ̈ ʕ ɞ ɞ ɞ

ɞΓ ɞ ữ

τ N : 0.05 ɟ 1 ɟ

2.2 ˘ غ Ά ´ logistic ع ŭ

ɞ̈H ɑ ɞ C ɞNAG ɞ

NGAL ɬ LFABP Ά ´ Ặ NAG ɞNGAL

ɬ LFABP ε ´ ● غ N : 0.05 ɟ

2 ɟ

2.3 ŭ ى ´ ROC

ɬ •'`"

3

Table 3 The diagnostic efficacy of risk scoring model for hepatorenal syndrome

			´				Ά̃
					%	%	%
NAG	35	71	33	11	75.0	67.0	42.0
LFABP	29	77	36	8	81.8	72.6	54.4
NGAL	56	50	37	7	84.1	47.2	31.3
ũ̃	27	79	36	8	81.8	74.5	56.3

Ά̃ = + 1 ɟ

3

I Ỉ ǵ ῨΕ ᆟ م ݜ Ỉ ; ꞕ ´ ζ Ɑ ǵ ɟ Ά ᆟ Ὼ ; ῨΕ ς ; Ɑ ǵ φm ɟ ς Ӄ [8] ɟ ж ꞕ φ Ὼ ; m ῨΕ ƒ ẹ ה ´ [9] ɟ ῴ ´ ה Ά̨ ᾲ ' ฿ C ꞵ2 ɞ C ℵ ݜ Ꮶ ǵ [10,11] ɟ ݹ O ũ̃ ᾲ ɥ Ђ ´ ' ݜῨH ǵ ' [12] '

ẹ e Ẩ є Y ی NAG ɞNGAL ɞLFABP NAG ж I ɔ m ɔ ɔ ᾲ Ỉ I NAG Ẩ [13] ɟ NGAL ݜ LFABP ũ̃ ᾲ ᆟ ũ̃ ݹ Ꮶ NGAL ݜ LFABP ╗ ǵ ' Ђ Ţ ' Ꮶ [14,15] ɟ ũ̃ ´ ה NAG ɞNGAL ɞLFABP є Ђ ´ ج m ɵ e ũ̃ ´ AUC e Ђ є Y ' Ꙓ ی є Y m є Ђ ´ ج ݹ 70% ɯ ɔ Ӂ ȳ ẹ NGAL с 50% ũ̃ ی ݹ ᄀ ݼ ɔ ئ Ђ ╗ Ђ є Y ی í ɵ e ɟ

φ ζ ݹ Ђ щ ˜ m ẅ ᾲ ε ὐ ɟ ẹ ε ╓ Ψ ݹ Ψ ´ Ә ɟ Ő Ђ m ẅ ˜ ی ɟ ɔ ݼ Ђ NAG ɞNGAL ɞLFABP ũ̃ ی ɸ ´ m í ῴ ɟ

1 Ὼ . 2004 2013 Ψ ɑ ɸ ی J . Ψ ɑ ᾱ̃ ├ 2017 20 23 2879 2883.

2 Ở – . ´ ݜ J . 2020 25 1 86 88.

3 Bashir MH Iqbal S Miller R et al. Management and outcomes of hepatorenal syndrome at an urban academic medical center a retrospective study J . Eur J Gastroenterol Hepatol 2019 31 12 1545 1549.

4 δ ῑ ╪ . ɸ ی 10 ˜ ݜ ẹ ῑ ǵ J . ᆟ 2020 29 4 438 441.

5 Bonavia A Singbartl K. Kidney Injury and Electrolyte Abnormalities in Liver Failure J . Semin Respir Crit Care Med 2018 39 5 556 565.

6 . ɸ ɸ ی ' ῑ ݜ ẹ ● ǵ ũ̃ J . Ở ├ 2019 37 8 14 16.

7 Angeli P Ginès P Wong F et al. Diagnosis and management of acute kidney injury in patients with cirrhosis revised consensus recommendations of the International Club of Ascites J . Gut 2015 62 4 968 974.

8 ˝ Ὼ . ´ J . Ψ ɑ 2017 9 1 1 6.

9 Rice JB White AG Galebach P et al. The burden of hepatorenal syndrome among commercially insured and Medicare patients in the United States J . Curr Med Res Opin 2017 33 8 1473 1480.

miRNA 320a fRadψ2 β catenin

[1] [2] [3]

RNA miRNA 320a 4 fRadψ2 β β catenin 2017 6 2019 8 122 miRNA 320a fRadψ2 mRNA β catenin 1 0

2018 ZJ 216

1. 810000
2. 810007
3. 810100
E mail hy67825@163.com

correlated with the degree of differentiation and negatively correlated with tumor T stage tumor size and lymph node metastasis N : 0.05 . The expression level of fRadᶙ2 mRNA and β catenin were negatively correlated with the degree of differentiation and positively correlated with tumor T stage tumor size and lymph node metastasis N : 0.05 . The expression level of miRNA 320a in the survivors was higher than that in the dead and the expression level of fRadᶙ2 mRNA and β catenin was lower than that in the dead N : 0.05 there were significant differences in the survival curves of miRNA 320a fRadᶙ2 mRNA β catenin expression level between high risk and low risk patients *P* : 0.05 . There was a negative correlation between the expression level of miRNA 320 and fRadᶙ2 mRNA and β catenin N : 0.05 . Conclusion The expression of miRNA 320a in liver cancer tissue is low and the expression of hTcf 4 and β catenin are high which are related to the degree of differentiation tumor T stage tumor size and lymph node metastasis and can predict patient prognosis.

KEY WORDS Liver cancer tissue miRNA 320a *hTcf 4* β catenin Pathological characteristics

ῦ ɔ ɞ T ῦ í Ά ˜ ΎY Ặ ж ΐ ɞ ˜ Ặ ẫ [1] ɟ RNA MicroRNA miRNA 320a Ӊ Ѣ l 8q21.3 Ά ῴ Ώ ה Ά ה Ặ miRNA 320a ' Ά Ặ ж ῧ [2] ɟ β β catenin ɞ ж T غ 4 غ Human T cell factor 4 gene fRadᶙ2 Wnt/β catenin מ غ ẹ Ψ β catenin Ά ῴ Ώ Ặ fRadᶙ2 ῧ ˬ ﾍ Ψ [3,4] ɟ Ѣ miRNA 320a ɞfRadᶙ2 ɞ β catenin ש Ά ɞ ˜ Ặ ˥ ; ɟ

1

1.1

ר 2017 6 2019 8 122 ʒ ع ẹ Ψ 65 ʒ 57 ʒ 41~75 ج 55.97±7.36 ɟ Ẩ Ά ́ ɑ ה Ά [5] í ẹ ђ ɑ ה Ẩ ῴ ɔ Ặ ́ ɟ Ά ה ʬ ɟ Ӊ Ж ج ש ɟ

1.2

א Reverse Transcription Polymerase Chain Reaction RT PCR Ά miRNA 320a ɞfRadᶙ2 mRNA ʬ 2 Ct ῦ ẍ ɔ J

β catenin ﾍ ῦ ɟ ó [6] 11%~50% ε 1 ῦ 51%~80% ε 2 ῦ >80% ε 3 ῦ ε 1 ῦ Ψ ε 2 ῦ ε 3 ῦ β catenin ε Ά φ >3 ῦ ε ɟ ῦ ɟ 1 ɟ

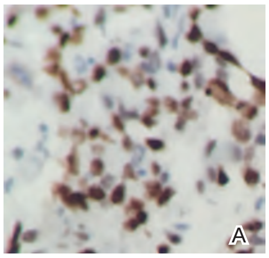

A

B

A ε B ε ɟ

1 β catenin -

×200

Figure 1 β catenin immunohistochemistry Biotin Avidin staining method ×200

1.3

miRNA 320a ɞfRadᶙ2 mRNA ɞβ catenin ῧ Ά Ψ ɟ miRNA 320a Ӊ Ά ɞfRad 4 Ά ɞ catenin Ά í ɞ ɟ ῦ Ά í Ặ ɟ ɟ ῦ ɵ ɟ ● Ά Ӊ ● ɟ ῦ Ặ ɟ

1.4

SPSS 22.0 Ɵ ῦ ʬ Ξ Ξ r l

% ² Spearman ŏ ˘
Ά í Ą ɔ Ə
Receiver operating characteristic ROC ѡ
ROC ; Area under the curve AUC ŏ ˘
~ ɵ e ▌ å Kaplan
Meier K M ŏ Log Rank Mantel
Cox ˘ ● ɵɳ ●
Pearson ŏ miRNA 320 mRNA Ά hTcf 4 mRNA ɵ
β catenin Ą ɟ N<0.05 ε
τ ɟ

2

2.1 miRNA 320a ɷfRadѰ2 mRNA ɷβ catenin ɡ̈
Ψ

miRNA 320a ɳ Ь
fRad 4 mRNA Ь
β catenin Ь
τ N<0.05 ɟ 1 ɟ

1 miRNA 320a fRadѰ2 mRNA β catenin
l % ¯

Table 1 miRNA 320a fRadѰ2 mRNA β catenin expression in liver cancer tissues l % ¯

ي	l	miRNA 320a	fRadѰ2 mRNA	β catenin
	122	4.62±0.89	0.78±0.16	96 78.69
	122	6.48±1.17	0.37±0.10	28 22.95
r/ ² e		13.975	24.002	75.824
N e		<0.001	<0.001	<0.001

2.2 miRNA 320a ɷfRadѰ2 mRNA ɷβ catenin ‴
í
miRNA 320a ɷfRadѰ2 kPL?
Ά ɳ ɷβ catenin Ά ɡ̈ ŏ ɔ
ɵ T ŏ ɵ ɵ
τ N<0.05 ɟ 2 ɟ

2.3 miRNA 320a ɷfRadѰ2 mRNA ɷβ catenin Ά í
Ą
miRNA 320a Ά ŏ ɔ ∖ Ą Ά T

2 miRNA 320a fRadѰ2 mRNA β catenin l %

Table 2 Comparison of clinical data of patients with different expressions of miRNA 320a hTcf 4 mRNA and β catenin l %

	miRNA 320a				fRadѰ2 mRNA				β catenin			
		ɳ	² e	N e		ɳ	² e	N e			² e	N e
<60	16 51.61	49 53.85	0.046	0.830	47 54.02	18 51.43	0.068	0.795	50 52.08	15 57.69	0.259	0.611
≥60	15 48.39	42 46.15			40 45.98	17 48.57			46 47.92	11 42.31		
ɋ̈												
	13 41.94	44 48.35	0.382	0.536	44 50.57	13 37.14	1.809	0.179	44 45.83	13 50.00	0.143	0.706
	18 58.06	47 51.65			43 49.43	22 62.86			52 54.17	13 50.00		
ɔ												
	14 45.16	43 47.25	0.041	0.840	39 44.83	18 51.43	0.437	0.509	46 47.92	11 42.31	0.259	0.611
	17 54.84	48 52.75			48 55.17	17 48.57			50 52.08	15 57.69		
' ŏ												
A	6 19.35	14 15.38			17 19.54	3 8.57			14 14.58	6 23.08		
B	15 48.39	48 52.75	0.309	0.857	47 54.02	16 45.71	5.067	0.079	51 53.13	12 46.15	1.108	0.575
C	10 32.26	29 31.87			23 26.44	16 45.71			31 32.29	8 30.77		
ŏ ɔ												
ɳ	6 19.35	37 40.66			33 37.93	10 28.57			36 37.50	7 26.92		
Ψ	11 35.48	49 53.85	27.925	<0.001	45 51.72	15 42.86	6.343	0.042	50 52.08	10 38.46	9.114	0.011
	14 45.16	5 5.49			9 10.34	10 28.57			10 10.42	9 34.62		
T ŏ												
	11 35.48	10 10.99			5 5.75	16 45.71			4 4.17	17 65.38		
	10 32.26	16 17.58	16.634	0.001	15 17.24	11 31.43	38.155	<0.001	22 22.92	4 15.38	54.738	<0.001
	8 25.81	43 47.25			44 50.57	7 20.00			48 50.00	3 11.54		
	2 6.45	22 24.18			23 26.44	1 2.86			22 22.92	2 7.69		
<5 cm	17 54.84	22 24.18	9.997	0.002	16 18.39	23 65.71	25.702	<0.001	18 18.75	21 80.77	36.184	<0.001
≥5 cm	14 45.16	69 75.82			71 81.61	12 34.29			78 81.25	5 19.23		
	8 25.81	51 56.04	8.467	0.004	28 32.18	31 88.57	31.778	<0.001	39 40.63	20 76.92	10.794	0.001
	23 74.19	40 43.96			59 67.82	4 11.43			57 59.38	6 23.08		

ǚ ɞ ɞ \ Ặ N<0.05 fRadɥ2 mRNA ɞβ catenin Ά ǚ ɔ \ Ặ Ά T ǚ ɞ ɞ \ Ặ N< 0.05 ɉ 3 ɉ

3 miRNA 320a fRadɥ2 mRNA β catenin

Table 3 Correlation between miRNA 320a fRadɥ2 mRNA β catenin and clinical characteristics

í	miRNA 320a		hTcf 4 mRNA		β catenin	
	p ᵉ	N ᵉ	p ᵉ	N ᵉ	p ᵉ	N ᵉ
ǚ ɔ	6.894	<0.001	-0.608	0.006	-0.626	<0.001
T ǚ	-5.771	<0.001	0.617	<0.001	0.449	<0.001
	-6.351	<0.001	0.544	<0.001	0.351	0.017
	-7.086	<0.001	0.589	<0.001	0.539	<0.001

2.4 miRNA 320a ɞfRadɥ2 mRNA ɞ β catenin

miRNA 320a Ҍ fRadɥ2 mRNA ɞβ catenin ӊ Ҍ τ N<0.05 ɉ 4 ɉ

4 miRNA 320a fRadɥ2 mRNA β catenin

Table 4 Comparison of miRNA 320a fRadɥ2 mRNA β catenin expression in patients with different prognosis

˜	l	miRNA 320a	fRadɥ2 mRNA	β catenin ǚ
	87	4.95±1.02	0.63±0.13	1.87±0.58
	35	3.81±0.56	1.15±0.22	2.93±0.90
r ᵉ		6.235	16.166	7.720
N ᵉ		<0.001	<0.001	<0.001

2.5 ROC ǚ

miRNA 320a AUC ɛ 0.799 73#AG 0.717~0.866 ᵉ ≤4.5 ɛ 82.86% ɛ 63.22% fRadɥ2 mRNA AUC ɛ 0.761 73#AG 0.676~0.834 ᵉ >0.98 ɛ 54.29% ɛ 93.10% β catenin AUC ɛ 0.730 73#AG 0.642~0.806 ᵉ >2 ǚ ɛ 65.71% ɛ 73.56% N< 0.05 ɉ 2 ɉ

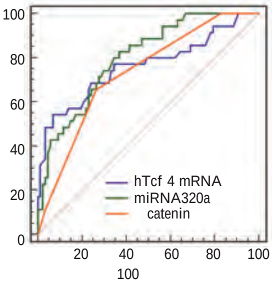

2

Figure 2 Prognostic value of each indicator

2.6

ɯ ROC ǚ ᵉ ɛ ǚ ǚ ɛ miRNA 320a ɞfRadɥ2 mRNA ɞβ catenin ● Ά ӊ ● K M ǚ ה miRNA 320a ²; 22.400 ɞ hTcf 4 ²; 26.292 ɞβ catenin ²; 22.267 ● Ά ӊ ● τ N< 0.05 ɉ 3 ɉ

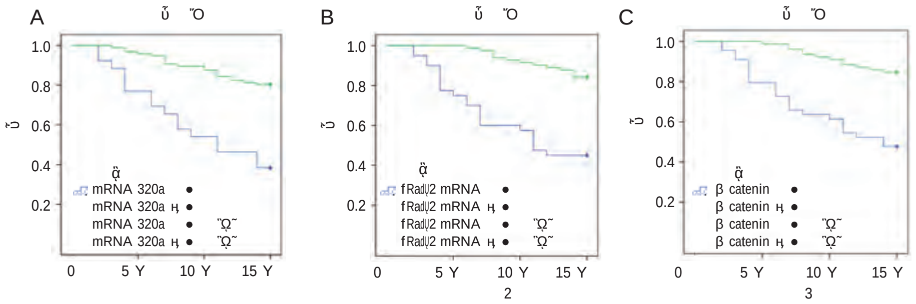

a ɛ miRNA 320a K M b ɛ hTcf 4 K M c ɛ β catenin K M ɉ

3 K M

Figure 3 K M curve

2.7 miRNA 320a Ά fRadɥ2 mRNA ɞβ catenin Ặ

miRNA 320a Ά fRadɥ2 mRNA \ Ặ p=-0.524 N<0.05 Ά β catenin \ Ặ p=-0.509 N<0.05 ɉ

3

miRNA 320a miRNA 320 φm miRNA 320a ' Ặ ɞ Ά [7] ɉ miRNA 320a

5 miRNA 320a fRadџ2 mRNA β catenin

Table 5 Correlation between miRNA 320a and fRadџ2 mRNA and β catenin

	hTcf 4 mRNA		β catenin	
	p e	N e	p e	N e
miRNA 320a	-0.524	<0.05	-0.509	<0.05

mRNA ң Ћ Ά ǖ ͻ \
Ặ Ά Τ ǖ ɞ ɞ \
Ặ ΄Υ miRNA 320a mRNA Ћ
miRNA 320a ' ΐ ǖ ͻ ɞΤ ǖ ɞ
ɞ ɞ ˜ ' ﻎﻧ
ͻ miRNA 320a ' Ћ ↄ
Ά ˜ ε ί w
Ђᵐ Υ ɟ Xiong W [8] Ό
miRNA 320a ң ΄Υ miRNA 320a
╗ Ά ˜ Ặ ɟ æ [9]
miRNA 320a ﯙ ͻ ◓ Ψ \ ң
Ά ǖ ɞǖ ͻ ɞ Ặ ɟ
Ά φ Ч ɟ miRNA 320a ˜ β catenin
מ ˝ ͻ ˛ ἕ Η ﻎﻧ ῎Ặ
ꭗ ъ ΐ Ά ˜ [10] ɟ
miRNA 320a Ȅ ˜ Ţ ɵ e ɟ
Wnt/β catenin מ ˝ ˧ ฿ ﻍ
Wnt ɕβ catenin ɞ ﻍ Τ ﻍ fRadџ2 Ћ
ﻍ Τ ﻍ [11 12] ɟ fRadџ2
mRNA Ά ǖ ͻ \ Ặ Ά Τ ǖ ɞ
ɞ \ Ặ fRadџ2 Ά
˦ ˜ Ặ ъ ﻎﻧ fRadџ2
' Ћ ῎Ặ ε ɟ
ה fRadџ4 Ά ฿ ɞ ı
Ặ ͻ ẹ Ӂ ƒ ꭗ ˦˛
fRadџ2 ᵐ ˛ ﻎﻧ [13 14] ɟ fRadџ2 ﻧ
Ә Ћ ﻧ ε
w˛ ἀ ﻎﻧ c myc ה Ә [15] ɟ
β catenin Wnt/β catenin מ ˝
ǖ ' ч Ά ꭗ
ꭗ ɕ Ặ ﻎﻧ ῎Ặ
β catenin ῎Ặ ˛
β catenin ᵐ ˛ ﻎﻧ [16] ɟ
β catenin Ћ Ά ǖ ͻ
\ Ặ Ά Τ ǖ ɞ ɞ
\ Ặ ﯙ Ψ ң Ћ ' ΐ

˜ ɟ [17] Ό Ψ β catenin
Ά ί ǖ ɞ ǖ ͻ ɞ Ặ
ж ẹ Ό β catenin Ά
Ặ Ά ' Ά Ẩ ʅ ɞ ʅ
Ặ ˜ ᵐ ɟ
ה miRNA 320a Ά fRadџ2 mRNA ɕβ catenin
\ Ặ ˘ ' Ặ ΐ ж ẹ Ә
ɟ ͻ Ћ Ϋ
˜ ʅ Ẩ ɟ
ͻ miRNA 320a \ ң
fRadџ2 ɕβ catenin \ ﺞ Ά ǖ ͻ ɞ Τ ǖ
ɞ ɞ Ặ ˜ ɟ

1 ῎ı . Ɑ ה ǖ J . ǖ Ά 2020 12 1 1 5+38.

2 Lieb V Weigelt K Scheinost L et al. Serum levels of miR 320 family members are associated with clinical parameters and diagnosis in prostate cancer patients J . Oncotarget 2017 9 12 10402 10416.

3 Sun J Li B Jia Z et al. RUNX3 inhibits glioma survival and invasion via suppression of the β catenin/TCF 4 signaling pathway J . J Neurooncol 2018 140 1 15 26.

4 ΐ ȳ . HIF 1α/β catenin מ ˝ ל Ά ч ж ῴ῎Ω J . Ψ ╞ ├ 2018 98 32 2552 2558.

5 Ψ ╞ ж Ă ˦ ˷ ► ˦ ῷ ˧ Ж ├ ├ . Ɑ ה 2017 J . Ψ ╞ ͻ 2017 16 7 705 720.

6 æ џ . HGF ˦ MMP 9 ﯙ ♥ Ψ ί τ J . Ψ ˷ 2018 27 12 74 77.

7 Li YS Zou Y Dai DQ. MicroRNA 320a suppresses tumor progression by targeting PBX3 in gastric cancer and is down regulated by DNA methylation J . World J Gastrointest Oncol 2019 11 10 842 856.

8 Xiong W Ran J Jiang R et al. miRNA 320a inhibits glioma cell invasion and migration by directly targeting aquaporin 4 J . Oncol Rep 2018 39 4 1939 1947.

9 æ ẳ ữ . ͻ ◓ miR 320a SKOV3 ꭗ ˦˛ ΐ J . Ψ ╞ 2019 26 14 1026 1030+1035.

10 Wu F Li J Guo N et al. MiRNA 27a promotes the proliferation and invasion of human gastric cancer MGC803 cells by targeting SFRP1 via Wnt/β catenin signaling pathway J . Am J Cancer Res 2017 7 3 405 416.

11 Su H Qiao Y Xi Z et al. The Impact of High mobility Group Box Mutation of T cell Factor 4 on Its Genomic Binding Pattern in Non small Cell Lung Cancer J . Transl Oncol 2020 13 1 79 85.

C CT

[1] [1] [2]

C Cys C CT
138 87
51 BUN Cr
Cys C CT Cys C CT
Cys C CT
BUN Cr N<0.05 Cys C CT N<0.05
Cys C CT N<0.05 Cys C CT BUN Cr
N<0.05 Cys C CT
AUC 0.841 68.63%
86.21% Cys C CT

C CT

The clinical significance of cystatin C and CT value of renal effusion in patients with obstructive empyema of urinary tract stones

GUO Liang[1] XU Pengcheng[1] HU Henglong[2]

1. Department of Urology Lu an Hospital Anhui Medical University Liuan Anhui China 237000
2. Department of Urology Tongji Hospital Huazhong University of Science and Technology Wuhan Hubei China 430000

ABSTRACT Objective To explore the clinical significance of Cystatin C Cys C and CT value of renal effusion in patients with obstructive empyema of urinary tract stones. Methods A total of 138 patients with obstructive hydronephrosis of urinary tract stones in our hospital were selected including 87 patients with renal empyema as the study group and 51 patients with hydronephrosis as the control group. The general data of the two groups were statistically compared. The renal function indexes blood urea nitrogen BUN creatinine CR serum Cys C and CT value of renal effusion of the two groups were detected and compared. The correlation between serum Cys C and CT value of renal effusion and the relationship between the two and renal function indexes was analyzed and the diagnostic value was analyzed and the diagnostic value of serum Cys C and CT value of hydronephrosis on urinary tract stone obstructive empyema and hydronephrosis was explored. Results The serum BUN and Cr levels of the research group were higher than those of the control

81800626

1. 237000
2. 430000
E mail GL18756415019@126.com

group N<0.05 the CT values of the serum Cys C and renal effusion in the research group were higher than those in the control group N<0.05 . Serum Cys C was positively correlated with CT value of renal effusion N<0.05 serum Cys C and CT value of renal effusion were positively correlated with serum BUN and Cr levels N<0.05 . The area under the curve AUC of the combined diagnosis of serum Cys C and CT value of renal effusion combined with the differential diagnosis of urinary tract stone obstructive empyema and hydronephrosis was 0.841 which was greater than the single diagnosis of the two the best diagnostic sensitivity of combined diagnosis was 68.63% and specificity was 86.21%. Conclusion Serum Cys C level and CT value of hydronephrosis in patients with urinary tract stone obstructive empyema are abnormally increased and are positively correlated with the patient s renal function which can assist in the clinical differential diagnosis of urinary tract stone obstructive empyema and hydronephrosis guide clinical evaluation of patients renal function and develop targeted treatment plans.

KEY WORDS Urinary tract stone obstructive empyema Cystatin C Renal effusion CT value

[1,2] C Cystatin C Cys C [4] CT [5] CT [6] Cys C CT

1

1.1

2017 4 2019 9 138 20~79 47.41±19.59 90 48 Body mass index BMI 19.2~26.1 kg/m² 23.06±1.51 kg/m² 108 30 29 24 [7] 51 87

CT ≤70 P

1.2

12 h 5 mL 2 mL OTA 400 Blood urea nitrogen BUN Creatinine Cr 3 500 r/min 5 min -70 MR 96T Cys C CT 64 CT Brilliance nanoCT CT

1.3

BMI

BUN ɷCr ẇ Cys C ɷ CT e ɟ
Cys C Ά CT e Ą ẇ
Cys C ɷ CT e Ά '
Ą ɟ Cys C ɷ CT e
Ά ⷈ ɵ e ɟ

1.4

SPSS 22.0 Θ w
¯ Ξ Ξ r w
I % 2 Pearson Ą
ŏ ɔ Ə Receiver operating
characteristic ROC ŏ ⷈ ɵ e w N<
0.05 ε τ ɟ

2

2.1 Ξ m
BUN ɷCr Ћ
τ N : 0.05 1 ɟ

2.2 Ξ Cys C ɷ CT e
Cys C ɷ CT e Ћ
τ N : 0.05 2 ɟ Ξ
CT ḏ ₰ 1 ɟ

2.3 Cys C Ά CT e Ą
Cys C Ά CT e ∖ Ą p ;
0.800 N : 0.05 ₰ 2 ɟ

2.4 Cys C ɷ CT e Ά ' Ą
Cys C ɷ CT e Ά BUN ɷ
Cr ∖ Ą N : 0.05 3 ɷ₰ 3 ɟ

2.5 Cys C ɷ CT e ⷈ ɵ e
ROC Cys C ɷ CT e ´
ⷈ ; Area under the curve
AUC Ћ Cys C ɷ CT e ₸ ⷈ
´ ⷈ ȳ ε 68.63% ɟ $ 5e

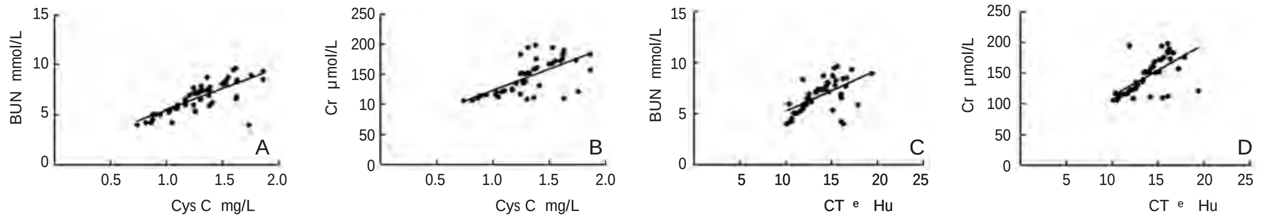

3 Cys C CT

Figure 3 Relationship between serum Cys C and CT value of renal effusion and renal function

4 Cys C CT

Table 4 Differential diagnosis value of serum Cys C and CT value of renal effusion

	AUC	95%CI	X		%	%	P
Cys C	0.758	0.678~0.827	5.973	>1.34 mg/L	64.71	77.01	<0.001
CT	0.770	0.690~0.837	6.362	>8.39 Hu	82.35	66.67	<0.001
	0.841	0.769~0.898	9.648	-	68.63	86.21	<0.001

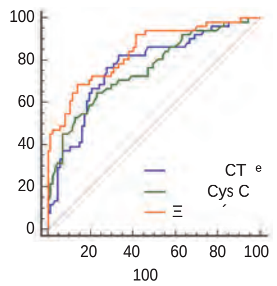

4 Cys C CT

Figure 4 Differential diagnosis value of serum Cys C and CT value of renal effusion

3

Cys C ... 13.3 KD ... Cys C ...[8] ... Cys C ... Cys C

Cys C ... Cys C ... Cys C[9] ... Cys C ... CT ... 95% ...[10] ... CT ...[11] ... CT ... CT

Ό ί
ա ῎Ặ Ҟ ה ג ˜ ɟ
ɘ ʼ ؤٞ
Ỉ ש ̇ Ҟ Cys C
ש ̇ CT ᵉ ╗ ʼ ί ἇ̣
Ά ΎΆ ˈ
ٰ ẶẶ ʼ ί Ţ ˈ ϭ῎Ặ
ɟ

1 ϋ . ᴛ ´ ɘ
ی ה ¥ J . Ψ ├ ´
Ψ 2019 5 4 50 53.
2 Ji DS. Effect observation of minimally invasive percutaneous nephrolithotomy in the treatment of upper ureteral calculi com bined with pyonephrosis J . Acta Med Sin 2018 31 2 68 72.
3 Wang YB He DH Zhang H et al. Diagnosis and treatment of upper urinary tract obstructive pyonephrosis J . Chin Comm Doct 2016 32 11 51+53.
4 . CysC αα1 MG ש̇ β2 MG ؤٞ ط
ɵ ᵉ ש̇ Ά Ҟ Ặ J . ǚ
Ά 2020 12 4 516 519.
5 Yuruk E Tuken M Sulejman S et al. Computerized tomog raphy attenuation values can be used to differentiate hydrone phrosis from pyonephrosis J . World J Urol 2017 35 3 437 442.
6 ٰ . CT ᵉ ؤٞ ǚ ש̇ Ỉ ί D . τ
├ 2018.
7 .ᵐ ٦ ɘ
´ 33 ʢ J . Ψ ﻪ ´ ί 2017 33 7 628 631.
8 . CysC α1 MG ש̇ β2 MG ؤٞ ط
ɵ ᵉ ש̇ Ά Ҟ Ặ J . ǚ
Ά 2020 12 4 124 127.
9 ٩ . C ؤٞ Ψ
ɵ ᵉ J . ├ מ 2016 29 11 366 366 367.
10 Cheng M Xiao XG Chen WJ et al. Value of spectral CT imaging on identifying hydronephrosis and simple renal cysts J . J Harbin yike daxue xuebao 2017 51 1 35 40.
11 ٰ Ẹ . CT ᵉ ´
ɵ ᵉ J . Ψ ╞ 2018 39 1 54 57.
12 ″ . CT ᵉ
ɵ ᵉ J . ├ 2018 49 6 449 452.
13 Aurégan C Berteloot L Pierrepont S et al. Xanthogranulo matous pyelonephritis with pyonephrosis in a 4 year old child J . Arch Pediatr 2015 22 3 287 291.

12 ٰ ˛ ˘ . miR 138 ῎Ặ TCF 4
CAL 62 ؞ ἕ H ᛀ Ә J . Ψ ﻪ ί
῎Ọ 2019 37 4 425 430.
13 Li R Liu S Li Y et al. Long noncoding RNA AFAP1 AS1 enhances cell proliferation and invasion in osteosarcoma through regulating miR 4695 5p/TCF4 β catenin signaling J . Mol Med Rep 2018 18 2 1616 1622.
14 θ . miR 204 5p ˜ TCF 4 Siha
؞ ḉ ᛀ Ә J . ├ ǚ
2018 15 6 373 378.
15 Yang B Xu Y Wang X et al. A serine , ├ _ʹᵐ ξ̌ є ḱ ﻊ

• •

←Ш ┘ ж † HPV ɞ Жی Ǖ
Ŷ ε HPV w ɟ ẉ PCR 2017 7 2019 7 3 650 ʢ Њ Ở ├ ظ├ Ψ HPV ﭺ ﻍ Жی 17 ی ῷ ฿ 15 ●ی ɻ 2 ң●ی Ǖ ɞ ɞ ی ῷ ɟ 3 650 ʢ ɔ 825 ʢ Ό ε 22.60% ẹ Ψ HPV ●ی 745 ʢ ▌90.30% 745/825 ң●ی 172 ʢ ▌20.85% 172/825 ңЖی ΄ 92 ʢ ▌11.15% 92/825 HPV w ╖ ε ζ Ã 553 ʢ ▌67.03% 533/825 272 ʢ ▌32.97% 272/825 HPV Жی A Жی ъ ῷ ε HPV 52 ȡHPV 6+11 ȡHPV 16 ȡHPV 58 ȡHPV 51 ی ɟ ←Ш ┘ HPV w HPV 52 ȡHPV 6+11 ȡHPV 16 ی Жی ε ζ ה † ۷ ɔ ˥ ң HPV ɟ HPV ﭺ ﻍ Ǖ ی ←Ш

Analysis of Female Human Papillomavirus infection in Haidian District Beijing

WANG Haibin ZHANG Dongqing ZHAO Jiao
Department of Clinical Laboratory the Fourth Medical Center Chinese PLA General Hospital Beijing China 100048

ABSTRACT Objective To investigate the infection rate subtypes and age distribution of human papillomavirus HPV among women in Haidian District Beijing and to provide evidence for preventing HPV infection. Method A total of 3650 outpatient women from the Fourth Medical Center of Chinese PLA General Hospital were checked for 17 HPV DNA types by fluorescence quantitative PCR assay. The HPV infection age distribution of the subjects HPV infection rate and HPV subtypes were analyzed. Result Among 3650 women there were 825 cases of HPV infection and the infection rate was 22.60% including 745 cases of high risk subtypes and 172 cases of low risk subtypes and 92 cases of mixed infection of high and low subtypes accounting for 11.15% 92/825 . Female HPV infection is dominated by single infection a total of 553 cases accounting for 67.03% 533/825 and 272 cases of multiple infection accounting for 32.97% 272/825 . Women in different age groups show different subtypes of HPV infection. The top five high risk HPV infection subtypes were 52 6+11 16 58 and 51 subtypes. Conclusion Female HPV infections in Haidian District of Beijing are mainly HPV 52 HPV 6+11 and HPV 16 subtypes. The incidence trend is younger. Effective measures should be taken to reduce HPV infection.

KEY WORDS Human papillomavirus Genotype Beijing

† papillomavirus Њ † rus HPV HPV ζ papovaviridae † ฿ ɨ Ʀ ж ɟ HPV ӝ Ẻ ζ † ɻ ж † human papillomavi ΎẺ ж ɻ

100048
E mail 1197131586@qq.com

100 HPV [1] HPV HPV HPV HPV HPV [2,3] HPV 3 650 17 HPV HPV HPV

1

1.1

2017 7 2019 7 3 650 15~80 43.9± 11.8 <20 22 20 ~381 30 ~989 40 ~1141 50 ~745 60 ~296 70 ~76

1.2

PCR SLAN 96P HPV HPV DNA 15 16、18、31、33、35、39、45、51、52、56、58、59、66、68、82 HPV DNA 2 6、11

1.3

1.3.1

3 mL 4 48 h

1.3.2 DNA

DNA

1.3.3 PCR

PCR dNTP、Taq DNA 36 μL 4 μL DNA H_2O 40 μL 3 000 r/min 4 s 94 2 min 93 10 s 62 31 s 40 62

1.3.4

HPV Ct ≤38 No Ct Ct 38~40 38~40 HPV IC PCR VIC Ct >32 PCR

1.4

SPSS 19.0 % χ² P<0.05

2

2.1 HPV

3 650 HPV 825 22.60% 825/3650 HPV HPV 745 90.30% 172 20.85% 92 11.15% 1

1 HPV

Table 1 Multiplex HPV infection results of women from Haidian District of Beijing

		%
	553	67.03
	178	21.85
	64	7.76
	17	2.06
	8	0.97
	2	0.24
	2	0.24
	1	0.12
	825	22.60

2.2 HPV

3 650 40~49 <20 20 ~ 59.09% 45.67% 2

2 HPV l %

Table 2 HPV positive rate of each group of women from Haidian District of Beijing l %

	l		╥m		²e	N e
<20	22	13 59.09	6 27.27	7 31.82	15.925	<0.001
20~	381	174 45.67	88 23.10	86 22.57	70.7146	<0.001
30~	989	224 22.65	155 15.67	69 6.98		
40~	1 141	227 19.89	176 15.42	51 4.47		
50~	745	127 17.05	94 12.62	33 4.43		
60~	296	53 17.91	30 10.14	23 7.77		
70~	76	7 9.21	4 5.26	3 3.95		

2.3 HPV Жی Ȯ Ỹ

825 ҙ HPV ŭ l A Жیъ ᾇ ε HPV 52 ɞ HPV 6+11 ɗHPV 16 ɗHPV 58 ɗHPV 51 ی ╥m ⁄ є Жیъ ᾇ ε HPV 52 ɗHPV 6+11 ɗHPV 16 ی 3 ɟ

2.4 HPV Жی Ỹ ŭ

HPV Жی ж ѫ w HPV 52 ɗHPV 6+11 ɗHPV 16 ی ε ζ Ά ѫ m 4 ɟ

3

ɟ φ m ҩ Ά Ә ж ה ҙ щ \ † ה ɔ ɟ HPV ᾅ ● ی HPV ǵ [4,5] ɟ ה ‶H ω ' w ᾇ HPV ΄Y

3 HPV l %

Table 3 HPV positive rate of each group of women from Haidian District of Beijing l %

HPV Жی	l n=825	╥m n=553	n=272
HPV 16	139 16.85	70 12.66	69 25.37
HPV 18	55 6.67	28 5.06	27 9.93
HPV 31	37 4.48	13 2.35	24 8.82
HPV 33	32 3.88	13 2.35	19 6.99
HPV 35	26 3.15	6 1.08	20 7.35
HPV 39	84 10.18	24 4.34	60 22.06
HPV 45	22 2.67	5 0.90	17 6.25
HPV 51	95 11.51	44 7.96	51 18.75
HPV 52	193 23.39	93 16.82	100 36.76
HPV 56	77 9.33	35 6.33	42 15.44
HPV 58	113 13.70	54 9.76	59 21.69
HPV 59	67 8.12	29 5.24	38 13.97
HPV 66	49 5.94	21 3.80	28 10.29
HPV 68	52 6.30	25 4.52	27 9.93
HPV 82	27 3.27	8 1.44	19 6.99
HPV 6+11	171 20.73	80 14.47	91 33.46

ל ΄Y HPV ی У ĩ ς ² ɟ

4 HPV l %

Table 4 HPV infection distribution of each age group of women from Haidian District of Beijing l %

HPV Жی	ж	<20	20~	30~	40~	50~	60~	70~
HPV 16	139 16.85	5 0.61	47 5.70	35 4.24	34 4.12	12 1.45	5 0.61	1 0.12
HPV 18	55 6.67	5 0.61	14 1.70	11 1.33	14 1.70	7 0.85	3 0.36	1 0.12
HPV 31	37 4.48	3 0.36	5 0.61	12 1.45	9 1.09	3 0.36	3 0.36	2 0.24
HPV 33	32 3.88	0 0.00	11 1.33	10 1.21	7 0.85	3 0.36	1 0.12	0 0.00
HPV 35	26 3.15	0 0.00	7 0.85	3 0.36	4 0.48	8 0.97	3 0.36	1 0.12
HPV 39	84 10.18	6 0.72	16 1.94	23 2.79	20 2.42	13 1.58	6 0.72	0 0.00
HPV 45	22 2.67	0 0.00	3 0.36	5 0.61	10 1.21	3 0.36	1 0.12	0 0.00
HPV 51	95 11.51	1 0.12	26 3.15	17 2.06	26 3.15	16 1.94	8 0.97	1 0.12
HPV 52	193 23.39	5 0.61	36 4.36	58 7.03	44 5.33	30 3.64	18 2.18	2 0.24
HPV 56	77 9.33	3 0.36	14 1.70	16 1.94	23 2.79	11 1.33	8 0.97	2 0.24
HPV 58	113 13.70	2 0.24	28 3.39	25 3.03	25 3.03	19 2.30	13 1.58	1 0.12
HPV 59	67 8.12	4 0.48	18 2.18	18 2.18	14 1.70	8 0.97	5 0.61	0 0.00
HPV 66	49 5.94	0 0.00	12 1.45	14 1.70	14 1.70	7 0.85	2 0.24	0 0.00
HPV 68	52 6.30	1 0.12	9 1.09	12 1.45	11 1.33	15 1.82	4 0.48	0 0.00
HPV 82	27 3.27	0 0.00	3 0.36	11 1.33	9 1.09	2 0.24	2 0.24	0 0.00
HPV 6+11	171 20.73	6 0.73	62 7.52	58 7.03	26 3.15	16 1.94	4 0.48	0 0.00

HPV Җ ﻍ ﺉﻯ ┘ ⅟ ж ᵕ̉ م ε 1.4%~25.6% ǚ ε ζ Ɑ ﻍ ﻪ ﻃﺉﻯ ʚ ғ ˘ ﺉﻯ ┘ ה ᵕ ͻ ⅟ Ө ᵕ̉ [6] ɟ ᵕ ┘ ה Ђ˘ ﺉﻯ ┘ HPV Ỹ ↿ ╧ Ш ﺉﻯ ┘ ε 33.47% [7] ɔ Z ﺉﻯ ┘ ε 23.43% [8] Ӥ ﺉﻯ ┘ ε 25.31% [9] ╧ ε 22.64% [10] Z ﺉﻯ ┘ ε 29.38% [11] ﺉﻯ ┘ ε 30.45% [12] ɟ H PV Ḫ Ꙥ ẹ ђ ﺉﻯ ┘ ● ﻯ HPV ʢ Ꙥ Ḫ ● ﻯ HPV ʢ ɟ Garg [13] HPV Ж ﻯ ǚ Ά ʚ ʚ ﻃﺉﻯ Ặ ẫ ĭ م Ĭ Ẫ̉ Ж ﻯ ε 16 ɗ18 ɗ31 ﻯ ɟ Ά ﻪ HPV Ҕ † ﻯ ᾇ ﻧﺤﻯ m ﺉﻯ ┘ HPV 52 ɗHPV 81 ɗHPV 16 ﻯ [14] ﺉﻯ ┘ HPV 52 ɗHPV 16 ɗHPV 58 ﻯ [15] ╧ Ш ﺉﻯ ┘ HPV 16 ɗHPV 58 ɗHPV 52 ﻯ [7] ﺉﻯ ┘ HPV16 ɗHPV 52 ɗHPV 58 ﻯ [16] ɔ Z ﺉﻯ ┘ HPV 52 ɗHPV 16 ɗHPV 58 ﻯ [17] ← Ш ﺉﻯ ┘ ﻋﺞ ├ HPV 52 ɗHPV 58 ɗHPV 16 ﻯ [6] ɟ Ӝ ˘ ﺉﻯ ┘ Ό Ά ẫ ĭ م Ĭ Ẫ̉ ε HPV 16 HPV 18 ﻯ Ḫ J Ḫ HPV 52 ɗHPV 58 ﻯ ﺋﻭ ﻪ Ĭ ẹ ђ ﺉﻯ ┘ ı ς HPV 18 ﻯ Ꙥ m ɟ HPV ﻯ ᾇ Ẻ ж ﻃﺉﻯ Ж ﻯ ǚ Ɑ ﻍ ʼ ᵕ ̉ ʚ Ḣ ᵕ̉ Ặ Ӝ ς ʼ Ά ﺉﻯ ﻃﻬﻯ ʚ Җ ﻍ Ҝ ẍ ﻍ Ặ ς ˘ ﺉﻯ ┘ ﺋﻭ ⅟ HPV ʚ HPV ﺉﻯ ┘ Ж ﻯ Ặ Ә [6] ɟ <20 ε 59.09% 13/22 <20 Ɑ ﻍ ʼ Ά ה ᵕ ı ẍ ﺋﻭ ל ͻ ʻ Ặ ﻣﺤﻪ ɟ HPV m Y ẻ ● HPV ˜ ʼ Ӥ ﺋﻭ Ĭ ı ẍ Ḫ ; HPV [18] ● ﻯ HPV Җ ה [19,20] ɟ ῷ HPV ╥m Ά ל ĭ̃ m Ẫ ʚ ⱳ ﯾﮟ ﺉﻯ ┘ ɟ ɔ ← Ш ┘ Ở ├ ﻁ ├ Ψ HPV ˜ Ḫ ͻ ⱳ ╥m ε ζ ᵕ̉ HPV Ж ﻯ ˘ ᵕ

̉ ı Α Ж ﻯ ъ ᾇ ̈ ε HPV 52 ɗHPV6+11 ɗHPV16 ɗHPV58 ɗHPV51 ﻯ <20 ⅟ 20~29 ɟ HPV Ὼ Ẫ ⅟ HPV Ặ̈ ´ ´ Ꙥ ж Ḫ HPV ɟ

1 ╞ Ὼ . í M . 2 . ← Ш Ψ ﻪ ├ Ό 2010 490 492.

2 ╥ Ở . ﻪ ж † HPV J . Ψ ╞ Ặ̈ 2017 21 1 89 93.

3 Ὼ ˥ Ὼ . ж † Ά ﻍ Ặ J . Ψ ╞ 2016 38 4 277 282.

4 ╞ . ᵕ̉ Ж ﻯ HPV Ά Ặ J . ǚ Ά 2017 9 3 196 200.

5 Maggino T Sciarrone R Murer B et al. Screening women for cervical cancer carcinoma with a HPV mRNA test first results from the Venic pilot program J . Br J Cancer 2016 115 5 525 532.

6 ´ ъ . ← Ш ﻋﺞ ├ 5512 ʢ HPV ﻧﺢ ﻯ ﻍ ǚ J . ẍ ǚ Ά í 2016 23 10 1158 1162.

7 ┌ ╙ . ╧ Ш ǚ ﺉﻯ ┘ HPV Ỹ Ά ǚ J . պ ├ 2012 29 39 5686 5707.

8 Ὼ ╞ . ɔ Z ﺉﻯ ┘ HPV Ỹ ǚ J . Ψ ﻪ պ ├ 2019 57 33 136 139.

9 . Ӥ ﺉﻯ ┘ HPV Ỹ ǚ J . Ĭ ǚ 2019 6 32 12 14.

10 i . ╧ HPV ǚ J . ← £ ├ 2020 37 1 58 61.

11 ╬ . Z ﺉﻯ ┘ ж † Ж ﻯ ʚ Ỹ ﯾﮟ ǚ J . Ψ ﻪ Ặ̈ ɫ 2016 29 1 57 60.

12 ể . ﺉﻯ ┘ Җ HPV Ỹ ǚ J . ╧ ├ 2017 28 18 3004 3006.

13 Garg A Suri V Nijhawan R. Prevalence of human papilloma virus infection in young primiparous women during postpartum period study from a tertiary care center in northern india J . J Clin Diagn Res 2016 10 10 6 9.

14 ʠ ╞ . ﺉﻯ ┘ ᵕ̉ HPV J . պ ├ 2020 28 10 1753 1756.

15 δ ŵ . ﺉﻯ ┘ 5151 ʢ ├ HPV Ж ﻯ ǚ J . ﻪ ├ 2019 40 23 2827 2831.

1418

1 2 1

˜ ˈ ˜ Ά SUA ש ̉ CK MB
Ặ ɟ ˥ 2018 1 2019 12 Њ Ҷ 173 ʢ ǘ ợ
SUA ש CK MB Ţ Ĩ LVEDd Ĩ LVEDs
ǘ LVEF ⁄ Gensini ợ ל ǘ ı ǘ ɟ Ξ
ᵐ í ﭻ ˈ τ N<0.05 ˊ
CK MB ᵉ ẹ ẖ ╖ N : 0.05 ΎΌ ᵉ ̋ ̉ ˈ Killip ǘ
SUA ᵉ Ά CK MB ᵉ ̋ ̉ τ N : 0.05 Killip ǘ SUA ᵉ Ά CK MB
ᵉ ST ى STEMI SUA ᵉ Ά CK MB ᵉ ST ى NSTEMI
╖ τ N : 0.05 SUA ᵉ Ά CK MB ᵉ Ά LVEF \
Ặ Ά LVEDs ɑLVEDd ɑGensini ǘ \ Ặ τ N : 0.05 ɟ ˈ ʬ SUA
ש CK MB ᵉ Ţ ˈ ש ˜ ɟ

Correlation between the prognosis of cardiac function and serum uric acid and CK MB levels after acute myocardial infarction

HU Chaoyong[1] ZOU Huawei[2] GAO Pengzhi[1]

1. Department of Cardiology Taihe County People s Hospital Fuyang Anhui China 236600 2. Department of Cardiology Fuyang Hospital of Anhui Medical University Fuyang Anhui China 236000

ABSTRACT Objective To explore the relationship between the prognosis of cardiac function and the level of serum uric acid and CK MB after acute myocardial infarction. Methods 173 patients with acute myocardial infarction who were hospitalized in our department from January 2018 to December 2019 were selected. All patients were tested for blood uric acid and CK MB and the patients were assessed for end diastolic left ventricular diameter LVEDd end systolic left ventricular diameter LVEDs left ventricular ejection fraction LVEF and Gensini coronary artery disease score depending on whether they had the hyperuricemia group was compared. Results The general clinical data of the two groups of patients were balanced and comparable and the difference was not statistically significant N<0.05 . The peak level of CK MB in patients with myocardial infarction combined with hyperuricemia was significantly higher than that of other patients N<0.05 . The peak time is earlier the SUA value of patients with different cardiac function Killip grades is different from the peak CK MB and the difference is statistically significant N<0.05 . The higher the Killip grade the higher the SUA value and the peak CK MB. The levels of SUA and CK MB peak

---

12010402c193

1. 236600
2. 236000
E mail shinei44936859@163.com

in patients with ST segment elevation myocardial infarction STEMI were significantly higher than those in patients with non ST segment elevation myocardial infarction NSTEMI N<0.05 The SUA value of patients with acute myocardial infarction was negatively correlated with the peak level of CK MB and LVEF it was positively correlated with LVEDs LVEDd and Gensini score the difference was statistically significant N< 0.05 . Conclusion The cardiac function and prognosis of patients with acute myocardial infarction can be assessed indirectly through SUA and CK MB values.

KEY WORDS Acute myocardial infarction Cardiac function Serum uric acid Creatine kinase isoenzymes MB

ῴ ж Ѩ ל
ה ϛ ǘ ̏ ╗ acute myocardial infarction AMI ᵐ Ẻ ה ɞ ל ɔ ɞ H ợ [1 2] ɟ ├ Ə Њ ɞ ̏ ϛ ˥ Ѣᵐ Ӂ ה ̎ ǘ э ╗ [3] ɟ ˜ ˈ ש̇ ˜ ẹ ש̇ Ặ ɟ ש̇ ̉ creatine kinase isoenzymes MB CK MB ó AMI ˈ ש̇ ˜ í τ ɟ ΰ̃ ש̇ CK MB ᵈ Ά ẹ ˈ ש̇ ˜ Ặ ɟ

1

1. ŒÀ ŏ Ṛ ΰ̃

1 l % ¯

Table 1 Comparison of general data between 2 groups

l % ¯

	l=91	l=82	r/ ²ᵉ	Nᵉ
	78 85.7	75 91.5	1.394	0.238
	59.6±9.2	60.3±10.1	0.477	0.634
BMI kg/m²	24.3±3.2	23.9±3.8	0.751	0.453
Ⴗ	83 91.2	79 96.3	1.908	0.167
	84 92.3	77 93.9	0.170	0.680
♥	50 54.9	47 57.3	0.099	0.754
	23 25.3	18 22.0	0.264	0.608
♥ mmHg	133.4±18.4	131.9±16.7	0.559	0.577
♥ mmHg	78.2±6.8	77.6±7.1	0.567	0.571
g/L	145.3±10.6	146.8±9.2	0.989	0.324

τ N<0.05 ΎY CK MB Њ τ N<0.01 ɉ 2 ɉ

2.3 Killip ǚ SUA ᵉ Ά CK MB ᵉ

Killip ǚ ~ Ж SUA Ά CK MB ᵉ ΎY τ N : 0.05 ɉ 3 ɉ

2.4 STEMI Ά NSTEMI ᵉ Ά CK MB ᵉ

STEMI SUA ᵉ Ά CK MB ᵉ Њ NSTEMI SUA ᵉ Ά CK MB ᵉ τ N<0.05 ɉ 4 ɉ

2 CK MB ¯

Table 2 Two groups of patients at different times CK MB comparison ¯

ǚ	l	6 h	12 h	18 h	1 d	2 d	3 d
	91	93.2±10.7	247.8±23.2	208.9±21.8	150.2±18.6	35.6±5.7	15.8±3.1
	82	91.8±11.2	176.3±19.4	210.4±20.9	142.9±15.1	24.9±3.1	12.3±2.7
r ᵉ		0.840	21.857	0.460	2.814	15.102	7.879
N ᵉ		0.401	0.001	0.645	0.005	0.001	0.001

3 Killip SUA CK MB ¯

Tab 3 Different Killip grading patients with serum uric acid and CK MB peak value ¯

Killip ǚ	l	ᵉ μmol/L	CK MB ᵉ ng/mL
	68	357.1±40.2	175.9±18.4
	52	386.3±38.1	194.2±17.6
	38	420.9±41.8	237.4±20.5
	15	453.7±42.4	256.8±23.2
D ᵉ		132.54	77.85
N ᵉ		<0.001	<0.001

4 STEMI NSTEMI SUA CK MB ¯

Table 4 STEMI and NSTEMI patients with serum uric acid and CK MB peak value comparison ¯

ǚ	l	ᵉ μmol/L	CK MB ᵉ ng/mL
ST	101	428.7±36.5	214.7±19.6
ST	72	375.2±33.0	184.3±15.3
r ᵉ		9.885	10.986
N ᵉ		<0.001	<0.001

2.5 SUA ᵉ Ά CK MB ᵉ Ά Ặ Ặ

SUA ᵉ Ά CK MB ᵉ Ά LVEF Ⴤ Ặ Ά LVEDs ɞLVEDd ɞ Gensini ǚ Ⴤ Ặ N<0.05 ɉ 5 ɉ

5 SUA CK MB

Table 5 Relationship between serum uric acid value and the peak value of CK MB and degree of coronary artery disease

			CK MB	
	p ᵉ	N ᵉ	p ᵉ	N ᵉ
LVEF	-0.689	<0.001	-0.723	<0.001
LVEDs	0.358	0.019	0.845	<0.001
LVEDd	0.388	0.016	0.037	0.013
Gensini ǚ	0.867	<0.001	0.694	<0.001

3

Ǿ ǚ Ợ ɞ ɞ Ợ ɞ ǟ O H[8] ɉ Ặ ɉ ~ Ặ Ş Ḩ H[9] ɉ SUA ĩ ~ Ḩ Ɔ[10] Ŵ Қ Î Ợ Î[11] ɉ CK MB Ά Қ ΎY Ặ[12] Ά Ş[m] ɉ

SUA Ŵ CK MB ȞΆ ~ Ặ ɉ

SUA Ά CK MB J

SUA

Ά CK MB ST

STEMI SUA Ά CK MB

ST NSTEMI

STEMI NSTEMI [13]

SUA Ά CK MB

SUA CK MB Ά

LVEF Ă Ά

LVEDd LVEDs

Ă SUA Ά CK MB

[14]

SUA Ά CK MB Ά Gen

sini Ă J

Ă G

[15] CK MB

SUA Ά CK MB

[16]

1 ≐ θ . J . 2017 12 4 486 490.

2 . miR 499 miR 16 Ά Ă θ J . Ά 2020 12 6 728 732.

3 . Ά J . 2017 9 4 502 503.

4 ST ≐ 2019 J . 2019 47 10 766 783.

5 Schaitza GA Faria Neto JR Francisco JC et al. Surgical treatment of a giant left ventricular aneurysm a case report J . Rev Bras Cir Cardiovasc 2014 29 4 663 666.

6 J . ≐ 2017 28 1 20 23.

7 . ST Ă J . 2015 6 780 783.

8 . J . P 2015 36 1 135 140.

9 . J . Ά 2015 10 130 131.

10 Edwards NL. The role of hyperuricemia in vascular disorders J . Curr Opin Rheumatol 2009 21 2 132.

11 Kaya EB Yorgun H Canpolt U et al. Serum uric acid levels predict the severity and morphology of coronary atherosclerosis detected by multidetector computed tomography J . Atherosclerosis 2010 213 1 178.

12 . CK MB cTn θ J . Ά 2020 12 8 1018 1021.

13 . B Ά Ă J . P 2016 30 5 426 429.

14 . J . 2015 24 3 530 532.

15 . ST B Ά Ă J . 2017 32 2 137 140.

16 . IMA H FABP CK MB J . ≐ 2016 22 1 27 29.

1414

16 . 8744 Ÿ J . 2019 23 10 1273 1278.

17 . Z 11822 HPV J . 2019 34 19 4523 4526.

18 Haeggblom L Ursu RG Mirzaie L et al. No evidence for human papillomavirus having a causal role in salivary gland tumors J . BMC Infect Dis 2018 18 1 338 342.

19 Lechner M Vassie C Kavasogullari C et al. A cross sectional survey of awareness of human papillomavirus associated oropharyngeal cancers among general practitioners in the UK J . BMJ Open 2018 8 7 e023339.

20 Zhang D Li T Chen L et al. Epidemiological investigation of the relationship between common lower genital tract infectionsand high risk human papillomavirus infections among women in Beijing China J . Plos One 2017 12 5 e0178033.

• •

miR 22 3p IL 1β

miR 22 3p IL 1β Ꮶ ΐ ש ẹ Ə ῍Ạ ɟ ŭ ݹ
Ế IL 1β 48 h Ꮶ ی ɟ qRT PCR Ά Western blot Con ɗIL 1β ɗIL 1β+miR NC ɗIL 1β+miR 22 3p ɗIL 1β+si NC ɗIL 1β+si TRIM8 ɗIL 1β+miR 22 3p+pcDNA ɗIL 1β+miR 22 3p+pcDNA TRIM8 Ψ miR 22 3p ɞTRIM8 ELISA ˘ IL 6 ɗIFN γ ɞTNF α ˘ ἕ H אָ w ᷉ miR 22 3p Ά TRIM8 ˜ Ə Western blot ˘ Bcl 2 ɞBax ɟ Ά IL 1β Ψ miR 22 3p ɞBcl 2 ȟ N<0.05 ἕ H ╗ N<0.05 TRIM8 ɞ Bax Ά IL 6 ɞIFN γ ɞTNF α ╗ N<0.05 miR 22 3p mimics si TRIM8 ' ȟ IL 6 ɗIFN γ ɞTNF α Ά ἕ H ש Bax N<0.05 ݸ Bcl 2 N<0.05 אָ w ᷉ miR 22 3p ' ˜ ´ TRIM8 Ǻ miR 22 3p mimics Ά pcDNA TRIM8 ' ȟ miR 22 3p mimics ἕ H ש א ῍Ạ Ə ɟ miR 22 3p ' ˜ ῍Ạ TRIM8 ъ ῍E IL 1β Ꮶ ש ῍Ạ ἕ H ɟ
miR 22 3p TRIM8 IL 1β ἕ H

Effect of miR 22 3p on IL 1β induced chondrocyte damage by regulating the expression of TRIM8

LI Wei FENG Shenghua ZHAO Jingming
Spinal Surgery Trauma Center Qingdao Haici Medical Group Qingdao Shandong China 266033

ABSTRACT Objective To investigate the effect of miR 22 3p on IL 1β induced chondrocyte injury and its mechanism. Methods Rat chondrocytes were isolated and cultured and IL 1β treated the cells for 48 h to construct a cell injury model. qRT PCR and Western blotting were used to detect the expression levels of miR 22 3p and TRIM8 in Con group IL 1β group IL 1β+miR NC group IL 1β+miR 22 3p group IL 1β+si NC group IL 1β+si TRIM8 group IL 1β+miR 22 3p+pcDNA group IL 1β+miR 22 3p+pcDNA TRIM8 group. The levels of IL 6 IFN γ and TNF α in each group were detected by ELISA. Flow cytometry was used to detect the apoptosis rate of each group. The dual luciferase report assay was used to verify the targeted regulation of miR 22 3p and TRIM8. Western blotting was used to detect the expression of Bcl 2 and Bax in each group. Results Compared with the control group the expression levels of miR 22 3p and Bcl 2 protein in IL 1β treated cells were significantly reduced N<0.05 . The apoptosis rate was significantly increased N<0.05 and the expression levels of TRIM8 and Bax and the levels of IL 6 IFN γ and TNF α were significantly increased N<0.05 . Transfection of miR 22 3p mimics or transfection of si TRIM8 can significantly reduce the levels of IL 6 IFN γ TNF α apoptosis rate and the protein level of Bax N<0.05

2019 0599

266033

E mail 13678895761@yeah.net

and increase the protein Level of Bcl 2 N<0.05 . The dual luciferase report experiment confirmed that miR 22 3p could target TRIM8. Co transfection of miR 22 3p mimics and pcDNA TRIM8 can significantly reduce the inhibitory effect of miR 22 3p mimics on cell apoptosis and inflammation. Conclusion miR 22 3p overexpression can target the inhibition of TRIM8 expression toreduce IL 1β induced chondrocyte inflammatory damage and inhibit cell apoptosis.

KEY WORDS miR 22 3p TRIM8 IL 1β Chondrocytes Inflammation Apoptosis

[1,3] miR 22 3p ox LDL miR 22 3p ox LDL [4] TRIM8 miR 22 3p TRIM8 [5] miR 22 3p TRIM8 IL 1β [6] IL 1β miR 22 3p TRIM8 miR 22 3p IL 1β

1

1.1

SD SPF SCXK 2016 0003 IL 1β Sigma miR 22 3p mimics miR NC si TRIM8 si NC anti miR 22 3p anti miR NC pcDNA3.1 IL 6 IFN γ TNF α ELISA Lipofectamine2000 Invitrogen Trizol PCR TaKaRa Promega TRIM8 Abcam Bcl 2 Bax CST RIPA BCA HRP IgG

1.2

1.2.1

[7,8] Con miR NC miR 22 3p mimics si NC si TRIM8 miR 22 3p mimics pcDNA miR 22 3p mimics pcDNA TRIM8 10 ng/mL IL 1β 48 h IL 1β+miR NC IL 1β+miR 22 3p IL 1β+si NC IL 1β+si TRIM8 IL 1β+miR 22 3p+pcDNA IL 1β+miR 22 3p+pcDNA TRIM8

1.2.2 qRT PCR

miR 22 3p TRIM8 mRNA Trizol RNA RNA RNA cDNA qRT PCR cDNA 2 μL Real Time Master Mix 10 μL 1 μL RNase Free ddH_2O 20 μL 95 2 min 95 15 s 60 1 min 72 30 s 40 miR 22 3p U6 TRIM8 GAPDH $2^{-\Delta\Delta Ct}$ miR 22 3p TRIM8 mRNA

1.2.3 ELISA IL 6 IFN γ TNF α

IL 6 IFN γ TNF α

1.2.4

l MUT TRIM8 ┐ ŏ ą̈
miR NC ɷmiR 22 3p mimics Á WT TRIM8 ɷMUT
TRIM8 Ă ˘ ẉ
ɟ

1.2.6 ẍ ○ Western blot TRIM8 ɷ
Bcl 2 ɷBax
˘ Ấ RIPA ┐
SDS PAGE ŏ
ẋ ˜ ɷ Ấ TRIM8 1Ƃ500 ɷBcl 2
1Ƃ1 000 ɷBax 1Ƃ1 000 m 4
TBST Ấ J 1Ƃ2 000 Ỉ ẉ
Ңь ˝H ḍ ŏ ˘ ɟ

1.3
SPSS 21.0 Ɵ ŏ
ℭ ´ ŏ ẉ ¯ Ξ
r ╥ Ė ŏ ẉ N<
0.05 ε Ė τ ɟ

2

2.1 miR 22 3p ∤ TRIM8 ɡ̈ IL 1β
Ƙ Ψ
Á Con IL 1β Ψ miR 22 3p
ң τ N<0.05
TRIM8 mRNA ẇ
╗
τ N<0.05 1 ɟ

1 miR 22 3p TRIM8 IL 1β
¯

Table 1 Expression of miR 22 3p and TRIM8 in IL 1β induced chondrocyte injury ¯

ŏ	l	miR 22 3p	TRIM8 mRNA	TRIM8
Con	9	1.00±0.06	0.99±0.05	0.39±0.04
IL 1β	9	0.41±0.05	3.11±0.29	0.78±0.07
r e		22.663	21.612	14.512
N e		0.000	0.000	0.000

2.2 miR 22 3p IL 1β
Ƙ ĭ
Á Con IL 1β IL 6 ɷIFN γ ɷTNF α
ɷ ĕ H ẇ Bax
╗
τ N<0.05 Bcl 2 ң
τ N<0.05 Á IL 1β+miR NC
IL 1β+miR 22 3p IL 6 ɷIFN γ ɷTNF α
ɷBax ɷ ĕ H ң
τ N<0.05 Bcl 2
╗
τ N<0.05 2 ɟ

2.3 Ą TRIM8 IL 1β Ƙ
ĭ
Á IL 1β+si NC IL 1β+si TRIM8
IL 6 ɷIFN γ ɷTNF α ң N<0.05
ĕ H ң N<0.05 Bcl 2
╗ N<0.05 Bax ң N<0.05
3 ɟ

2 miR 22 3p IL 1β
¯

Table 2 The effect of miR 22 3p overexpression on chondrocyte injury induced by IL 1β ¯

ŏ	l	miR 22 3p	IL 6 ng/L	IFN γ ng/L	TNF α ng/L	ĕ H %	Bcl 2	Bax
Con	9	1.01±0.06	2.45±0.25	11.54±1.12	7.22±0.71	6.32±0.61	0.73±0.07	0.22±0.03
IL 1β	9	0.46±0.04[a]	7.55±0.71[a]	62.33±6.14[a]	31.65±3.11[a]	24.13±2.11[a]	0.30±0.03[a]	0.63±0.06[a]
IL 1β+miR NC	9	0.44±0.04	7.61±0.72	64.28±6.32	33.27±3.35	25.36±2.32	0.28±0.03	0.65±0.05
IL 1β+miR 22 3p	9	0.82±0.08[b]	3.56±0.35[b]	17.25±1.54[b]	10.87±1.01[b]	11.25±1.14[b]	0.64±0.05[b]	0.33±0.03[b]
D e		213.159	214.146	355.917	297.734	279.116	209.054	211.861
N e		0.000	0.000	0.000	0.000	0.000	0.000	0.000

Á Con [a]N<0.05 Á IL 1β+miR NC [b]N<0.05 ɟ

3 TRIM8 IL 1β
¯

Table 3 The effect of inhibiting TRIM8 expression on IL 1β induced chondrocyte injury ¯

ŏ	l	TRIM8	IL 6 ng/L	IFN γ ng/L	TNF α ng/L	ĕ H %	Bcl 2	Bax
Con	9	0.36±0.03	2.67±0.26	10.32±1.04	7.01±0.69	7.36±0.71	0.72±0.06	0.21±0.03
IL 1β	9	0.77±0.07[a]	7.84±0.77[a]	61.39±6.11[a]	32.45±3.22[a]	23.66±2.31[a]	0.31±0.03[a]	0.62±0.06[a]
IL 1β+si NC	9	0.79±0.08	7.91±0.76	63.54±6.21	34.67±3.41	24.87±2.43	0.30±0.03	0.63±0.06
IL 1β+si TRIM8	9	0.43±0.04[b]	3.86±0.38[b]	24.15±2.44[b]	15.28±1.52[b]	13.58±1.36[b]	0.59±0.05[b]	0.39±0.04[b]
D e		131.196	190.634	220.852	261.030	185.700	198.987	150.773
N e		0.000	0.000	0.000	0.000	0.000	0.000	0.000

Á Con [a]N<0.05 Á IL 1β+si NC [b]N<0.05 ɟ

2.4 miR 22 3p ˜ TRIM8

StarBase TRIM8 3′UTR Ψ Ά miR 22 3p Ў Ώ 1 ɟ ẉ Ã ﻳ l WT TRIM8 Ψ Ά miR NC miR 22 3p ẉ ɥ N<0.05 Ã ﻳ l MUT TRIM8 Ψ miR 22 3p ẉ Ά miR NC τ N<0.05 4 ɟ Ά miR NC miR 22 3p Ψ TRIM8 ɥ N<0.05 Ά anti miR NC anti miR 22 3p Ψ TRIM8 ╗ N<0.05 ɟ 5 ɟ

1 TRIM8 3 UTR miR 22 3p

Figure 1 TRIM8 3 UTR contains a nucleotide sequence complementary to miR 22 3p

4 miR 22 3p TRIM8

Table 4 Dual luciferase reporting assay was used to detect the targeted relationship between Mir 22 3p and TRIM8

ŭ	l	WT TRIM8	MUT TRIM8
miR NC	9	1.02±0.06	0.99±0.05
miR 22 3p	9	0.48±0.04[a]	1.00±0.05
r e		22.465	0.424
N e		0.000	0.677

Ά miR NC [a]N<0.05 ɟ

2.5 TRIM8 Ђ miR 22 3p IL 1β Ƙ Ə

Ά IL 1β+miR 22 3p+pcDNA IL 1β+

5 miR 22 3p TRIM8

Table 5 Effect of knockout or overexpression of miR 22 3p on TRIM8 protein expression

ŭ	l	TRIM8
miR NC	9	0.41±0.04
miR 22 3p	9	0.20±0.02[a]
anti miR NC	9	0.38±0.03
anti miR 22 3p	9	0.83±0.07[b]
D e		328.154
N e		0.000

Ά miR NC [a]N<0.05 Ά anti miR NC [b]N<0.05 ɟ

miR 22 3p+pcDNA TRIM8 IL 6 IFN γ TNF α ╗ N<0.05 ἔ H ╗ N<0.05 Bcl 2 ɥ N<0.05 Bax ╗ N<0.05 ɟ 6 ɟ

3

miR 22 3p ﯚ ל Ψ ɥ Ά ɔ Ƙ [9] ɟ miR 22 3p ' Έ ﻳ Ƙ [10] ɟ miR 22 3p ' Έ א ' ŭ ɔ [11] ɟ miR 22 3p ɥ ' Ƙ ה ɟ ε miR 22 3p ﯚ Ƙ Ψ Ə Ά Ό IL 6 IFN γ TNF α ╗ ' א ъ ה [12] ɟ miR 22 3p ' Έ IL 1β Ƙ ɟ IL 1β ˜ ἔ H miR 22 3p ˜ ἔ H ɥ miR 22 3p ' Ά IL 1β ἔ H ɟ ε m ẹ ' Ά ἔ H Bcl 2 ἔ H Bax ɟ ἔ

6 TRIM8 miR 22 3p IL 1β

Table 6 TRIM8 overexpression reverses the effect of miR 22 3p overexpression on IL 1β induced chondrocyte injury

ŭ	l	TRIM8	IL 6 ng/L	IFN γ ng/L	TNF α ng/L	ἔ H %	Bcl 2	Bax
IL 1β+miR NC	9	0.76±0.07	7.71±0.69	63.54±6.33	32.48±3.22	26.14±2.63	0.29±0.03	0.64±0.06
IL 1β+miR 22 3p	9	0.33±0.03[a]	3.42±0.34[a]	16.47±1.65[a]	11.25±1.13[a]	12.36±1.23[a]	0.66±0.05[a]	0.31±0.03[a]
IL 1β+miR 22 3p+pcDNA	9	0.32±0.03	3.40±0.33	16.24±1.62	10.52±1.06	11.47±1.15	0.67±0.04	0.29±0.03
IL 1β+miR 22 3p+pcDNA TRIM8	9	0.65±0.06[b]	7.12±0.71[b]	52.13±5.21[b]	26.33±2.61[b]	20.33±2.13[b]	0.41±0.04[b]	0.53±0.05[b]
D e		175.340	161.510	295.322	234.315	122.120	193.591	132.873
N e		0.000	0.000	0.000	0.000	0.000	0.000	0.000

Ά IL 1β+miR NC [a]N<0.05 Ά IL 1β+miR 22 3p+pcDNA [b]N<0.05 ɟ

H מ ˝ Bcl 2 ; Bax ɔ ’
caspase א ъ ἕ H [13] ɟ
IL 1β ˜ Ψ Bcl 2 ;
Bax ɔ miR 22 3p ˜
Ψ Bcl 2 ɔ Bax ; miR 22 3p
’ Bcl 2 Bax ъ
Ἇ ἕ H ɟ

TRIM8 ﯚ OGD/R ẃ Ƙ Ψ
ɔ ӊ ẹ ’ ╗ OGD/R ẃ
ӊ ἕ H ῎E ROS У [14] ɟ
TRIM8 ﯚ Ố Ƙ ﯾ Ψ
ẹ ’ Ἇ Ố Ƙ ᛀ

ἕ H [15] ɟ IL 1β ˜
Ψ TRIM8 ╗ m
Ἇ TRIM8 ˜ ’ ӊ IL 1β
Ψ IL 6 IFN γ TNF α ’ ӊ
ἕ H ’ ˛ Bcl 2 ש Ἇ Bax
Ἇ TRIM8 ’ ῎E IL 1β
Ƙ ɟ א w ֏ Ά
Western blot miR 22 3p ’ ˜ ˊ
TRIM8 ’ ˜ TRIM8 ש ε
miR 22 3p ı ’ ˜ TRIM8 ъ ל Ά
Ƙ pcDNA TRIM8 Ά
miR 22 3p mimics Ẵ ˜ ʄ
IL 1β IL 6 IFN γ TNF α
╗ ἕ H ╗ Bcl 2
ӊ Bax ╗ miR 22 3p
’ ; TRIM8 ӊ א ש
Ἇ ἕ H ɟ
ɔ IL 1β Ψ miR 22 3p
; TRIM8 ɔ miR 22 3p
’ TRIM8 ъ ῎E IL 1β
Ƙ ’ Ἇ ἕ H
’ ε Ặ w ̉ ɟ

1 Chώ

• •

1

1 2 3

NPP ц ЖΨ‖ΰ m Ẻ l
Ą̈ Ύ Ό ɟ ה ɔ ɮ Ḩ
TRP ℶ Ά Ĩ א ẹ Ψ ɔ ɮ Ḩ ɔ l 1 TRPV1 Ά Ặ
ε Ύ ' φm ɟ Ђ Ỹ Ά TRP
Ά ' Ђ TRPV1 Ą̈ Ḥ Ə ε ˜ ǚ Ψ ǚ ε
w ˜ ɟ
ɔ ɮ Ḩ ɔ l 1 Ą̈ Ḥ

Research progress of transient Receptor Potential Vanilloid 1 inhibitors in neuropathic pain

SHENG Shuyue[1] TIAN Yinghong[2] ZHANG Xingmei[3]

1. The First Affiliated Hospital Southern Medical University Guangzhou Guangdong China 510515 2. Experimental teaching management center School of Basic Medical Science Southern Medical University Guangzhou Guangdong China 510515 3. Department of Neurobiology School of Basic Medical Science Southern Medical University Guangzhou Guangdong China 510515

ABSTRACT Neuropathic pain NPP is a very common symptom in current society. However the mechanism of NPP is still unclear and there are no effective drugs which can effectively treat NPP. In recent years Transient Receptor Potential TRP channels are found to be involved in multiple intracellular responses. Transient Receptor Potential Vanilloid 1 TRPV1 isclosely related to NPP which makes its inhibitors as important drugs targeted for NPP. This article summarize the overview of NPP and the composition and function of the TRP channel family. The focus is on the research progress of TRPV1 inhibitors as targeted drugs in neuropathic pain and provides a new research direction for drug therapy of neuropathic pain.

KEY WORDS neuropathic pain transient Receptor Potential Vanilloid 1 inhibitor

neuropathic pain NPP Ẻ l Ą̈
l [1] ฿ ⁴ Ą̈ ⁴ Ψ Ą̈ [3] ɟ ⁴ Ą̈ ฿ ⁴
⁴ ฿ ɔ ɞP ặ Ặ ' ێ
ℶ ɞɔ ˜ ℶ ɞ ێ Ặ ⁴ P [3] ɟ Ψ
˜ ɞ Ƙ ⁴ [2] ɟ Ą̈ ฿ Ą̈ ⁴ ɔ Ψ Ą̈ ɟ

81771484 2018A030313835

1. 510515
2. 510515
3. 510515
E mail zxmray@hotmail.com

Na+ Ca2+ K+ [3] transient receptor potential TRP TRP TRPV1 transient receptor potential vanilloid 1 TRPV1 [4] TRPV1 [5]

1

transient receptor potential TRP [6] TRP TRPC TRPV TRPM TRPP TRPML TRPA TRPN [7] TRPC TRPM TRPA TRPV 6 TRP TRP box TRP TRP [8] TRP [9] TRP TRPC6 TRPA1 TRPM6 TRPM1 [5]

TRPV1 transient receptor potential vanilloid 1 Ca^{2+} TRPV1 PH TRPV1 TRP Ca^{2+} [10] TRPV1 [11,12]

2 TRPV1

5 [13] 1989 TRP TRPV1 TRPV1

2.1 capsazepine

1994 S [14] S TRPV1 4

ɥ Ὼ ئۆ 5 ˝ Ḩ ɔ ᢩ ﯿ ɥ ɥ 2E 4Z N 3R 3 hydroxy 2 oxo 1 2 3 4 tetrahydro 5 quinolyl 5 4 isopropoxyphenyl 5 4 trifluoromethylphenyl 2 4 pentadienamide R 36b Ὼ ɟ Ι Ỉ ɔ ΄ Ἃ Ca[2+] Ə Ύ w Ḥ Ύ ئۆ سخ Ƙ ی Ψ [18] ɟ

2.4 α α spinasterol

α m Ẻ ɞ ɔ ⅂ Ƙ ɔ Ə TRPV1 Ḥ ˀ ς m ɔ cyclooxygenase COX Ἃ Ḥ ɟ ئۆ У Ἃ Ψ COX א У ῴ Ὼ E2 PGE2 ’ ɯ Ə ɛ Ỉ TRPV1 ɟ غ α ˆ c Ἃ COX Ἕ PGE2 У TRPV1 Ə ɛ [19] ɟ ئۆ Ψ ἰ α Ἕ Ђ ˜ Ἕ Ƙ Ψ [20] ɟ ᾆ α ئۆ ˆ ל Ι Ỹ ; Ἃ COX 1 ⅂ COX 2 ɟ α m Ύ ẫ TRPV1 Ḥ ⅂ COX Ἃ Ḥ ئۆ ˜ ⅂ ی Ψ Ẻ Ə [20] ɟ

2.5 SZV 1287 3 4 5 diphenyl 1 3 oxazol 2 yl propanal oxime

SZV 1287 3 4 5 J ﯿ 1 3 Ս 2 ﯿ Γ 3 4 5 diphenyl 1 3 oxazol 2 yl propanal oxime m ی ɔ semicarbazide sensitive amine oxidase SSAO Ἃ Ḥ ɟ SSAO ǖ ç ﯿ Γ ɞ ⅂ ɔ [21] ’ Ə Ҍ TRPV1 ɔ Ι ʆ φ ɥ ɟ Ι Ỉ ئۆ ὰ Ƙ ی Ψ SZV1287 Ἃ Ђ TRPV1 ɔ ɔ ɔ ɟ ئۆ ی ⅂ TRPV1 ﯿ غ Ψ سخ ی ئۆ SZV1287 7 ˜ ╚ ɥ ئۆ ﯿ غ Ψ ᾆ ɟ ɔ SZV1287 ˆ c Ἃ SSAO Ἕ У ˀ ς ’ Ἃ TRPV1 Ə ʆ φ ɛ ی

[22] ɟ

2.6 TRPV1 ǖ RNA

RNA small interfering RNA siRNA m ئۆ 20 50 Y RNA RNA Ά ζ mRNA Ў ΄ ʆ φ Ἃ ζ ﯿ غ ɟ ئۆ ی Ψ Ά ╥ ΄ سخ ♥ Ƙ CCI Chronic constriction injury ῃ ⅂ ῃ ﭺ ╗ ɟ ה TRPV1 ئۆ ῴ ع ɞ ⅂ ﯿ ɟ Ỉ ˜ TRPV1 siRNA Ι ὰ ῃ Ἕ ɟ ˀ ˀ Ђ Ψ מ ˝ Extracellular signal regulated kinases ERK ɞ CaM dependent kinases CaMKs ɟ Ẃ ῴ ERK ɔ ˜ ئۆ ẃ ’ ﺵ ⅂ Ψ Ə CaMKs ל Ά ERK [4] ъ ל Ά У ɟ ئۆ CCI ی Ψ CaMKII ɞ ERK ɔ Ə Ξ ﭺ ╗ TRPV1siRNA ; TRPV1 ˜ TRPV1 ⅂ CaM KII Ἕ ɥ ERK ɔ Ə ς Ἕ TRPV1siRNA ч Ə ’ Ά ; CaMKII ⅂ Ἕ ERK ɔ Ặ [23] ɟ ה RNA short hairpin RNA shRNA m ה RNA ǖ ’ RNA Ἃ ﯿ غ ɟ Hirai [24] ˜ TRPV1 AAV9 Ι AAV9 shTRPV1 ˜ Ƙ spared nerve injury SNI ی Ỉ AAV9 shTRPV1 ئۆ ˜ 10 28 50 ῃ ӣ ﻫ ẹ ђ Ξ ῃ Ξ ᾆ ɟ ئۆ 4 ⅂ ˜ AAV9 shTRPV1 DRG Ψ TRPV1 ɥ 55% ئۆ Ψ ɥ 95% ɟ TRPV1 ئۆ Ψ Ặ Ə ς AAV9 sh TRPV1 Ə ئۆ Ψ ᾆ Ἕ Ə ɟ Ђ ˜ TRPV1 siRNA ɞ shRNA Ə ς ˜ RNA long noncoding RNAs lncRNA ’ ɯ TRPV1 У Ə [25] ɟ Lnc RNAs RNA ΄ II

È У ѽ lnc RNA ‟
’ ğ Ǐ Ψ ה Ə ɟ
Lnc RNA BC168687 lnc RNAs ŏ φᵐ Ė I Ə
‟ ж Liu [25] ה ğ
Diabetic neuropathic pain DNP
DRG Ψ lnc RNA BC168687
ѫ ɟ Liu [26] ה lnc RNA
BC168687 siRNA DNP
ṇ [e] mechanical withdrawal thresholds
MWT ﾉ ṇ ѝ thermal with
drawal latencies TWL Ą DRG Ψ
TRPV1 mRNA ˀ Ş ң DRG

loid 1 antagonist attenuates mechanical allodynia in a mouse model of neuropathic pain J . Biol Pharm Bull 2011 34 7 1105 1108.

18 Saku O Ishida H Atsumi E et al. Discovery of novel 5 5 diarylpentadienamides as orally available transient receptor potential vanilloid 1 TRPV1 antagonists J . J Med Chem 2012 55 7 3436 3451.

19 Marwaha L Bansal Y Singh R et al. TRP channels potential drug target for neuropathic pain J . Inflammopharmacology 2016 24 6 305 317.

20 Brusco I Camponogara C Carvalho FB et al. α Spinasterol a COX inhibitor and a transient receptor potential vanilloid 1 antagonist presents an antinociceptive effect in clinically relevant models of pain in mice J . Br J Pharmacol 2017 174 23 4247 4262.

21 Payrits M Sághy É Mátyus P et al. A novel 3 4 5 diphenyl 1 3 oxazol 2 yl propanal oxime compound is a potent Transient Receptor Potential Ankyrin 1 and Vanilloid 1 TRPA1 and V1 receptor antagonist J . Neuroscience 2016 324 151 162.

22 Horváth Á Tékus V Bencze N et al. Analgesic effects of the novel semicarbazide sensitive amine oxidase inhibitor SZV 1287 in mouse pain models with neuropathic mechanisms Involvement of transient receptor potential vanilloid 1 and ankyrin 1 receptors J . Pharmacol Res 2018 131 231 243.

23 Guo SH Lin JP Huang LE et al. Silencing of spinal Trpv1 attenuates neuropathic pain in rats by inhibiting CAMKII expression and ERK2 phosphorylation J . Sci Rep 2019 9 1 2769.

24 Hirai T Enomoto M Kaburagi H et al. Intrathecal AAV serotype 9 mediated delivery of shRNA against TRPV1 attenuates thermal hyperalgesia in a mouse model of peripheral nerve injury J . Mol Ther 2014 22 2 409 419.

25 Liu C Tao J Wu H et al. Effects of LncRNA BC168687 siRNA on Diabetic Neuropathic Pain Mediated by P2X 7 Receptor on SGCs in DRG of Rats J . Biomed Res Int 2017 2017 7831251.

26 Liu C Li C Deng Z et al. Long Non coding RNA BC168687 is Involved in TRPV1 mediated Diabetic Neuropathic Pain in Rats J . Neuroscience 2018 374 214 222.

2020 8 ϴ Ό 3 ;

1. 2020 8 1018 CK MB ȼTnI ɓơ ܫ ঌ ΄ ɵ ᵉ Ə
ӥ Ѝ Ώ ᵛ Ψł ▌52.44% Ń εł ▌33.33% Ń Å ł 43 ད 84.31% Ń εł 43 ད 52.44% Ń

2. 2020 8 1026 RDW ♥ ה Ə Ọ̈ æ ᛃ
є Ψł ה 61 ད A 53 ད B π 29 ད C Ń εł ה 96 ད A 28 ད B π 19 ད C Ń Ψ ݎ ł 61 Ń εł 96 Ń A Ψł 53 Ń εł 28 Ń A Ψł 29 Ń εł 19 Ń מ Ə zhi56223390@163.com ε qiu cx200508hs@163.com

3. 2020 9 1257 HLA B27 ɞASO ܫ ẍ í τ Ə
╓ 1 Ψ ད ł 85 Ńłł 35 Ń Ḩ ặ Ώ Ψł 48/37 Ńłł 20/15 Ń Ḩ

ђ ǚ Ά ŋ
2020 10 14

60

26 1 12 8 5

40

1997 WHO 1999

H9N2 2005 2003

PCR

40

SARS H1N1 H7N9

2020

1 Uϑ"n Ëë@ž g ῶ Ä بخ

2016 3

18

6 IVD

“ — — —

— ”

IVD

IVD

gzivdleague@163.com

http //yxyq.cbpt.cnki.net
020-32290789 206 jmdt@vip.163.com
020-32290789 201